Sedimentary Petrology and Paleocurrents of the Harebell Formation, Pinyon Conglomerate, and Associated Coarse Clastic Deposits, Northwestern Wyoming

GEOLOGICAL SURVEY PROFESSIONAL PAPER 734-B

Sedimentary Petrology and Paleocurrents of the Harebell Formation, Pinyon Conglomerate, and Associated Coarse Clastic Deposits, Northwestern Wyoming

By DAVID A. LINDSEY

GEOLOGY OF GOLD-BEARING CONGLOMERATES IN NORTHWESTERN WYOMING

GEOLOGICAL SURVEY PROFESSIONAL PAPER 734-B

A detailed study of the petrography and sedimentary structures of Upper Cretaceous and Paleocene gold-bearing conglomerates in northwestern Wyoming and adjacent States

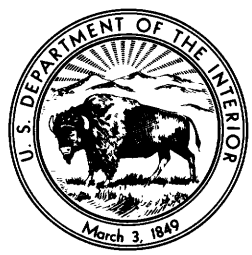

UNITED STATES GOVERNMENT PRINTING OFFICE, WASHINGTON : 1972

UNITED STATES DEPARTMENT OF THE INTERIOR

ROGERS C. B. MORTON, *Secretary*

GEOLOGICAL SURVEY

V. E. McKelvey, *Director*

Library of Congress catalog-card No. 72-600277

For sale by the Superintendent of Documents, U.S. Government Printing Office
Washington, D.C. 20402 - Price $1.50 (paper cover)
Stock Number 2401–00249

CONTENTS

ILLUSTRATIONS

TABLES

SEDIMENTARY PETROLOGY AND PALEOCURRENTS OF THE HAREBELL FORMATION, PINYON CONGLOMERATE, AND ASSOCIATED COARSE CLASTIC DEPOSITS, NORTHWESTERN WYOMING

By DAVID A. LINDSEY

ABSTRACT

The quartzite roundstone conglomerates of the Harebell Formation and the Pinyon Conglomerate in Jackson Hole are part of a series of Upper Cretaceous and lower Tertiary coarse clastic deposits that crop out discontinuously from the Centennial Range in Idaho to the Green River and Bighorn Basins in northwestern Wyoming. Inasmuch as most of these conglomerates contain small quantities of fine-grained gold of supposed detrital origin, a petrographic and paleocurrent study was undertaken to determine the source of the conglomerates.

The Harebell Formation (Upper Cretaceous) and the Pinyon Conglomerate (Upper Cretaceous and Paleocene) can be divided into four lithofacies: a lower, sandstone lithofacies and three quartzite roundstone conglomerate lithofacies. The sandstone facies underlies and perhaps intertongues with two of the conglomerate facies; it contains some highly tuffaceous sandstones as well as nontuffaceous sandstones and minor amounts of conglomerate, shale, and coal. The conglomerate facies are divisible into (1) the western facies, located at the north end of the Teton Range and characterized by abundant roundstones of quartzite and soft sedimentary rocks; (2) the northern facies, located north of Spread Creek in Jackson Hole and characterized by abundant quartzite, few soft sedimentary rocks, few volcanic rocks, and almost no welded-tuff roundstones; and (3) the southern facies, located between Spread Creek and the Gros Ventre River, which contains abundant quartzite and also more volcanic and welded-tuff roundstones than the northern facies. Commonly, only a few thin lenses of sandstone and shale are found in the conglomerates.

Paleocurrent directions in the Harebell Formation and the Pinyon Conglomerate were determined by measuring crossbedding orientation in the sandstone facies and both imbrication and crossbedding orientation in the conglomerate facies. Paleocurrents that deposited the western conglomerate facies flowed southeasterly; those that deposited the sandstone facies and the overlying northern conglomerate facies, east-northeasterly; and those that deposited the southern conglomerate facies, south-southeasterly. Maximum and mean maximum quartzite roundstone sizes show a downstream decrease. Regions of maximum roundstone size may define the courses of major paleostreams: two in the northern facies and as many as three in the southern facies.

Quartzite-bearing conglomerates in part of the Beaverhead Formation of southwestern Montana and adjacent Idaho and in the Fort Union Formation of the Bighorn Basin were studied to assess their possible relation to the Harebell and Pinyon. The Divide conglomerate lithosome (Ryder, 1967) of the Beaverhead Formation contains quartzite, soft sedimentary rock, and volcanic roundstones that are petrographically identical with those of the Harebell and Pinyon and suggest a similar source terrane. Imbrication and variation in quartzite roundstone size suggest derivation from the southwest. In contrast, the Fort Union conglomerates near Heart Mountain contain quartzite roundstones and heavy-mineral species that suggest a source terrane different from that of the Harebell and Pinyon. Crossbedding orientations indicate a source to the southwest, perhaps the Paleozoic terrane of the Late Cretaceous–Paleocene Washakie Range uplift.

Although alternative explanations cannot be entirely ruled out, I favor long-distance transport of coarse detritus from western and northwestern sources in Idaho and Montana to explain the present composition and distribution of conglomerates in the Harebell and Pinyon. Much of the quartzite probably came from the present region of Precambrian quartzites of the Belt Supergroup in Idaho and Montana and Precambrian and Cambrian quartzites in southeastern Idaho; Paleozoic orthoquartzites and quartzose sandstones from a wide area to the west and northwest may also have contributed significantly. Many of the volcanic roundstones in the Harebell and Pinyon can be explained by derivation from similar rocks in the Upper Cretaceous Elkhorn Mountains Volcanics and Livingston Group to the north. Paleozoic and Mesozoic sedimentary rocks to the west and northwest supplied soft sedimentary roundstones to the conglomerates.

Plant and vertebrate fossils and sedimentary features suggest a warm, humid terrestrial environment of deposition for the conglomerates, but microfossils and a few invertebrate fossils suggest the proximity of marine conditions in Late Cretaceous time. The conglomerates probably accumulated as alluvial fans next to rapidly rising highlands to the west and north of Jackson Hole.

479-609 O - 72 - 2

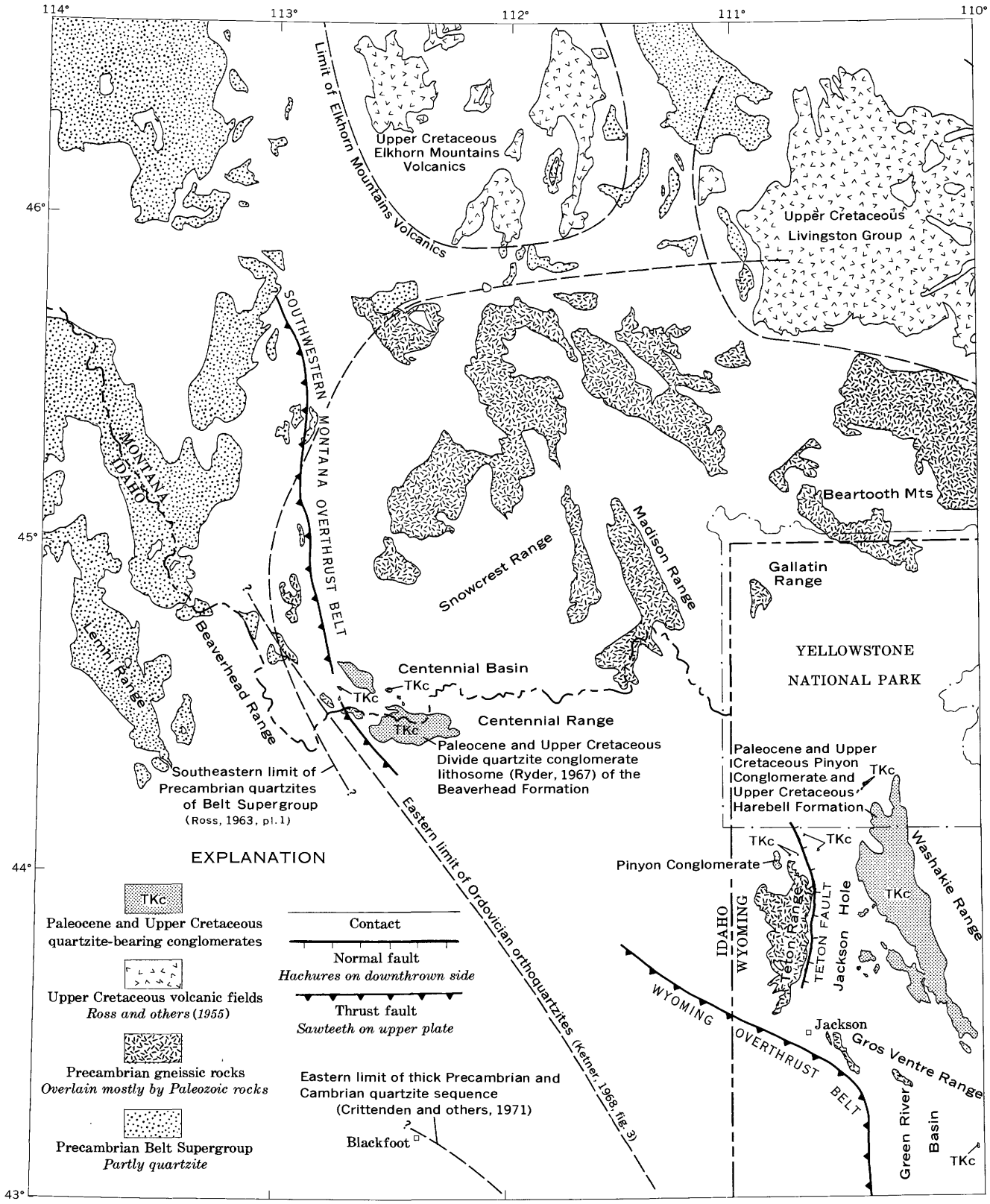

FIGURE 1. — Geographic and geologic setting of Upper Cretaceous and Paleocene quartzite-bearing conglomerates

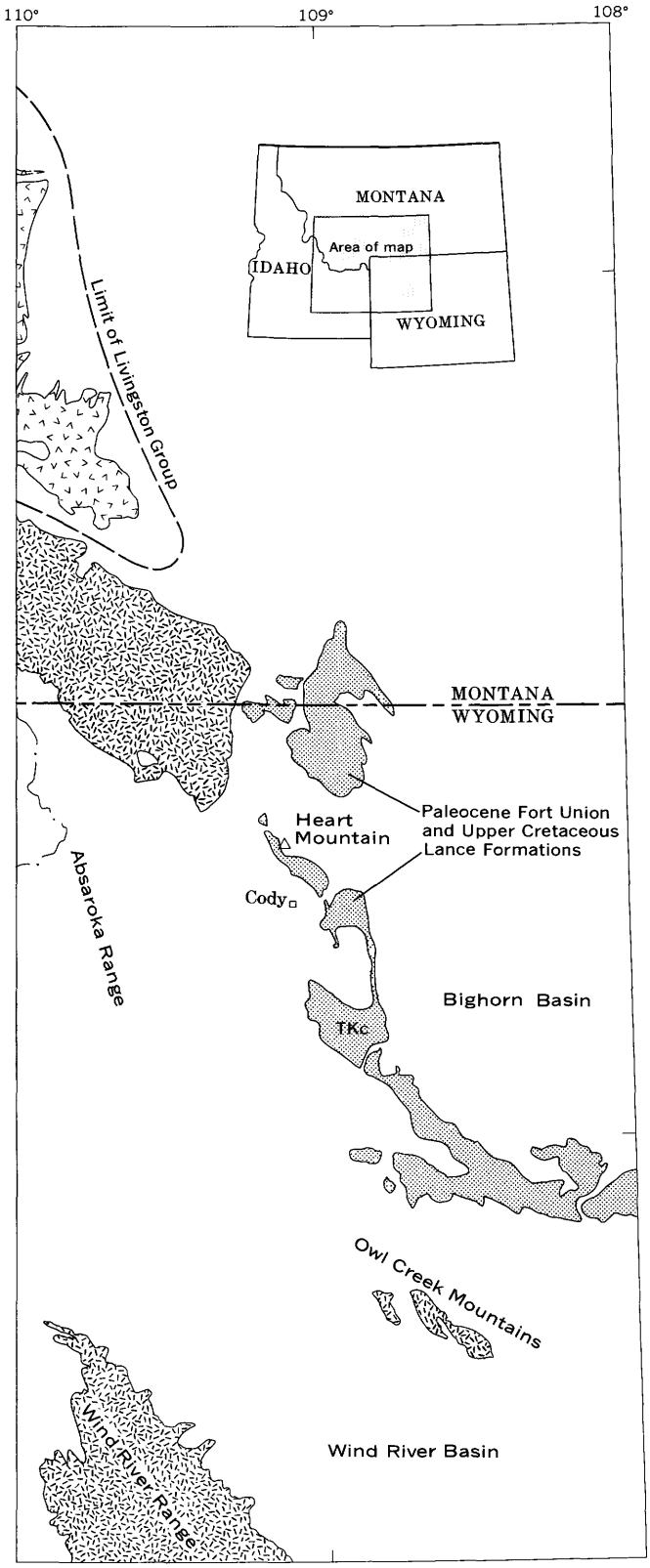

in northwestern Wyoming and adjacent areas.

INTRODUCTION

PURPOSE OF STUDY

This is the second in a series of reports on the gold-bearing conglomerates of northwestern Wyoming, designated the Harebell Formation (Upper Cretaceous) and the Pinyon Conglomerate (Upper Cretaceous and Paleocene). The first report in the series, by Love (1972), covered the stratigraphy of the conglomerates. The conglomerates are characterized by a very large volume of quartzite boulders, cobbles, and pebbles and by small quantities of fine-grained detrital gold (Antweiler and Love, 1967). The absence of abundant quartzite nearby in present-day uplifts suggests that these terranes were not the source of either the conglomerates or the gold contained within them. The purpose of the present study is to present petrographic and paleocurrent evidence bearing on the source or sources of the conglomerates.

GEOLOGIC AND GEOGRAPHIC SETTING

The Harebell Formation and the Pinyon Conglomerate are part of a series of Upper Cretaceous and Paleocene coarse clastic deposits which extend discontinuously from southwestern Montana and adjacent Idaho to the Bighorn Basin of Wyoming (fig. 1). All the deposits shown in figure 1 are distinguished by abundant quartzite boulders, cobbles, and pebbles and by at least small amounts of fine-grained gold. These deposits consist of the Upper Cretaceous to Paleocene quartzite conglomerates in the Beaverhead Formation, the Pinyon Conglomerate at the north end of the Teton Range, the Harebell Formation and the Pinyon Conglomerate in Jackson Hole, and local conglomerates in the Paleocene Fort Union Formation along the west flank of the Bighorn Basin.

Certain regional geologic features which are pertinent to possible sources of the conglomerates, and which are also shown in figure 1, are the east margins of the Wyoming overthrust belt (Armstrong and Oriel, 1965) and of the southwestern Montana overthrust belt (Scholten, 1968); the present eastern limits of Precambrian quartzites of the Belt Supergroup (Ross, 1963, pl. 1), of Precambrian and Cambrian quartzites (Crittenden and others, 1971), and of thick Ordovician orthoquartzites (Ketner, 1966, 1968); the present distribution of Precambrian gneissic rocks overlain mostly by Paleozoic rocks (taken from State geologic maps by Love and others, 1955; Ross and Forrester, 1947; and Ross and others, 1955); and the present distribution of Upper Cretaceous volcanic fields (Ross and others, 1955).

The Harebell Formation and the Pinyon Conglomerate are situated mainly in the highlands between the Gros Ventre River and the south boundary of

Yellowstone National Park, to the east and northeast of the lowest part of Jackson Hole (figs. 1 and 2). Jackson Hole itself is a structural and topographic basin, about 30–50 miles across, bounded by high mountain ranges on three sides. The Teton, Gros Ventre, and Wind River Ranges comprise a chain of uplifts which expose Precambrian gneissic cores mantled by Paleozoic and Mesozoic sedimentary rocks; these uplifts form the western and southern boundaries of Jackson Hole. With respect to regional structure, Jackson Hole and the ranges to the south and west are partly fault-bounded large blocks situated on the edge of the stable foreland Rocky Mountains of Wyoming; nearby and to the southwest is the overthrust belt of Idaho and western Wyoming (Horberg and others, 1949). Tertiary volcanic terranes of the Yellowstone National Park area and the Absaroka Range bound Jackson Hole on the north and east. Partially exposed beneath the Eocene Absaroka Volcanic Supergroup is the Washakie Range, a northwest-trending uplift of Paleozoic rocks that was beveled by erosion prior to deposition of the Absaroka Volcanic Supergroup.

METHODS OF STUDY

The present study deals mainly with the petrography and paleocurrents of the gold-bearing conglomerates. Information on stratigraphy is cited from various reports by J. D. Love. Field measurements were made to determine roundstone lengths and imbrication and crossbedding orientations. Pebbles and cobbles were identified in field counts and in specimens selected for laboratory study, as were conglomerate matrix and sandstone. The petrography of specimens was studied by conventional laboratory techniques, including use of thin sections, hydrofluoric acid-etched and cobaltinitrite-stained rock slices, and bromoform separation of heavy minerals. The data derived from these studies were grouped accordng to rock units (formations, lithofacies) and summarized by descriptive statistics; statistical tests were applied to answer pertinent geologic questions. Some of the groupings involve data from rocks of more than one age, and results of additional tests are presented to show that stratigraphic variation is not major. Finally, the data are summarized in relation to the geologic framework of northwestern Wyoming and adjacent parts of Montana and Idaho in an attempt to provide a clearer understanding of the sources of the conglomerates and the regional geologic events which led to their deposition.

Throughout the present study, I followed a uniform procedure of field observation and sampling. Under the procedure, the standard field sampling unit is termed the "station"; all station localities in the Harebell Formation and the Pinyon Conglomerate are shown in figure 2; those for the other formations studied are shown in figures accompanying later discussions. The station is an outcrop where as many types of observations as proved feasible were made: measurement of roundstone length, measurement of imbrication and crossbedding orientations, counting of identified roundstones, and collection of specimens for laboratory study. Measurements of roundstone length in traverses as much as 1,000 feet long were grouped under one station; at some stations measurements from small adjacent outcrops were combined to assure that all stations were comparable. The stations were dispersed as evenly as possible over much of the area of occurrence of the formations studied in order to achieve as representative a sample of the whole as possible, but the stations and samples were not selected by random methods. Uneven distribution of outcrop, inaccessibility of some areas, and uncertain stratigraphic control all hindered the collection of representative measurements and samples. However, I believe that the outcrops studied (in some formations, a large part of the total) are for the most part geologically representative of the formations studied.

ACKNOWLEDGMENTS

I thank J. C. Antweiler and J. D. Love for introducing me to the geology of Jackson Hole and providing many hours of stimulating discussion and advice. Harold Ganow and Steven Rudy assisted me in fieldwork. Margaret Roberts and Robert Terrazas wrote computer programs and assisted with computer analysis of data. D. A. Seeland provided a computer program for rotation and analysis of crossbedding orientations. F. S. Fisher donated samples and laboratory notes. W. L. Rohrer, H. J. Prostka, W. H. Hays, and S. S. Oriel contributed by discussion; R. H. Tschudy identified pollen samples; E. T. Ruppel, W. R. Keefer, and D. E. Trimble loaned rock samples for comparative studies; and I. J. Witkind identified rock samples and contributed by discussion of the geology of southwest Montana. All those acknowledged are employed by the U.S. Geological Survey.

STRATIGRAPHY

CRETACEOUS AND TERTIARY SECTION

Table 1 summarizes the post-Jurassic stratigraphic section of Jackson Hole and vicinity. In general, the section is divisible into four parts: marine, mixed marine and continental, continental, and continental volcanic. Marine sandstones and shales dominate the lower part of the section from the Lower Cretaceous Cloverly Formation to the

Upper Cretaceous Bacon Ridge Sandstone. Evidence of marine environments persists into the Late Cretaceous Harebell Formation (Love, 1972), but abundant fossil remains and coals indicate recurrent continental environments from the deposition of the coaly sequence through Harebell time. Continental conglomerates, sandstones, and shales were deposited from Late Cretaceous and Paleocene Pinyon time into Eocene Wind River time. Beginning with the Eocene Wind River Formation, a thick succession of continental volcaniclastic rocks completes the Tertiary section.

TABLE 1. — *Quaternary, Tertiary, and Cretaceous stratigraphic section of Jackson Hole, Wyo.*

[Modified from Love (1956b); asterisk (*) indicates supplemental information from Love (1972), Rohrer (1966a, 1968, 1969), Rohrer and Obradovich (1969), and Smedes and Prostka (1972)]

System	Series	Formation and rock types	Maximum thickness, in feet
Quaternary		Alluvium, alluvial terraces, volcanic ash, basalt flows, till, and glacial outwash	Variable
Quaternary or Tertiary	Pleistocene or Pliocene	Bivouac Formation: conglomerate, welded tuff, and pumicite	1,000
Tertiary	Pliocene	Teewinot Formation: limestone, tuff, pumicite, claystone, and conglomerate	5,000
	Miocene	Colter Formation: pyroclastic conglomerate, sandstone, and claystone	7,000
	Eocene	*Wiggins Formation: Volcanic conglomerate and tuffaceous claystone	2,500
		*Tepee Trail Formation: tuffaceous sandstone, mudstone, and claystone	*1,500
		*Wind River Formation: sandstone, tuffaceous sandstone, claystone, mudstone, arkosic conglomerate, quartzite-bearing conglomerate, and coal	*1,800
	Paleocene	Unnamed sandstone and claystone sequence: sandstone, claystone, and minor coal	*1,500
Tertiary and Cretaceous	Paleocene and Upper Cretaceous	Pinyon Conglomerate: quartzite-cobble and pebble conglomerate with minor sandstone, shale, and coal	*3,000
Cretaceous	Upper Cretaceous	Harebell Formation: sandstone, shale, and quartzite cobble and pebble conglomerate	5,000
		Meeteetse Formation: tuff, bentonite, sandstone, shale, and coal	675
		Mesaverde Formation: sandstone	982
		Lenticular sandstone and shale sequence	2,400
		Coaly sequence: shale, coal, and sandstone	1,000
		Bacon Ridge Sandstone: sandstone and minor shale, coal, and bentonite	1,250
		Cody Shale: shale and sandstone	2,200
		Frontier Formation: sandstone, shale, porcellanite, and bentonite	1,100
	Lower Cretaceous	Mowry Shale: shale, bentonite, tuff, and sandstone	700
		Thermopolis Shale: shale and sandstone	300
		Cloverly Formation: sandstone	?

HAREBELL FORMATION

The Harebell Formation was named by Love (1956a) for Harebell Creek, along the southern margin of Yellowstone National Park (fig. 2). Parts of the Harebell had previously been referred to the Laramie Formation (Hague, 1896), the Mesaverde Formation (Foster, 1947; Bengston, 1956), the conglomeratic sandstone sequence (Love and others, 1948), and the Lance Formation (Love and others, 1955). Angular unconformities are reported at the base and top of the Harebell Formation (Love, 1956a, b; 1972).

Love (1971) defined two members in the Harebell: an unnamed lower, sandstone member and an upper, quartzite roundstone conglomerate member, which he named the Bobcat Member. In the type section of the Harebell, the lower member contains about 5,000 feet of sandstone, siltstone, and claystone, with lenses of quartzite conglomerate. The Bobcat Member near Bobcat Ridge consists of more than 3,000 feet of quartzite roundstone conglomerate. North of Pacific Creek, the lower member contains abundant volcanic detritus and is probably equivalent in part to the Landslide Creek Formation (Fraser and others, 1969, p. 34–37) less than 50 miles to the north. Along Blackrock Creek, the lower member contains about 3,000 feet of sandstone, siltstone, and claystone. Here the lower member is overlain by about 1,000 feet of quartzite roundstone conglomerate of the Bobcat Member, and this sequence, in turn, is overlain by nearly 2,000 feet of sandstone and claystone. To the south, along the Gros Ventre drainage, the Harebell is locally present as sandstone, siltstone, and shale, with lenses of conglomerate; it ranges in thickness from 50 to more than 800 feet. The conglomerate lenses are composed mainly of pebbles derived from Paleozoic and Mesozoic rocks, but some quartzite pebbles are present.

The age of the Harebell, as determined on the basis of fossil evidence (plants, fresh-water invertebrates, fragmentary dinosaur remains, and pollen), is Late Cretaceous (Love, 1956a, b; 1972). Plant fossils indicate that both the Harebell and the Pinyon were deposited in a warm, humid terrestrial environment (Love, 1956c, 1972). Possible marine microfossils, including acritarchs and dinoflagellates and, in the Harebell Formation, *Mytilus*? clams (Love, 1972), suggest the occasional proximity of marine waters during Late Cretaceous time.

PINYON CONGLOMERATE

The Pinyon Conglomerate was named by W. H. Weed (in Hague, 1896) for exposures on Pinyon Peak, a few miles south of Yellowstone National Park (fig. 2). It overlies the Harebell Formation, and the contract in some places is an angular unconformity (Love, 1956b, 1972). The Pinyon is unconformably overlain by Tertiary volcanic rocks on Pinyon Peak (Hague, 1896) and conformably overlain by an unnamed sandstone and claystone sequence in the area from Cottonwood Creek to Park Creek (Love, 1947; Rohrer, 1969).

Love (1956b) divided the Pinyon into two members. The lower member consists of 50–140 feet of

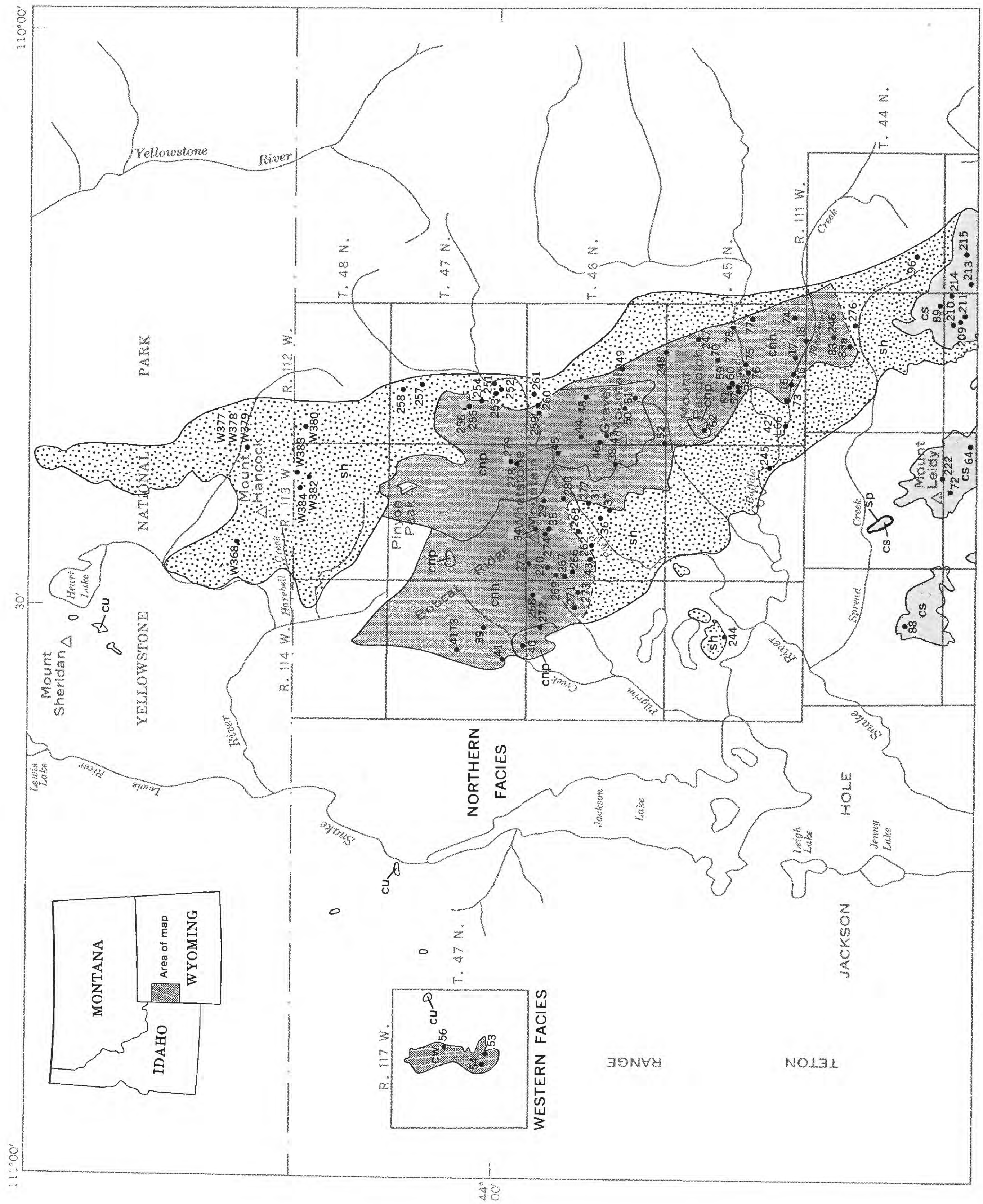
YELLOWSTONE NATIONAL PARK
Yellowstone River
Mount Sheridan
Heart Lake
Mount Hancock
Pinyon Peak
Whetstone Mountain
Bobcat Ridge
Gravel Mountain
Mount Randolph
Mount Leidy
Jackson Lake
Leigh Lake
Jenny Lake
JACKSON HOLE
TETON RANGE
NORTHERN FACIES
WESTERN FACIES
MONTANA
IDAHO
WYOMING
Area of map
110°00'
111°00'
44°00'

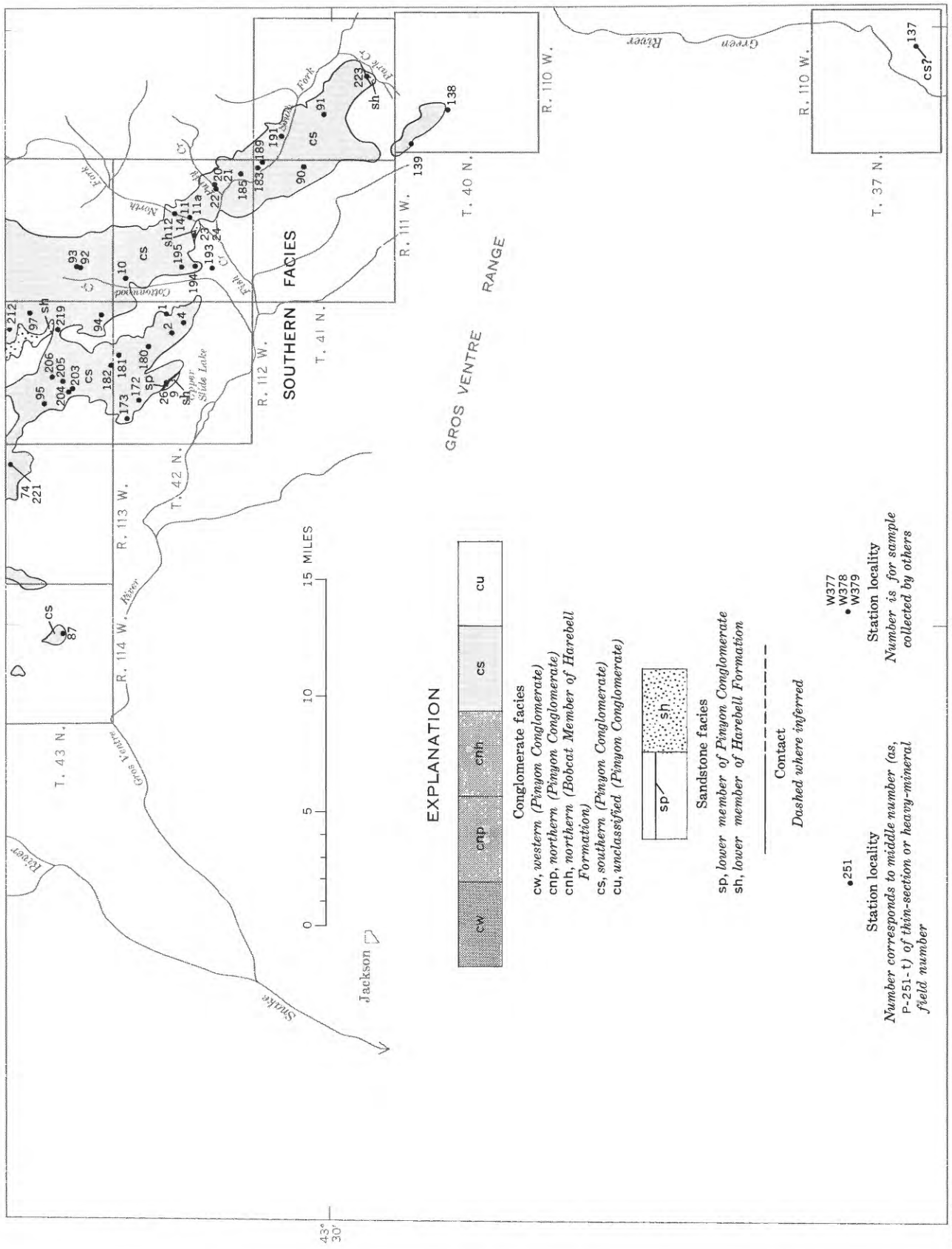

FIGURE 2. — Distribution of the Harebell Formation and the Pinyon Conglomerate and station localities where samples used in this study were measured or collected.

coal, sandstone, and claystone. In most places it is obscured by covered slopes, but it crops out north of Upper Slide Lake and north of Mount Leidy, where it is interbedded with the overlying conglomerate. The overlying conglomerate member consists almost entirely of quartzite roundstone conglomerate with only thin lenses of sandstone and shale. The conglomerate member is about 3,000 feet thick at the principal reference section (Love, 1972), more than 1,000 feet thick on Gravel Mountain (Love, 1956b), and 1,000–1,500 feet thick in complete measured sections on Cottonwood Creek and on the North Fork of Fish Creek (Love, 1947). To the southeast, on Park Creek, the conglomerate thins to slightly more than 200 feet. Remnants of similar conglomerate north of the Teton Range, on Mount Sheridan in Yellowstone National Park (Love, 1956c; Love and Keefer, 1969), and along the upper Green River (Richmond, 1945) have been considered part of the Pinyon Conglomerate (fig. 2).

The Pinyon Conglomerate was originally assigned to the Eocene (Hague, 1896), when that epoch was considered to be the base of the Tertiary. Love (1947, 1956b) considered the Pinyon to be Paleocene and cited as evidence the species of fossil vertebrates, invertebrates, and plants. Pollen from the coal beds in the lower member north of Upper Slide Lake confirms a Paleocene age for much of the southern part of the Pinyon (Love, 1972). The lower 150 feet of strata at the principal reference section, however, is considered, on the basis of a dinosaur tooth found here, to be Late Cretaceous in age (McKenna and Love, 1970).

REGIONAL LITHOFACIES[1]

During the present study I found that the conglomerates in the Harebell Formation cannot be distinguished from those in the Pinyon Conglomerate on the basis of their petrography and paleocurrent directions. Variations in petrography and paleocurrent directions were found to be regional rather than stratigraphic. Other criteria have been used to distinguish between the two formations (Love, 1972, table 1). For the present report, however, the two formations are rearranged into lithofacies, and variations between and within the facies are emphasized (fig. 2).

The conglomerates are divided, on the basis of regional differences in roundstone lithology, into the western, northern, and southern conglomerate facies (fig. 2). The western facies, north of the Teton Range, is regarded as part of the Pinyon Conglomerate, but its exact age is uncertain. The northern facies, north of Spread Creek in Jackson Hole, comprises both the Bobcat Member of the Harebell Formation and the overlying Pinyon Conglomerate. As defined, the northern facies ranges in age from Late Cretaceous to Paleocene. The southern facies, south of Spread Creek and in the Gros Ventre drainage, consists entirely of the Paleocene part of the Pinyon Conglomerate.

The sandstones of the lower members of both the Harebell Formation and the Pinyon Conglomerate constitute a fourth lithofacies. Although both Upper Cretaceous and Paleocene strata are included, the sandstone facies generally underlies and perhaps intertongues with the conglomerates. North of Blackrock Creek, sandstone of the lower member of the Harebell Formation underlies conglomerate of the Bobcat Member of the Harebell Formation as well as conglomerate of the Pinyon Conglomerate. South of Blackrock Creek, sandstones of the Harebell Formation and of the lower member of the Pinyon Conglomerate are found locally under the upper member of the Pinyon Conglomerate.

QUARTZITE-BEARING CONGLOMERATES OF OTHER AGES

Quartzite roundstones similar to those of the Upper Cretaceous and Paleocene conglomerates dominate conglomerates of the Eocene Pass Peak Conglomerate of Eardley, Horberg, Nelson, and Church (1944; Dorr, 1956; Steidtmann, 1969, 1971) and the Eocene Wind River Formation (Rohrer, 1968, 1969). Quartzite roundstones occur also in the tuffaceous conglomerates of the Miocene Colter Formation (Love, 1956b) and in numerous Pleistocene and Holocene alluvial terraces in and around Jackson Hole.

LITHOLOGY AND PETROGRAPHY

CONGLOMERATE

GENERAL DESCRIPTION

Quartzite roundstone conglomerate is the most distinctive lithology of the Harebell Formation and the Pinyon Conglomerate. It occurs in thick beds, and more than 1,000 feet is exposed in single outcrops. Stratification is generally crudely defined by sandstone lenses and carbonate-cemented ledges (fig. 3). Commonly only a few thin sandstone and shale lenses are present, but thick crossbedded sandstones similar to those in the overlying unnamed Paleocene sandstone and claystone sequence occur near the top of the conglomerate along the South Fork of Fish Creek. The conglomerate consists mainly of rounded quartzite pebbles, cobbles, and boulders — termed "roundstones" (Fernald, 1929; Love, 1956b) — set in a sandstone matrix (figs. 4 and 5). The

[1]The terms "lithofacies" and "facies" as used here refer only to aspect (appearance and composition) and do not imply spatial relationships, such as lateral continuity or equivalence (Weller, 1960, p. 503–522).

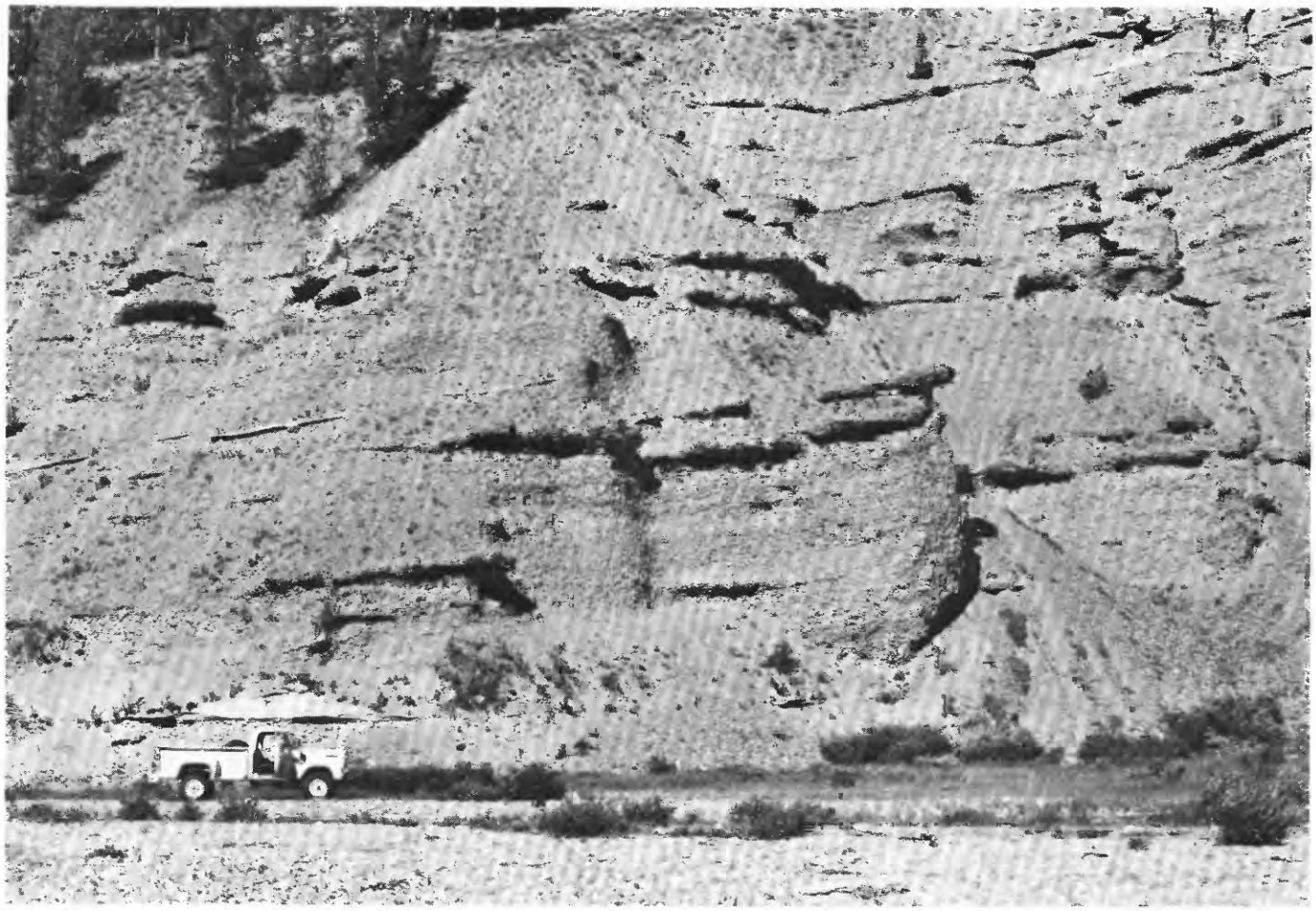

FIGURE 3. — Quartzite roundstone conglomerate in the Pinyon Conglomerate along the South Fork of Fish Creek. Note crude stratification and general scarcity of sandstone beds.

roundstones are packed closely together; in most outcrops they show a pronounced imbricate arrangement (fig. 4), and in a few outcrops, crossbedding. The stones are marked by pressure marks and by extensive cracking and crushing (figs. 4 and 5).

SIZE, SHAPE, AND SURFACE MARKINGS OF ROUNDSTONES

The long dimension of quartzite roundstones was systematically measured at stations throughout the Harebell Formation and the Pinyon Conglomerate (fig. 2). In Jackson Hole, the largest roundstones were as much as 21 inches in length. At one station (56) north of the Teton Range, several large sandstone boulders as much as 90 inches in length and one large quartzite boulder 50 inches in length were seen (fig. 6); none of the other quartzite roundstones exceeded 18 inches in length. Generally, roundstones of less common rock types in the conglomerates are smaller than those of the accompanying quartzite, but in the southern facies of the Pinyon Conglomerate those of volcanic rock are as long as 12 inches.

Three-dimensional measurements were made to determine the shape of quartzite roundstones at stations 1, 4, and 57. Zingg plots (Pettijohn, 1957, p. 54–57) show nearly identical shape distributions for all three stations, with most roundstones at each locality being oblate, or flattened (fig. 7). Inspection of roundstones at many other stations indicates the prevalence of oblate shapes.

Surfaces of the quartzite roundstones show crescentic percussion marks, pressure marks, and polish (fig. 8). The crescentic percussion marks are curvilinear cracks which typically are 1–3 cm long and about 1 mm deep (fig. 8*A*). Counts at eight stations show that about 5 percent of the quartzite stones bear at least a few percussion marks. Similar markings were described by Klein (1963), who considered them to result from impact during transport. Klein reported that percussion marks are known mainly from fluvial deposits, where the energy required to produce them is most commonly available. The marks may therefore be evidence of fluvial transport.

479-609 O - 72 - 3

FIGURE 4. — Typical conglomerate containing well-rounded moderately sorted quartzite roundstones in hard sandstone matrix, Harebell Formation north of Blackrock Creek.

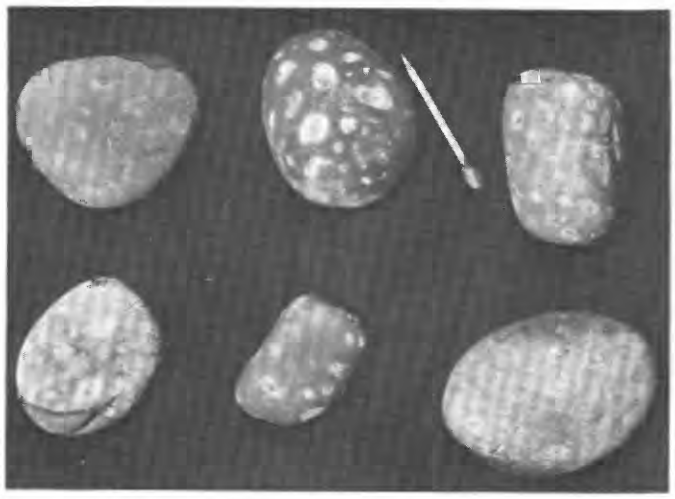

FIGURE 5. — Typical shapes and rounding of quartzite stones from conglomerate of the Harebell Formation, Whetstone Mountain. Pocklike spots are pressure marks.

Pressure marks are found on most roundstones in the conglomerates (figs. 4, 5, and 8*B*). Most are 1–2 cm across and are slightly indented below the surrounding surface. On roundstones extracted from the matrix each mark is located where the stone touches another stone. Similar marks have been described by Klein (1963) and Turnit (1968), both of whom concluded that the marks were caused by pressure solution.

The third surface marking, polish, occurs on a small percentage of the stones. Under the binocular microscope, the polished areas are seen to consist of parallel striae or grooves about 0.1 mm wide and as much as 1 cm long. In some examples two striae sets of different orientation are superposed. Similar parallel striae sets have been described by Judson and Barks (1961) and Clifton (1965), who suggested tectonic movement or compaction as a probable cause.

LITHOLOGY OF ROUNDSTONES

One hundred roundstones were identified in each of 98 counts in the conglomerates (table 2). Quartz-

A

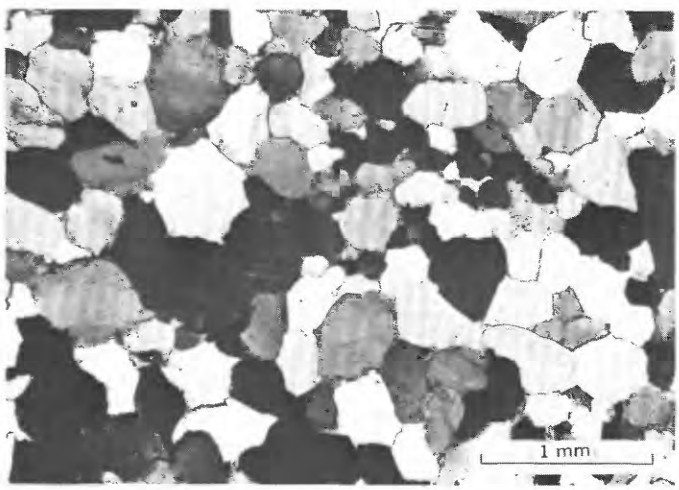

B

FIGURE 6. — Large quartzite boulder in Pinyon Conglomerate north of the Teton Range. *A*, Photograph shows size, rounding, and percussion marks. *B*, Photomicrograph shows same boulder to be orthoquartzite with detrital grain outlines and quartz cement. Crossed nicols.

ite was found to be the most abundant rock type everywhere; lesser quantities of soft sedimentary rocks (limestone, sandstone, shale, and chert), volcanic rocks (welded tuff and porphyritic rocks), and plutonic rocks (granitic rocks and gneiss) were found at most localities. The less common roundstone types were used to define three conglomerate lithofacies (figs. 9 and 10):

1. A western facies, north of the Teton Range, characterized by about 20 percent soft sedimentary roundstones and only very few volcanic roundstones.
2. A northern facies, generally north of Spread Creek in Jackson Hole, characterized by few soft sedimentary roundstones and generally 5

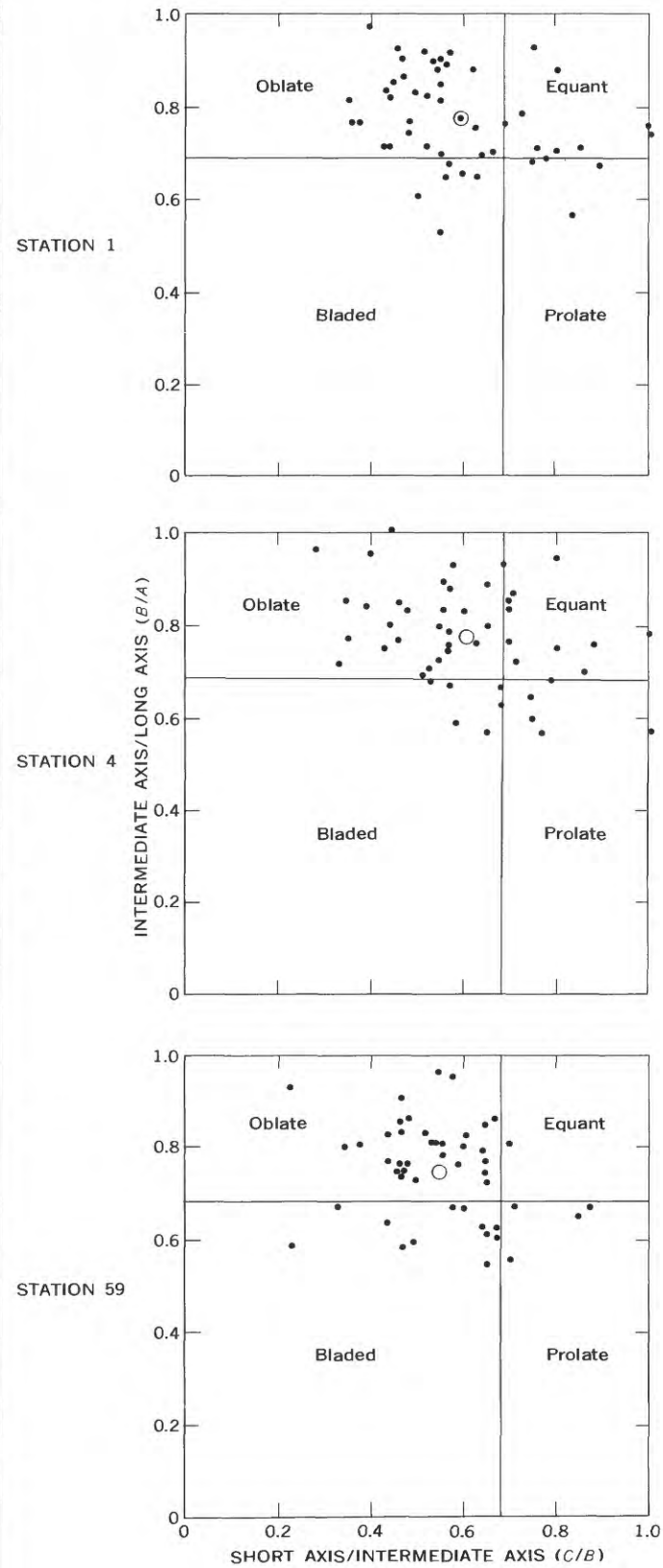

FIGURE 7. — Zingg plots of quartzite roundstone dimensions at three stations. *A*=long axis; *B*=intermediate axis; *C*=short axis. Circle is average shape at station.

percent or less total volcanic roundstones. Welded-tuff roundstones are very rare in the northern facies.

3. A southern facies, extending from Spread Creek to the Gros Ventre River, characterized by few soft sedimentary roundstones and generally more than 5 percent total volcanic roundstones. Among the volcanic roundstones, welded tuff is conspicuous throughout the southern facies. These characteristics are easily observed in the field and are useful in mapping the extent of each facies.

A more detailed summary of roundstone lithology data for the northern and southern facies is presented in figure 10.

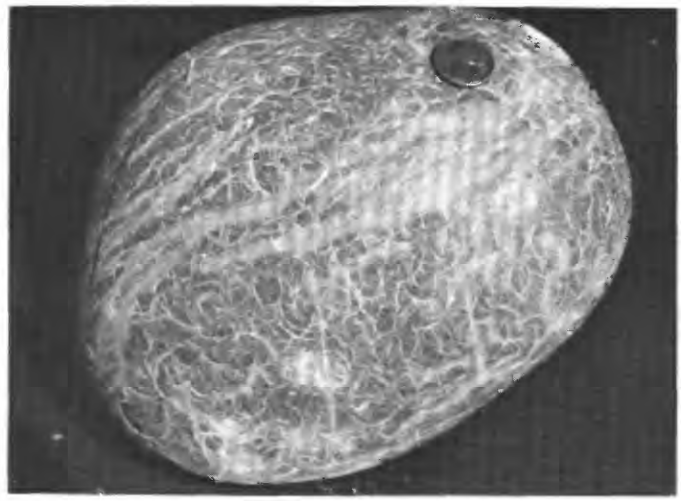

A

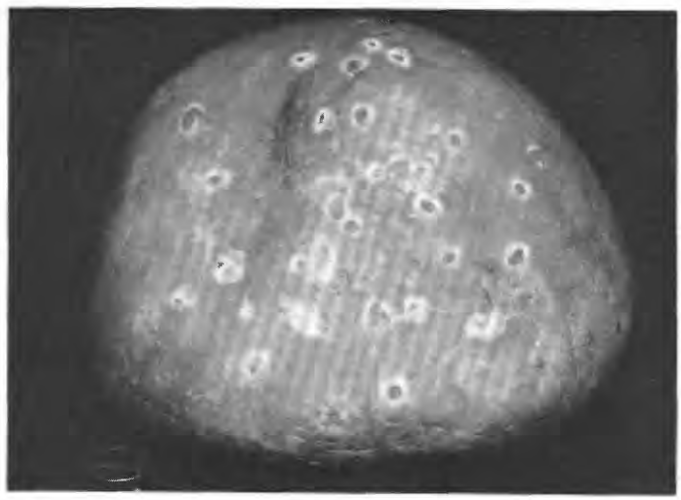

B

FIGURE 8. — Surface markings on quartzite roundstones. *A*, Crescentic percussion marks; *B*, pressure marks.

Statistical analysis of the pebble-count data supports the differentiation of the conglomerates into regional facies rather than stratigraphic units. Tests (Freund, 1960, p. 260–271) were made for differences in roundstone lithology between the northern and southern facies (table 3); they were not made for the western facies because of insufficient data. These tests show that:

1. The percentage of quartzite is significantly greater in the northern facies than in the southern facies.
2. The percentage of other sedimentary rocks is possibly greater in the southern facies than in the northern facies.
3. The percentage of total volcanic roundstones is significantly greater in the southern facies than in the northern facies.

In the northern facies, where the Pinyon directly overlies the Harebell, tests showed no significant differences between roundstone lithology in the Harebell Formation and that in the Pinyon Conglomerate (table 3). An additional qualitative test is provided by the abundance of welded-tuff roundstones, which were found to be sparse in both the Harebell and the Pinyon.

PETROGRAPHY OF ROUNDSTONES

Quartzite roundstones from each conglomerate facies were studied in thin section and freshly broken hand specimens. Each facies contains quartzite roundstones with a similar range of colors, microscopic textures, and feldspar contents (fig. 11). Predominant colors observed are white, gray, green, pink, red, brown, and black. Quartzite microtextures include detrital, solution, and metamorphic (based on the presence of metamorphic micas). Feldspar contents range from 0 to 20 percent or more by visual estimation; both orthoquartzites (fig. 12*A* and *B*) and feldspathic quartzites (fig. 12*C* and *D*) are common.

Surfaces of freshly broken orthoquartzite roundstones are commonly vitreous and may be any color mentioned in the preceding paragraph. Well-rounded undulose quartz with abundant quartz overgrowths or quartz cement forms the most common detrital microtexture (fig. 12*A*). Some orthoquartzites also contain interstitial sericite or scattered clots of carbonate; others show conspicuous solution textures, including extensive suturing, annealing, and recrystallization of grain margins. Surfaces of freshly broken subfeldspathic and feldspathic quartzite roundstones are commonly either dull or vitreous and also may be any color mentioned previously. Many feldspathic quartzites, however, are pink or red. Angular grains of plagioclase, micro-

TABLE 2. — *Composition (in percent) of roundstones counted in the western facies (Pinyon Conglomerate), the northern facies (Harebell Formation and Pinyon Conglomerate), and the southern facies (Pinyon Conglomerate)*

[Stations located in fig. 2; 100 roundstones were identified at each station. $\bar{x}$, arithmetic mean; s, standard deviation; s^2, variance; Tr., trace. Leaders (.....) indicate not present]

Station No.	Quartzite	Sedimentary rocks: Chert	Sandstone	Limestone	Shale	Total	Plutonic rocks[1]	Volcanic rocks: Welded tuff	Porphyritic rocks	Total
Western facies (Pinyon Conglomerate)										
53	76	2	15	3	1	21	3	Tr.	....	Tr.
54	77	1	13	1	3	18	3	....	2	2
56	73	Tr.	22	Tr.	2	24	3	Tr.	....	Tr.
$\bar{x}$	75.33	1.00	16.67	1.33	2.00	21.00	3.00	Tr.	0.67	0.67
Northern facies (Harebell Formation)										
15	92	....	2	....	1	3	2	....	3	3
17	93	....	....	....	2	2	....	....	5	5
31	97	....	1	....	....	1	....	....	2	2
34	87	....	6	....	....	6	1	....	6	6
39	94	....	2	....	....	2	....	....	4	4
41	94	3	....	....	1	4	1	....	1	1
49	98	....	1	....	....	1	....	....	1	1
52	96	....	1	....	Tr.	1	....	....	3	3
57	93	....	2	Tr.	....	2	Tr.	....	5	5
59	97	....	....	....	....	....	....	Tr.	3	3
60	99	....	....	....	....	....	....	....	1	1
73	95	....	....	2	....	2	1	....	2	2
75	98	....	....	....	1	1	1	....	....	....
76	94	....	1	....	....	1	1	....	4	4
77	94	....	1	....	....	1	1	....	4	4
78	96	....	....	....	....	....	1	....	3	3
247A	95	....	1	....	1	2	....	....	3	3
247B	93	....	2	....	1	3	....	....	4	4
248	98	....	....	....	....	....	....	....	2	2
260	98	Tr.	....	....	....	Tr.	....	....	2	2
265	96	....	1	....	1	2	....	....	2	2
267	92	1	1	....	1	3	....	....	5	5
268A	97	1	1	....	....	2	1	....	Tr.	Tr.
268B	94	....	2	....	....	2	....	....	4	4
269	97	....	1	....	....	1	....	....	2	2
270A	94	....	1	....	....	1	....	....	5	5
270B	93	....	1	1	....	2	....	Tr.	5	5
271	98	....	....	....	....	....	....	....	2	2
274A	96	....	....	....	1	1	....	....	3	3
274B	98	....	1	....	....	1	....	....	1	1
275A	98	....	1	....	....	1	....	....	1	1
275B	95	....	....	....	....	....	....	....	5	5
277	99	....	....	....	....	....	....	....	1	1
$\bar{x}$	95.39	0.15	0.91	0.09	0.30	1.45	0.30	Tr.	2.85	2.85
s	2.59	....	1.16	....	.53	1.33	.63	....	1.64	1.64
s^2	6.68	....	1.34	....	.28	1.76	.28	....	2.70	2.70
Northern facies (Pinyon Conglomerate)										
38	88	....	2	....	1	3	....	....	9	9
40	96	....	....	Tr.	1	1	Tr.	....	3	3
44	95	....	1	....	....	1	1	....	3	3
47	96	....	2	....	....	2	....	....	2	2
48	98	....	1	Tr.	....	1	Tr.	....	1	1
50	96	....	....	Tr.	....	Tr.	....	1	3	4
256A	97	....	2	....	....	2	Tr.	....	1	1
256B	94	....	2	Tr.	....	2	....	Tr.	4	4
259A	93	....	2	....	....	2	....	....	5	5
259B	98	....	....	....	....	....	....	....	2	2
272A	94	1	2	....	....	3	1	....	2	2
272B	96	....	1	....	....	1	....	....	3	3
278	94	2	2	....	....	4	....	....	2	2
$\bar{x}$	95.00	0.23	1.31	Tr.	0.15	1.69	0.15	0.08	3.07	3.15
s	2.61	....	.85	....	....	1.18	....	....	2.10	2.12
s^2	6.83	....	.73	....	....	1.40	....	....	4.41	4.47
Southern facies (Pinyon Conglomerate)										
1	92	....	....	....	1	1	1	1	5	6
2	77	....	5	....	5	10	4	3	6	9
4	79	....	2	....	4	6	3	Tr.	12	12
9	86	....	1	....	....	1	1	2	10	12
10	86	....	1	....	5	6	1	Tr.	7	7
11	92	....	....	....	....	....	2	1	5	6
14	83	....	1	....	2	3	2	Tr.	12	12
21	90	....	1	....	1	2	....	Tr.	8	8
64	89	1	1	1	1	4	Tr.	Tr.	7	7
71	94	....	....	....	....	....	Tr.	1	5	6
72A	91	....	2	....	1	3	....	Tr.	6	6
72B	88	....	1	....	1	2	1	2	7	9
87	78	....	4	....	5	9	....	1	12	13
88	91	1	1	....	....	2	2	1	4	5
89	88	1	....	....	1	2	Tr.	1	9	10
90	93	....	....	....	....	....	....	1	6	7
92	92	....	....	....	Tr.	Tr.	1	3	4	7
95	91	Tr.	3	....	....	3	1	2	3	5
96	85	....	....	....	....	....	1	3	11	14
97	89	....	3	....	....	3	....	2	6	8
172	90	....	....	....	....	....	Tr.	1	9	10
173	88	....	....	1	....	1	Tr.	1	10	11
180	95	....	1	....	....	1	....	1	3	4
181	88	....	2	....	1	3	....	2	7	9
183A	90	....	1	....	3	4	....	Tr.	6	6
183B	91	....	2	....	....	2	2	1	4	5
185	91	....	1	....	1	2	....	2	5	7
189	84	....	1	....	....	1	....	2	13	15
191	93	....	2	1	....	3	Tr.	2	2	4
193A	95	....	....	1	1	2	....	2	1	3
193B	96	....	1	....	....	1	....	1	2	3
194	93	1	1	1	....	3	....	2	2	4
195	92	....	3	....	....	3	....	Tr.	5	5
203	92	....	2	....	1	3	....	1	4	5
204	89	....	1	....	1	2	Tr.	2	7	9
206	91	1	2	....	....	3	Tr.	2	4	6
210A	89	....	1	1	....	2	1	2	6	8
210B	85	....	....	....	1	1	1	2	11	13
212	92	....	....	....	1	1	....	Tr.	7	7
213	95	....	....	....	1	1	....	Tr.	4	4
214A	96	....	1	....	1	2	....	1	1	2
214B	91	1	2	....	....	3	....	1	5	6
215A	94	....	....	....	....	....	....	Tr.	6	6
215B	94	....	2	....	....	2	....	2	2	4
219	93	....	....	1	1	2	....	3	2	5
222A	84	....	5	....	4	9	1	2	4	6
222B	89	....	2	....	1	3	1	1	6	7
223A	89	....	1	....	....	1	Tr.	1	9	10
223B	89	1	....	....	....	1	1	4	5	9
$\bar{x}$	89.63	0.14	1.22	0.14	0.92	2.43	0.55	1.33	6.06	7.39
s	4.37	....	1.26	....	1.41	2.25	.89	.99	3.09	3.07
s^2	19.07	....	1.59	....	1.99	5.08	.79	.97	9.56	9.45

[1]Plutonic refers to granitic and gneissic rocks and their relatives, except for stations 41 and 272A, where diabase was recorded.

TABLE 3. — *Student's t tests for significant differences in roundstone lithology between the northern and southern facies and between the Harebell Formation and Pinyon Conglomerate within the northern facies*

[$\bar{x}$, arithmetic mean; s^2, variance. Mean and variance are in percent. Numbers in parentheses are number of counts]

Roundstone lithology	Northern and southern facies: Northern facies (46) $\bar{x}$	Northern facies (46) s^2	Southern facies (49) $\bar{x}$	Southern facies (49) s^2	Student's t value	Significance	Harebell and Pinyon within the northern facies: Harebell (33) $\bar{x}$	Harebell (33) s^2	Pinyon (13) $\bar{x}$	Pinyon (13) s^2	Student's t value	Significance
Quartzite	95.28	6.61	89.63	19.07	7.74	0.01	95.39	6.68	95.00	6.83	0.01	None
Soft sedimentary rock	1.52	1.63	2.43	5.08	2.44	.10	1.45	1.76	1.69	1.40	.55	None
Volcanic rock	2.93	3.13	7.39	9.45	8.73	.01	2.85	2.70	3.15	4.47	.51	None

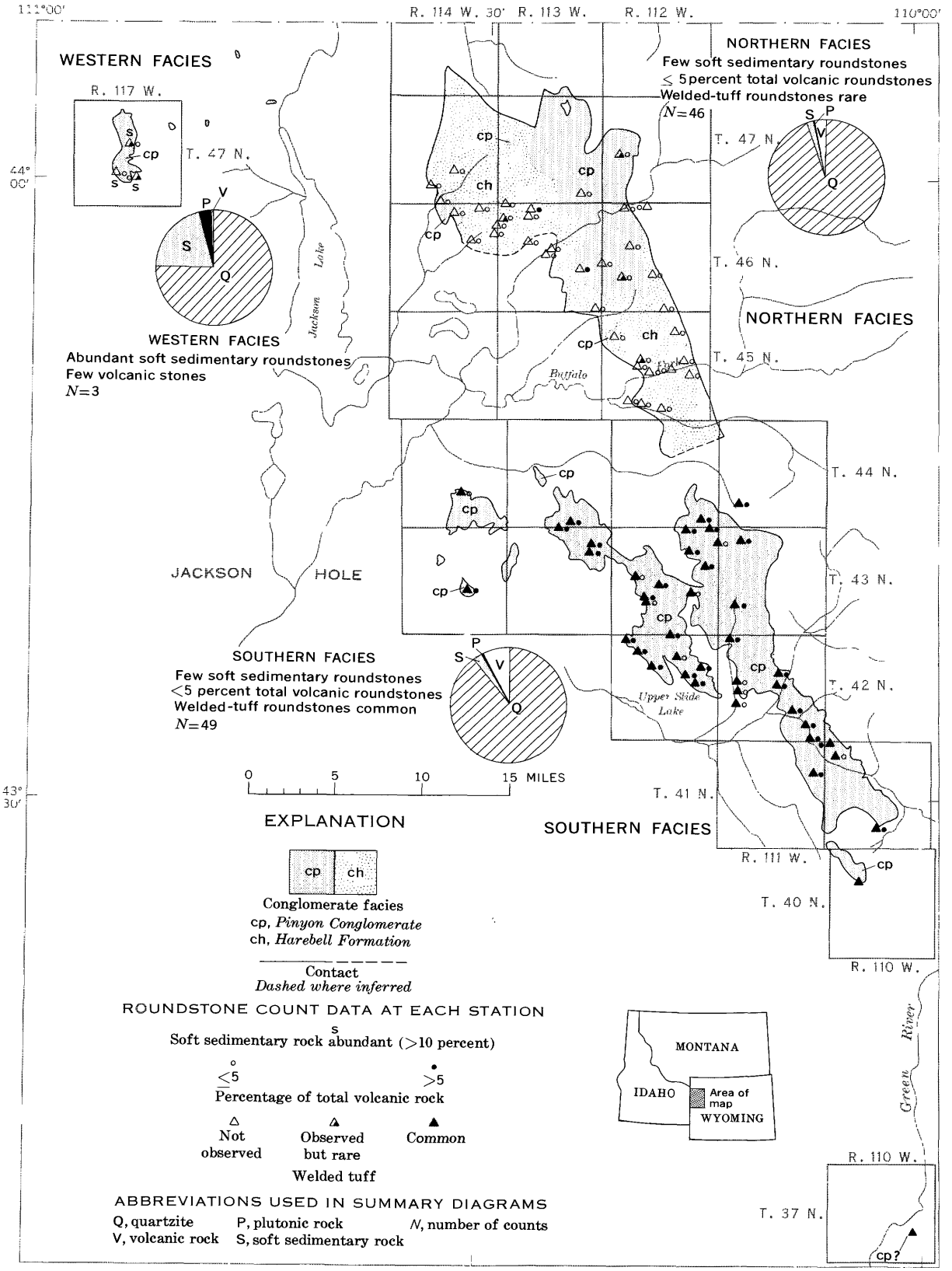

FIGURE 9. — Classification of the conglomerates of the Harebell Formation and the Pinyon Conglomerate into three lithofacies according to proportions of minor roundstone types present.

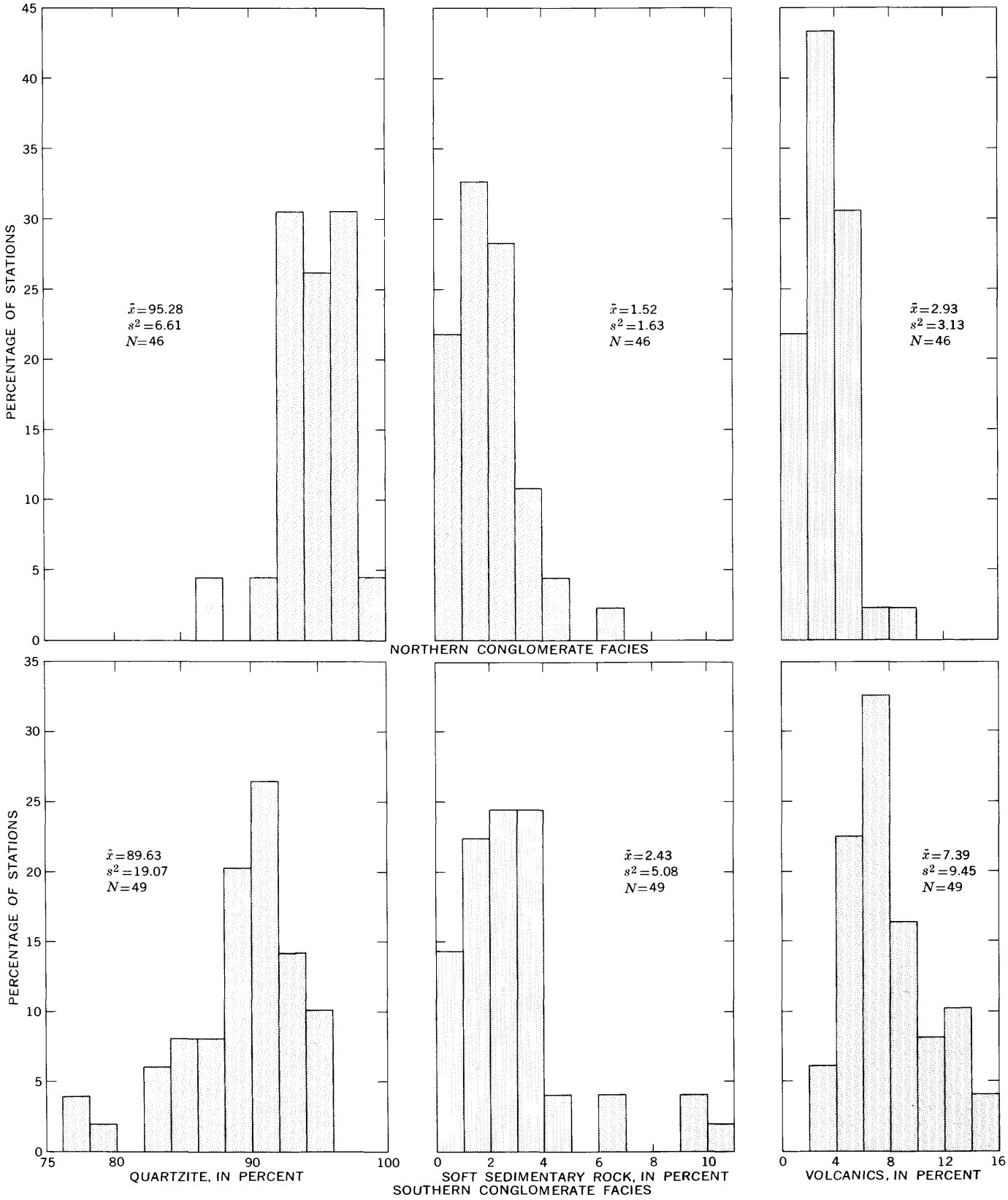

FIGURE 10. — Frequency distributions of quartzite, soft sedimentary rock, and volcanic roundstones in the northern and southern conglomerate facies. Frequencies are based on counts of 100 roundstones each as recorded in table 2. $\bar{x}$, arithmetic mean; s^2, variance; N, number of counts.

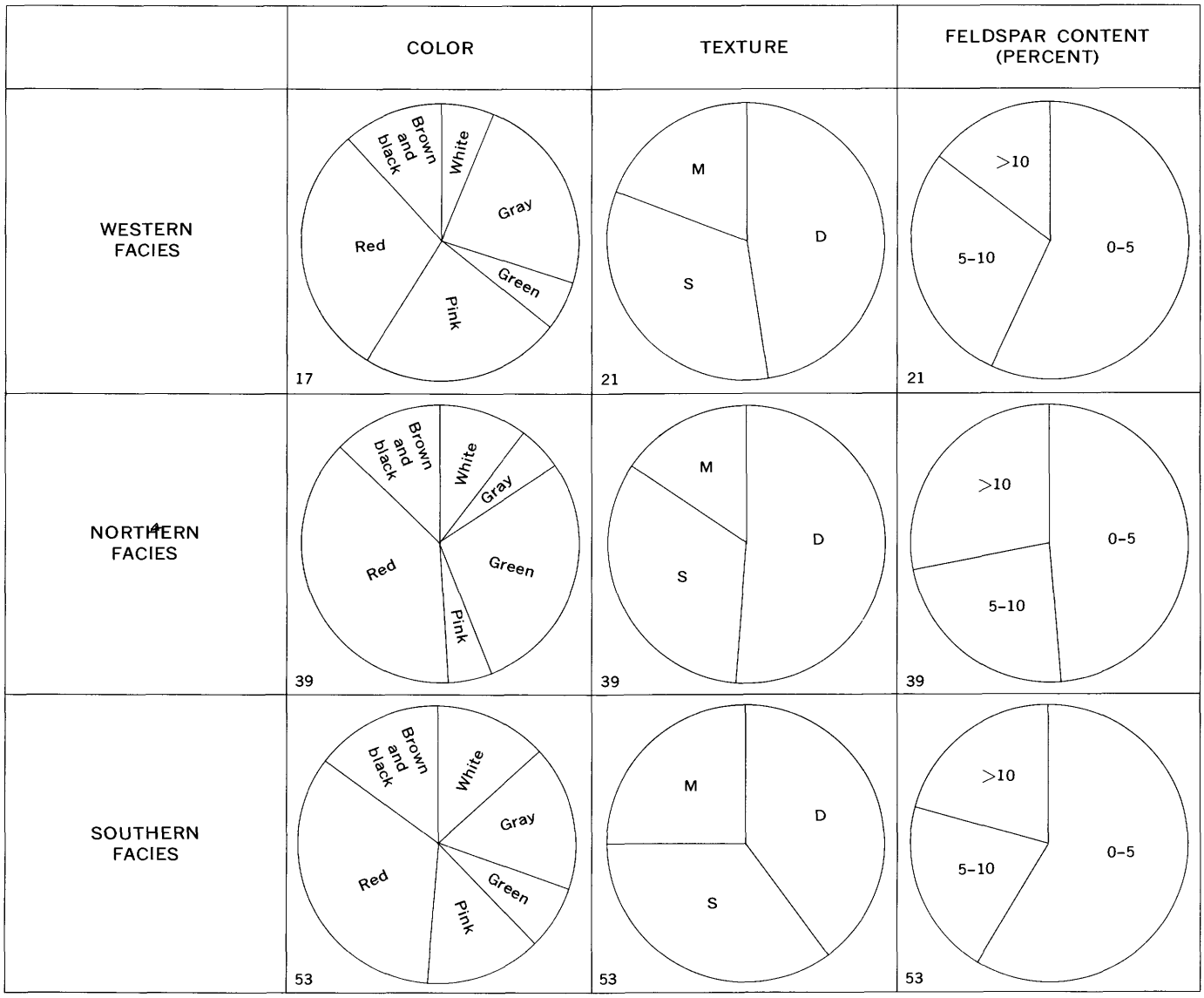

FIGURE 11. — Summary of color, texture, and feldspar content of quartzite roundstones from conglomerates in the western facies (two stations), the northern facies (five stations), and the southern facies (three stations). Number in lower left corner of each block is the number of specimens examined. Texture: D, detrital; S, solution; M, metamorphic.

cline, and detrital muscovite are common to abundant as seen under the microscope (fig. 12*C*), and many feldspathic quartzites are fine grained (fig. 12*D*). Solution textures and sericitic or chloritic matrix are common. A metamorphic origin is indicated for those orthoquartzites and feldspathic quartzites which exhibit a tectonic fabric or contain xenoblastic mica (fig. 12*B* and *D*), most commonly fine-grained biotite.

In hand specimen and thin section, most of the quartzite roundstones do not show unique characteristics that might aid in assigning them to a definite stratigraphic source. A few roundstones of chert and jasper pebble conglomerates do occur, and the jasper pebble conglomerates might be referred to similar rocks interbedded with quartzites of uncertain age in the Bayhorse region of central Idaho (W. H. Hays, oral commun., 1971). The quartzite roundstones are similar, however, to the following four broad groups of pre-Cretaceous quartzites found north and west of northwestern Wyoming: (1) Paleozoic Flathead, Kinnikinic, Swan Peak, and Quadrant Quartzites, (2) Precambrian and Cambrian quartzites, (3) quartzites of the Precambrian Belt Supergroup, and (4) pre-Belt quartzites.

The Cambrian Flathead Quartzite contains thin, discontinuous arkosic lenses at the base, but most of it is pink, tan, and gray quartz sandstone and orthoquartzite (Hanson, 1952; Miller, 1936; Parkinson, 1958). Probably more significant as a possible

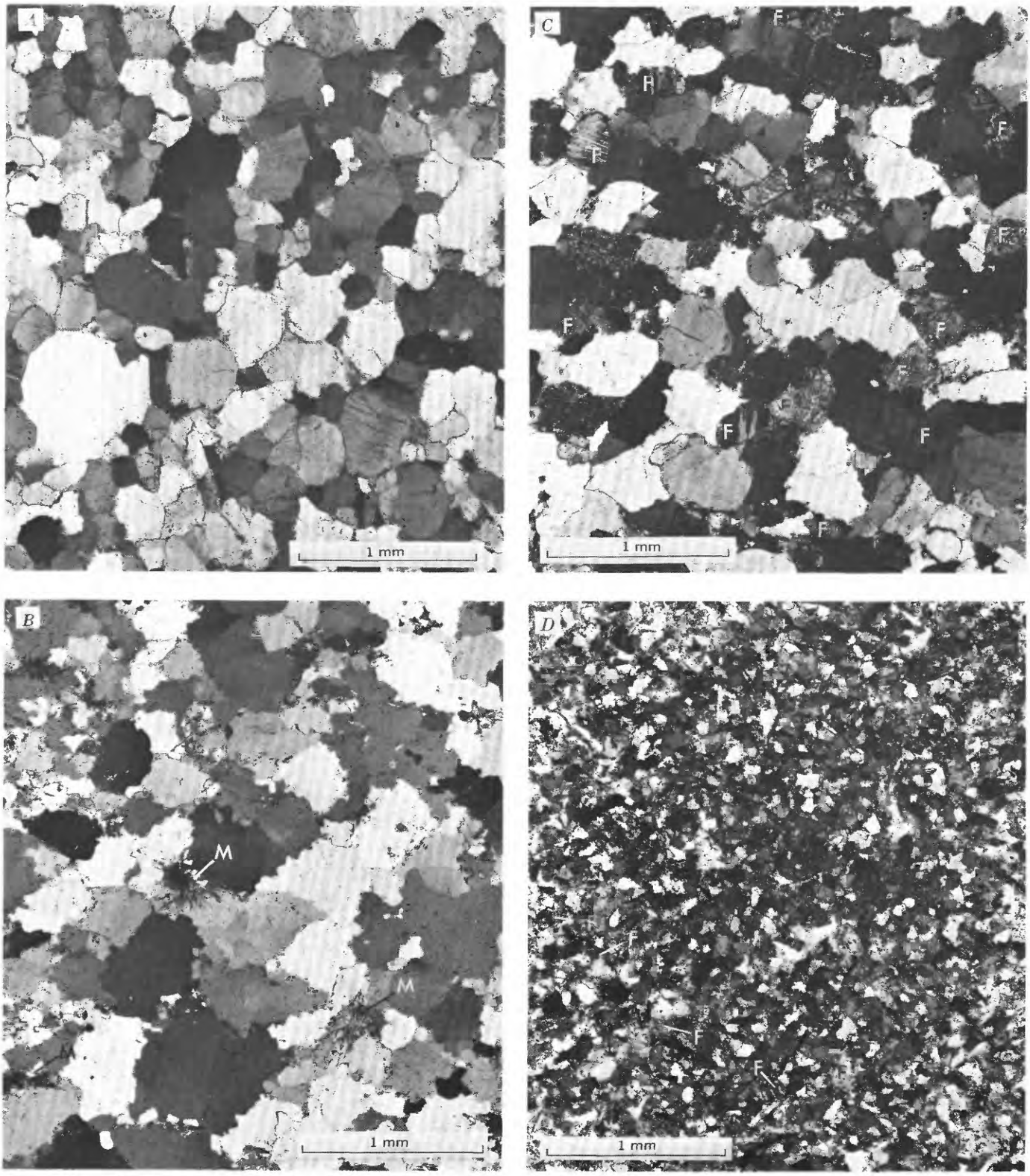

FIGURE 12. — Photomicrographs of the principal types of texture and mineralogy exhibited by the quartzite roundstones. *A*, Orthoquartzite with many detrital grain outlines and quartz cement. *B*, Metaquartzite consisting mostly of quartz grains with sutured and partially recrystallized grain contacts and scattered xenoblastic muscovite. *C*, Quartzite with as much as 20 percent feldspar; indented solution contacts between grains. *D*, Fine-grained feldspathic (10–20 percent) metaquartzite with detrital muscovite flakes and xenoblastic biotite. All samples are from the northern facies: *A* and *B* are from the Harebell Formation on Whetstone Mountain (sta. 34); *C* and *D* are from the Pinyon Conglomerate (sta. 48). Crossed nicols. M, muscovite; F, feldspar.

479-609 O - 72 - 5

source of the quartzite roundstones is the more than 1,000 feet of Ordovician quartzites known to extend over a wide area of Idaho and northern Utah (Ketner, 1966, 1968). These include the Kinnikinic Quartzite of Idaho, typically a light-gray to white quartz-cemented orthoquartzite (Hobbs and others, 1968), and the Swan Peak Quartzite of southeastern Idaho and northern Utah, which also contains much light-colored orthoquartzite (Vandorston, 1970). The Pennsylvanian Quadrant Quartzite also contains gray quartz sandstone and orthoquartzite. Many of the orthoquartzite roundstones in the Harebell and Pinyon conglomerates, including the large quartzite boulder north of the Teton Range (fig. 6), resemble the Paleozoic quartzites.

The Precambrian and Cambrian quartzites include the Precambrian and Cambrian Brigham Quartzite, the Precambrian Mutual Formation, and additional Precambrian quartzites below the Mutual in the region around Pocatello, southwest of Blackfoot, Idaho (Crittenden and others, 1971). Samples of the Brigham that I examined are light-gray orthoquartzites, but the Mutual Formation consists of much red feldspathic quartzite, some of it coarse grained to conglomeratic. Low-grade metamorphism was comparable to that in the conglomerate roundstones, being marked generally by development of abundant sericite.

The Precambrian quartzites of the Belt Supergroup of the Lemhi Range in Idaho include the Lemhi and Swauger Quartzites (Ross, 1947). Those that I examined display a wide range of colors and feldspar contents and a low grade of metamorphism comparable to that found in many roundstones from the Harebell and Pinyon conglomerates. Many contain abundant feldspar and metamorphic muscovite (Ross, 1947). Also, some quartzites in the LaHood Formation of the Belt Supergroup in southwestern Montana are feldspathic and may resemble the roundstones in the Harebell and Pinyon (McMannis, 1963).

The pre-Belt quartzites consist of the quartzites in the Cherry Creek Group and perhaps other unnamed metaquartzites from the pre-Belt terrane west of Yellowstone National Park. These quartzites are gray, green, or white; they show evidence of intense deformation; and they may contain high-grade metamorphic minerals (Reid, 1957, p. 5; Heinrich and Rabbitt, 1960, p. 5; Heinrich, 1960, p. 22). Only a few quartzite roundstones found in the Harebell and Pinyon resemble the pre-Belt quartzites.

A collection of 43 roundstones of soft sedimentary rocks was also studied in thin section. Many of these were collected from the Pinyon Conglomerate at the north end of the Teton Range (sta. 53, 54, and 56) and at Mount Randolph (sta. 62). The roundstones examined consisted of limestone, sandstone, phosphatic shale and siltstone, and chert, in decreasing order of abundance. Among the limestones, skeletal (fig. 13*A*) and oolitic limestones are the most common, but intraclastic limestone, micrite, and dismicrite are also present. Fragments of bryozoans, bivalves, crinoid stems, corals, and foraminifers are abundant in the skeletal limestones. In general, the petrography of the limestones resembles that of samples collected from the Mississippian Madison Limestone at the north end of the Teton Range. Some of the sandstones are phosphatic (fig. 13*B*), but many others are quartzitic, subfeldspathic, and chert bearing, with quartz or calcite cement. Most of the siltstones and shales examined are also phosphatic, and like the phosphatic sandstones, they resemble similar rocks in the Permian Phosphoria Formation. Chert roundstones are commonly derived from silicified limestone; some contain relict fossils.

Twenty-seven roundstones of plutonic rocks from widely separated localities were studied by means of thin sections and hydrofluoric acid-etched, cobaltinitrite-stained slices. The rocks fall into three textural categories: hypidiomorphic-granular igneous rocks (19), gneisses (five), and diabases (three). The hypidiomorphic-granular rocks range from granite to granodiorite, with biotite being the most common mafic mineral. Euhedral phenocrysts of both potassium feldspar and plagioclase are common, as are graphic intergrowths of quartz and feldspar (fig. 13*C*). An unusual feature seen in one pebble is the intrusive contact between grandodiorite and quartzite (fig. 13*D*). The gneissic roundstones consist of quartz-, feldspar-, and biotite-rich layers, and the diabases show typical subophitic textures of abundant plagioclase laths set in a mosaic of mafic minerals. Evidently most of the plutonic rocks were derived from small igneous plutons, some of which intruded the quartzite source terrane.

Two hundred and six roundstones of volcanic rock were studied by means of hydrofluoric acid-etched, cobaltinitrite-stained slices and thin sections. A wide variety of rock types were identified: porphyritic rhyolite, rhyodacite, dacite, trachyte, trachyandesite, and dacite as well as welded tuffs and volcanic breccias (table 4). In general the volcanic roundstones fall into four broad groups: (a) porphyritic with modal quartz (fig. 14*A*), (b) porphyritic with no modal quartz (fig. 14*B*), (c) welded tuffs (figs. 14*C* and *D*), and (d) breccias and miscellaneous lithologies.

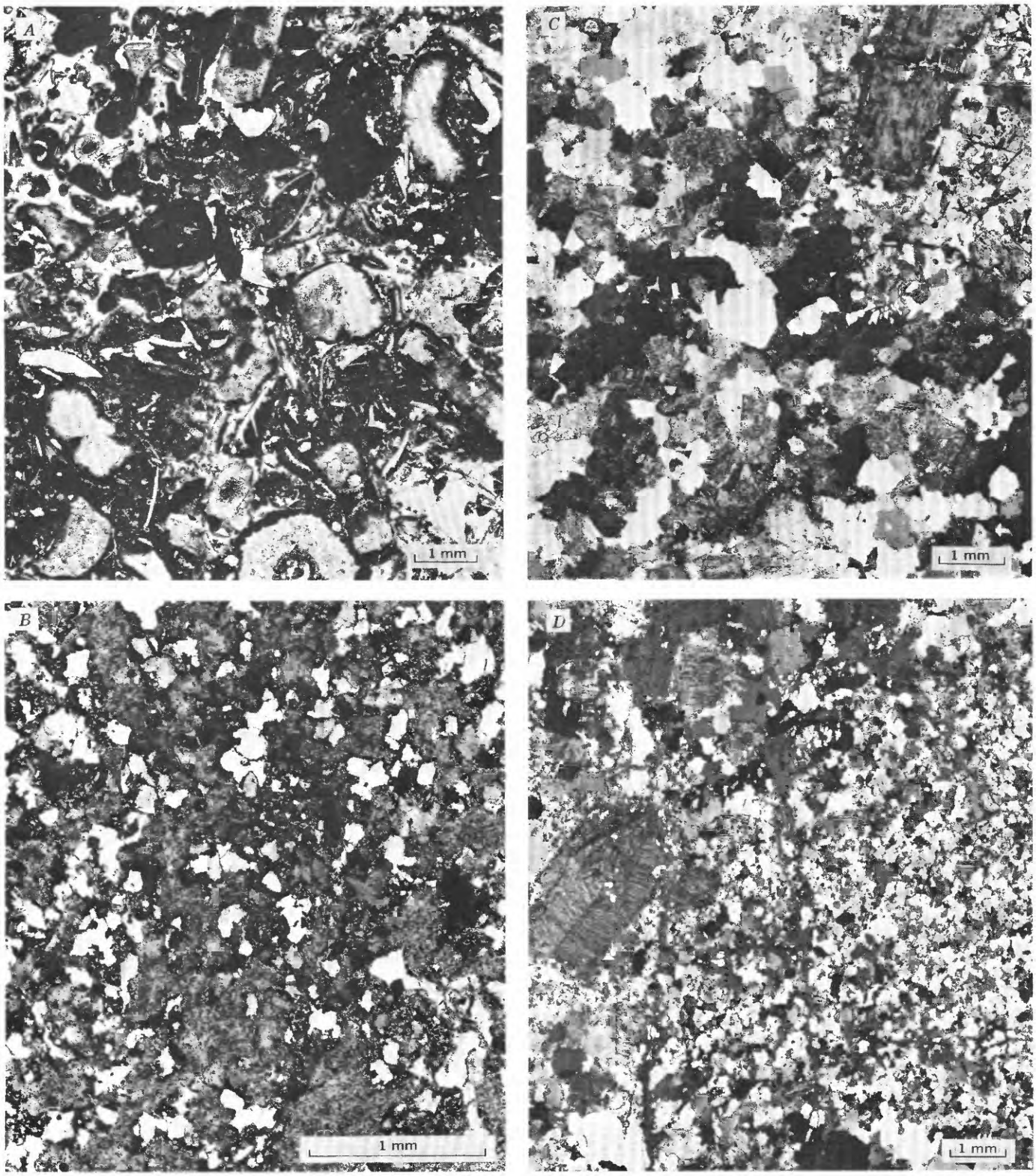

FIGURE 13. — Photomicrographs of roundstones derived from sedimentary (*A* and *B*) and plutonic (*C* and *D*) rocks. *A*, Skeletal limestone containing Paleozoic fossils; plain light. *B*, Phosphatic sandstone; plain light. *C*, Granite with hypidiomorphic and myrmekitic textures; crossed nicols. *D*, Granodiorite intrusive contact with quartzite; crossed nicols. *A* and *C* are from the northern facies (Pinyon Conglomerate) on Mount Randolph (sta. 62); *B* is from the western facies (Pinyon Conglomerate, sta. 56); and *D* is from the northern facies (Harebell Formation) on Whetstone Mountain (sta. 34).

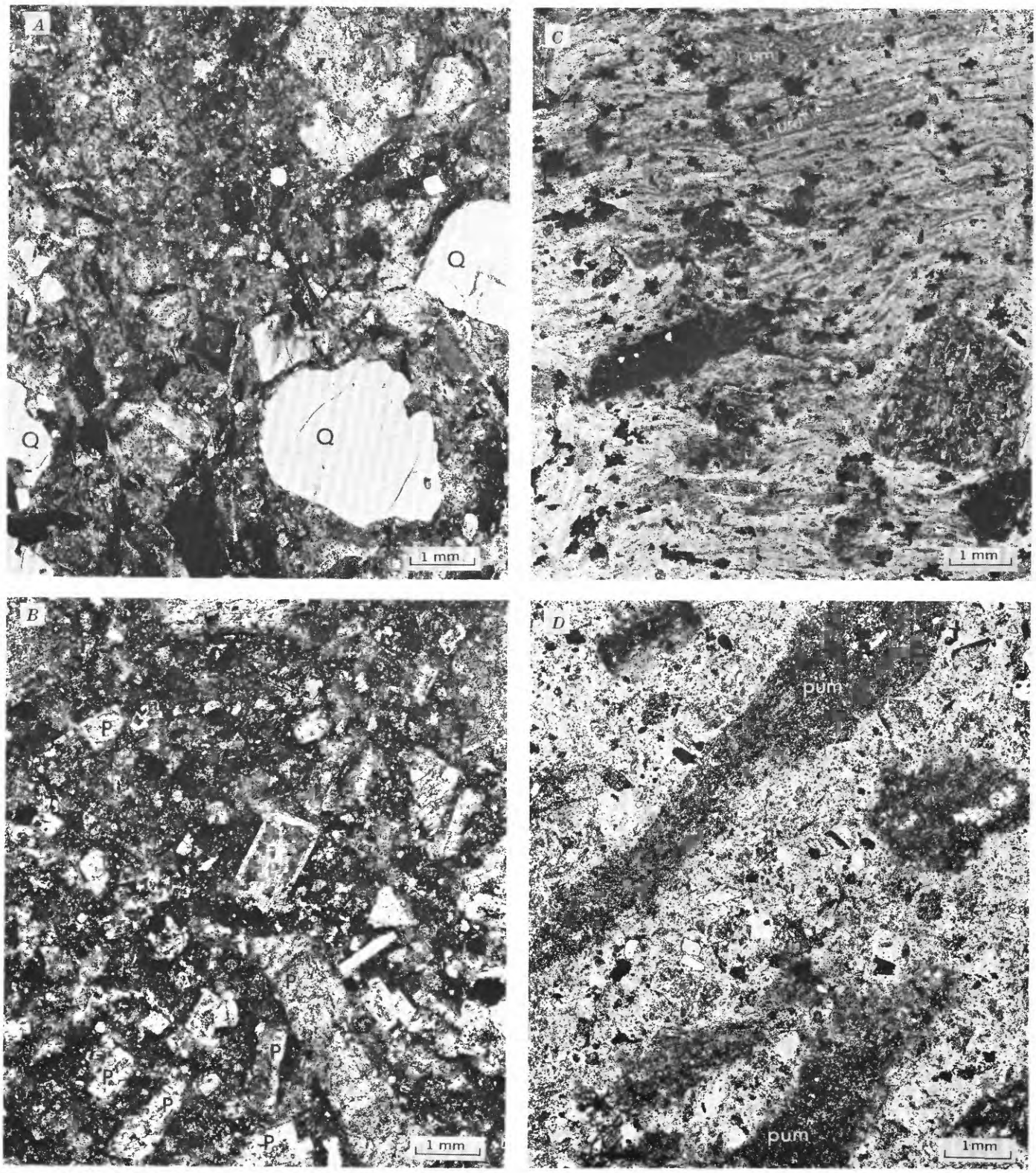

FIGURE 14. — Photomicrographs of typical volcanic roundstones. *A*, Porphyritic dacite with typical partially resorbed quartz phenocryst; crossed nicols. *B*, Porphyritic andesite with abundant zoned plagioclase phenocrysts; crossed nicols. *C*, Welded tuff with feldspar crystals, flattened pumice fragments, and flattened devitrified shards, which are typical in the southern conglomerate facies; plain light. *D*, Welded tuff with large uncollapsed pumice fragments; plain light. *A* is from the northern facies (Pinyon Conglomerate, sta. 40); *B*, *C*, and *D* are from the southern facies (Pinyon Conglomerate, sta. 71). Q, quartz; P, plagioclase; pum, pumice.

The sample of volcanic roundstones was not randomly selected and is only roughly indicative of the proportions of each rock type present. The 5 percent welded tuff recorded in table 4 represents every roundstone of this lithology that I saw in the northern facies, and roundstone counts indicate that the proportion of welded tuff is much less. Table 4 does suggest a predominance of porphyritic rocks with modal quartz over those with no modal quartz in roundstones of the northern facies and the reverse relationship in the southern facies.

TABLE 4. — *Proportions of volcanic rock types among roundstones from the northern and southern conglomerate facies*

[Based on identifications of HF-etched, cobaltinitrite-stained slices. Figures do not total to 100 percent because of rounding. Numbers in parentheses are number of specimens]

Rock type	Potassium feldspar (fraction of total feldspar)	Percent of rock type in conglomerate facies	
		Northern facies (79)	Southern facies (127)
Porphyritic volcanics with modal quartz ≥1 percent			
Rhyolite	>⅔	6	2
Rhyodacite	⅓–⅔	15	11
Rhyodacite?	[1]<⅓	46	9
Dacite	[2]<⅓	5	5
Total		72	27
Porphyritic volcanics with modal quartz <1 percent			
Trachyte	>⅔	1	2
Trachyandesite	⅓–⅔	1	8
Trachyandesite?	[1]<⅓	15	21
Andesite	[2]<⅓	1	13
Total		18	44
Welded tuffs		5	26
Volcanic breccias and miscellaneous lithologies		4	4

[1]Abundant potassium feldspar in matrix.
[2]No potassium feldspar in matrix.

Roundstones of quartz-bearing porphyritic volcanics contain 1–10 percent euhedral phenocrysts of quartz which show varying degrees of resorption. Rapid rock analyses of five such roundstones show ranges of 62–68 percent SiO_2, 15–16 percent Al_2O_3, and 5–6 percent Na_2O+K_2O (table 5), values which compare closely with those for dacites and rhyodacites (Nockolds, 1954, table 2). Fresh to altered phenocrysts of plagioclase and potassium feldspar are commonly abundant and may comprise as much as 40 percent of the rock. Plagioclase is almost everywhere zoned and may range up to An_{50}. Potassium feldspar occurs mostly as euhedral phenocrysts but also as rims on plagioclase and in micrographic intergrowths with quartz. Stained slices also suggest fine-grained potassium feldspar in the groundmass. Mafic phenocrysts, which commonly do not exceed a few percent of the rock, consist of pyroxene, amphiboles, and biotite. Opaque oxidation rims commonly accompany mafic phenocrysts, and chlorite, calcite, and apatite may replace the phenocrysts. The groundmass is typically altered to microcrystalline quartz, chlorite, clay(?) minerals, and disseminated iron oxides, although relict feldspar microlites can be seen in a few thin sections. In addition to the phenocryst and groundmass constituents, angular fragments of quartzite, sandstone, and other volcanics are commonly contained within roundstones

TABLE 5. — *Rapid rock analyses (in percent) of volcanic roundstones from conglomerates of the Harebell Formation and the Pinyon Conglomerate*

[Analysts: Leonard Shapiro, P. L. D. Elmore, G. W. Chloe, J. A. Kelsey, S. D. Botts, H. Smith, and Lowell Artis]

	Porphyritic volcanics with modal quartz					Porphyritic volcanics with no modal quartz			Welded tuffs		
Sample No.	1	2	3	4	5	6	7	8	9	10	11
SiO_2	64.1	62.4	64.4	64.9	68.0	61.2	61.2	62.0	62.4	69.6	69.5
Al_2O_3	15.4	16.3	15.8	15.6	14.5	16.2	16.0	16.3	15.5	15.7	14.6
Fe_2O_3	3.3	2.5	1.5	3.1	2.1	3.2	1.2	2.9	1.9	1.0	1.5
FeO	2.9	3.1	3.4	2.3	2.2	2.7	4.7	3.6	4.0	.96	1.6
MgO	1.9	2.0	2.1	2.0	1.7	2.0	2.2	2.2	1.8	.46	.83
CaO	1.3	3.3	2.0	2.7	2.2	3.3	3.2	2.9	2.8	1.6	1.5
Na_2O	2.1	3.0	3.3	2.4	2.7	2.1	2.3	2.0	2.6	3.2	3.4
K_2O	3.9	3.2	2.7	2.5	3.2	3.1	2.7	2.3	3.2	5.5	5.1
H_2O-	1.7	.47	1.3	.95	1.0	.94	1.4	1.1	.73	.25	.24
H_2O+	2.6	1.8	2.3	2.0	1.9	2.4	3.2	2.8	2.7	1.0	1.0
TiO_2	.61	.60	.77	.60	.46	.75	.61	.65	.78	.44	.52
P_2O_5	.21	.20	.26	.21	.12	.26	.26	.24	.39	.10	.12
MnO	.05	.10	.06	.12	.05	.11	.13	.13	.11	.08	.05
CO_2	<.05	.95	.09	.18	<.05	1.1	.70	.94	.78	.05	<.05
Sum	100	100	100	100	100	99	100	100	100	100	100

SAMPLE DESCRIPTIONS

Sample No.	Field No.	At or near station No.	Description
Northern facies (Harebell Formation)			
1	H–15–C2	15	Porphyritic rhyodacite.
2	H–15–C4	15	Porphyritic rhyodacite(?).
3	H–39–C2	39	Porphyritic rhyodacite.
Northern facies (Pinyon Conglomerate)			
4	P–47–C2	46	Porphyritic rhyodacite(?).
5	P–50–C2	50	Porphyritic rhyodacite.
Southern facies (Pinyon Conglomerate)			
6	P–71–C12	71	Porphyritic andesite.
7	FF–SF–CC–17	183	Porphyritic trachyandesite.
8	FF–SF–CC–26	183	Porphyritic andesite.
9	P–71–C3	71	Dacitic welded tuff.
10	P–71–C13	71	Rhyolitic welded tuff.
11	FF–SF–CC–28	183	Do.

of quartz-bearing volcanic rock. The presence of quartzite fragments similar to the quartzite roundstones of the conglomerates is significant in that it suggests a common source for roundstones of both quartz-bearing porphyritic volcanics and quartzite.

Except for the sparsity of quartz phenocrysts, roundstones of porphyritic rock with no modal quartz are petrographically similar to those with modal quartz. Rapid rock analyses of three such roundstones show them to contain 61–62 percent SiO_2, slightly more than 16 percent Al_2O_3, and 4–5 percent Na_2O+K_2O (table 5), also comparable to dacite (Nockolds, 1954, table 2). Petrographic study of thin sections and stained slices, however, results in classification of most of these rocks as andesite or trachyandesite (table 4). Although chemical evidence suggests that these rocks may be characterized as dacites, I will refer to them by their petrographic designation, andesite, to distinguish them from the porphyritic rocks with modal quartz previously described as dacites. Petrographic and chemical affinities suggest that both the dacitic and andesitic roundstones were derived from the same volcanic terrane; however, the general absence of quartzite fragments in the andesites suggests derivation from different sources.

Most of the welded-tuff roundstones are marked by numerous conspicuous dark pumice fragments; commonly the pumice fragments are collapsed and drawn out to form a pronounced compaction layering that gives the rock a distinctive striped appearance. In a few stones, equant angular pumice fragments retain their original form. Under the microscope, many stones are seen to contain numerous relict shards: hook- and spicule-shaped structures which commonly show deformation and flattening so that they conform to the plane of compaction layering. The shard interiors are now filled with quartz and feldspar devitrification products; no trace of glassy material was seen. A few highly altered plagioclase euhedrons commonly occur in the welded tuffs, and quartz euhedrons occur more rarely. Sparse mafic phenocrysts consist of light-green augite, brown and light-green amphiboles, and sparse pleochroic light-brown to deep-blue amphibole (riebeckite?). Many mafic phenocrysts are entirely replaced by chlorite, iron oxides, and apatite. The matrix of the welded tuff is generally a highly altered mass of microcrystalline quartz, chlorite, and iron oxides, with scattered veinlets and patches of calcite. Cobaltinitrite staining also reveals abundant potassium in the matrix. Rapid rock analyses of three stones showed widely varying SiO_2 contents — from about 62.5 to nearly 70 percent (table 5).

The petrography and chemistry of the volcanic roundstones is broadly indicative of two possible sources: (1) the Upper Cretaceous Elkhorn Mountains Volcanics and Livingston Group for volcanic rocks that contain no modal quartz (andesitic rocks) and for welded tuffs, and (2) an unknown source for volcanic rocks that contain modal quartz (dacitic rocks).

The porphyritic roundstones that contain no modal quartz are petrographically similar to the widespread andesitic rocks of the Elkhorn Mountains Volcanics described by Klepper, Weeks, and Ruppel (1957) and by H. F. Barnett (in Robinson, 1963). Chemical analyses of two "typical andesites" from the Elkhorn Mountains Volcanics (Robinson, 1963, table 9) are comparable to those obtained for andesitic roundstones from the Harebell and Pinyon (table 5). The welded-tuff roundstones are petrographically similar to the abundant welded tuffs found in the middle member of the Elkhorn Mountains Volcanics. Chemical analyses of welded tuffs in the Elkhorn Mountains Volcanics (Robinson, 1963, table 9; Smedes, 1966, table 2) show them to range in composition from rhyodacitic to rhyolitic, a range comparable to that obtained from analyses of three welded-tuff roundstones from the conglomerates of Jackson Hole (table 5). Andesite and welded tuff detritus probably derived from the Elkhorn Mountains Volcanics is also found in the Livingston Group volcaniclastic sediments (Roberts, 1963). In contrast, rhyodacites and dacites comparable to the quartz-bearing porphyritic roundstones found in the conglomerates are not known to be abundant in the Elkhorn Mountains Volcanics (Klepper and others, 1957). Hence, a second, unknown source must be postulated for the abundant quartz-bearing porphyritic roundstones found in the conglomerates.

PETROGRAPHY OF MATRIX

The matrix of the conglomerates, as seen in thin section, consists of poorly rounded, moderately well sorted sand grains set in either a calcite cement or a fine-grained argillic matrix. The grains consist of abundant quartz, feldspar, altered rock fragments, and chert, in addition to lesser amounts of quartzite, mica, and heavy minerals (table 6; fig. 15). Most of the clastic constituents, as shown by a triangular plot of 36 samples (fig. 16*A*), fall within the subfeldspathic lithic field of the Williams, Turner, and Gilbert (1954, p. 292–293) sandstone classification. A plot of grains, cement, and matrix (<0.02 mm) reveals two distinct rock types: calcite-cemented arenites and matrix-bound wackes (fig. 16*B*).

TABLE 6. — *Modal composition (in percent) of the sandstone matrix of conglomerates of the northern facies (Harebell Formation and Pinyon Conglomerate) and the southern facies (Pinyon Conglomerate)*

[300 points counted per slide. Middle of field number corresponds to station number in fig. 2. Leaders (.....) indicate not present]

Field No.	Quartz	K-feldspar	Plagioclase	Altered fragments	Chert	Quartzite	Muscovite	Biotite	Fine-grained altered matrix	Calcite cement	Heavy minerals
Northern facies (Harebell Formation and Pinyon Conglomerate)											
H–31–h1	29.4	6.3	2.3	15.0	5.0	1.3	....	0.7	1.7	38.0	0.3
31–t/h	42.3	6.0	.3	18.7	4.3	1.7	0.3	1.0	23.0	2.3	....
34–h2	31.0	3.0	1.7	11.3	2.0	4.0	.3	.7	45.3	.3	.3
35–h/t	50.0	4.7	2.0	4.7	2.7	.7	....	.7	25.6	9.0	....
37–h1	45.6	1.7	3.3	12.3	6.7	2.7	.3	.7	25.0	11.7	....
37–h2	34.0	2.0	2.7	9.7	1.7	1.7	.3	.3	.3	47.3	....
P–38–t/h	38.6	5.7	2.0	13.0	6.3	2.0	.3	1.7	27.7	2.7	....
H–39–t1	43.0	6.7	5.0	7.0	.7	....	.3	2.7	34.7	.....	....
39–t2	39.0	6.7	5.3	14.7	7.0	1.0	.3	2.0	24.0	.....	....
P–40–h2	21.0	5.0	1.3	10.7	1.0	1.3	1.0	....	1.3	57.0	.3
44–h	32.4	5.3	3.0	11.0	4.0	1.0	.3	.3	2.0	40.3	.3
44–h2	39.7	5.0	3.0	6.3	4.3	....	.3	2.0	32.0	6.3	1.0
47–h	29.4	5.3	5.0	6.7	2.7	1.3	.3	1.3	3.7	42.7	1.7
48–h	40.0	4.0	3.3	6.0	.7	....	.3	.3	9.7	34.7	1.0
H–49–t	46.7	5.0	2.0	5.7	7.3	....	.3	3.3	29.7	.....	....
P–51–t/h	48.7	5.0	3.3	4.7	10.0	....	.3	.3	21.7	6.0	....
62–t/h	37.4	4.3	.3	6.3	4.3	....	....	1.7	41.3	4.3	....
H–73–t/h	32.3	6.7	1.7	6.7	11.0	.7	.7	1.3	13.7	25.0	.3
Southern facies (Pinyon Conglomerate)											
P–1–t	33.6	4.7	4.7	4.3	4.0	0.3	0.7	1.3	0.3	45.3	0.3
2–h	42.0	3.3	4.0	6.7	....	....	1.3	2.3	39.3	.7	.3
2–t	41.7	6.3	3.7	10.3	1.3	....	....	1.7	33.7	.7	.7
10–t/h	25.3	5.0	2.3	8.7	1.0	.7	.3	.3	.3	55.3	.7
12–t	38.4	4.3	4.3	7.7	5.7	1.7	.7	1.3	.7	35.7	....
14–h	36.3	4.0	3.7	12.3	5.7	6.0	....	4.3	4.0	23.7	....
64–t/h	27.0	4.3	2.3	9.7	1.7	2.3	1.3	.7	.....	50.7	....
71–t	41.4	5.3	2.0	6.0	1.3	.3	1.0	.3	.....	41.7	.7
88–h	24.7	4.3	3.0	9.7	3.0	2.3	....	2.0	6.7	43.7	.7
89–t/h	25.3	5.0	4.0	8.3	1.7	1.0	1.0	.7	3.3	49.0	.7
90–t/h1	31.4	5.3	2.3	8.7	4.0	1.3	.3	1.7	.....	44.7	.3
90–t/h2	25.4	4.3	3.7	9.0	4.3	3.0	.3	1.0	1.7	47.3	....
91–t/h1	33.0	5.3	2.3	5.3	1.3	....	1.0	2.3	42.7	6.7	....
92–t/h	27.6	5.7	4.3	6.7	2.3	2.0	1.3	.7	.....	49.3	....
92–t/h2	40.0	4.0	3.3	6.7	3.7	2.3	.3	.7	7.7	20.7	.7
95–t/h3	31.7	5.0	4.3	9.0	1.0	1.0	.3	.3	2.7	43.7	1.0
96–t/h	22.0	5.3	2.0	9.7	2.0	1.3	.7	1.0	3.7	51.0	1.3
97–t/h1	24.3	4.0	2.7	7.7	4.0	1.3	.3	2.3	1.3	51.0	1.0

The quartz grains are everywhere almost evenly divided between two varieties which grade into each other: (1) quartz with straight extinction, which commonly has either straight, smooth, or irregular grain boundaries, and (2) quartz with undulose extinction, which generally has irregular grain boundaries. Both fresh and altered grains of orthoclase, microcline, perthite, and plagioclase are common, and total potassium feldspar generally exceeds plagioclase. Rarely plagioclase grains show normal or oscillatory zoning; most show only polysynthetic twinning. A wide variety of detritus, much of it unidentifiable, was included under the designation "altered fragments." However, grains of altered siltstone, volcanic rock with tiny plagioclase laths in a chloritic or silicified matrix, sparry calcite, and dusty micrite can be positively identified. Most of the altered fragments are brown grains composed chiefly of chlorite, microcrystalline quartz, and traces of carbonate and opaques. Grains identified as chert include both microcrystalline and chalcedonic quartz. Quartzite grains are similar to the quartzite pebbles and cobbles described previously. Large brown biotite flakes are generally more numerous than muscovite.

The sandstone matrix of the conglomerates is commonly cemented by sparry calcite which generally is clear but which appears dusty in the finer grained parts. Rhombs with high relief, probably dolomite, are present but sparse. One sample from an outlier of Pinyon Conglomerate at station 87 proved to be cemented by chalcedonic quartz. In samples where calcite is absent, a brown semiopaque matrix of clay minerals, microcrystalline quartz, disseminated opaque minerals, and possibly additional unidentified minerals occupy the interstices.

Heavy minerals were separated from 16 samples of conglomerate matrix by the following sequence of operations: Crushing, dissolving the carbonate cement in hydrochloric acid, drying, sieving to

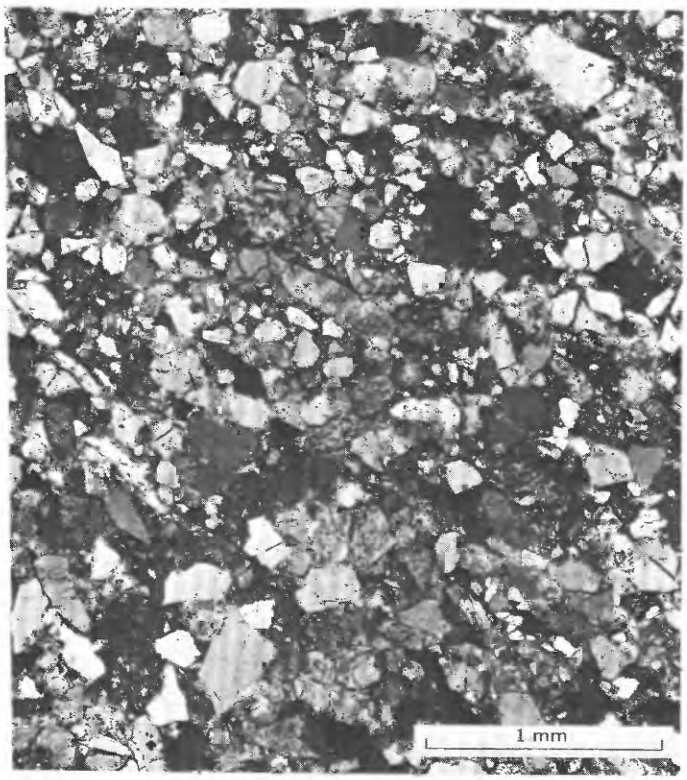

FIGURE 15. — Photomicrograph of typical subfeldspathic lithic wacke matrix of conglomerates; northern facies (Harebell Formation), station 35 on Whetstone Mountain; crossed nicols.

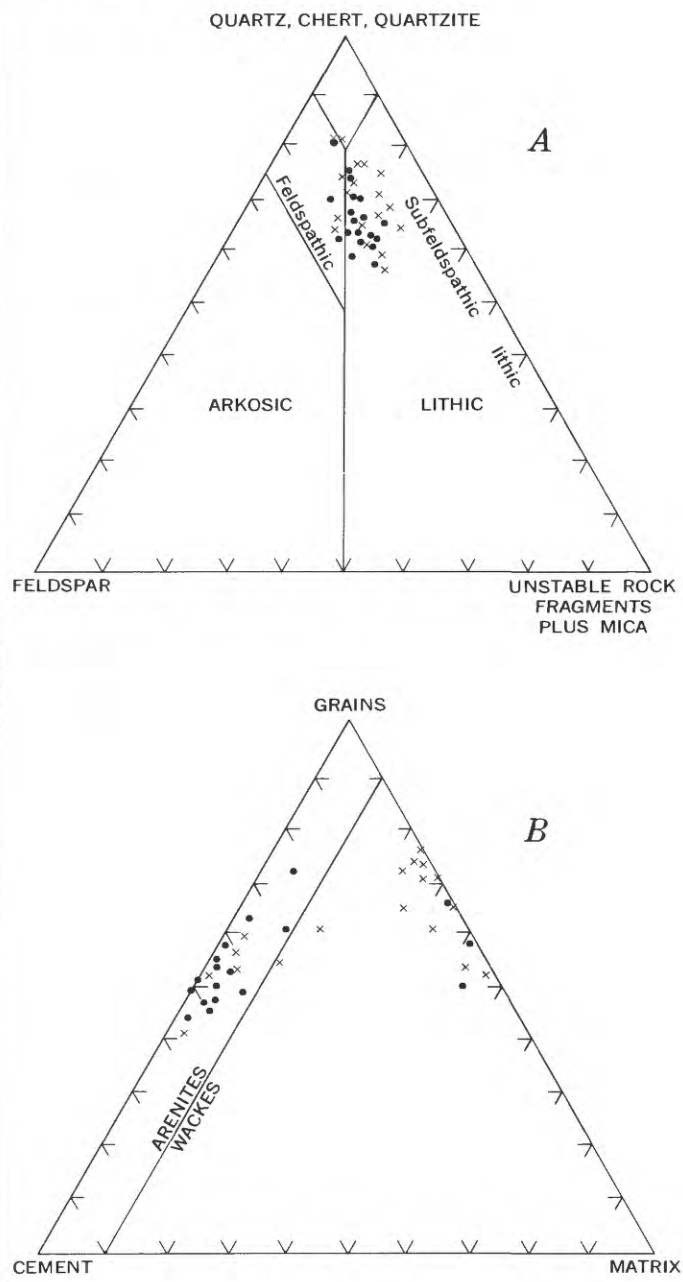

FIGURE 16. — Classification of sandstone matrix of conglomerates, modified from Williams, Turner, and Gilbert (1954, p. 292–293). *A*, Clastic constituents; *B*, relative proportions of grains, cement, and matrix. ×, northern facies; •, southern facies.

obtain the fractions 0.0625–0.125 mm and 0.125–0.25 mm, and centrifuging in bromoform. The 0.125- to 0.25-mm fraction proved to be mainly garnet and opaques. The 0.0625- to 0.125-mm fraction contained not only garnet and opaques but also significant quantities of zircon, tourmaline, sphene, and clinoamphibole (mainly pleochroic dark brown, but also light blue green and colorless) in addition to minor amounts of epidote, apatite, rutile, and pyroxene (table 7). Amphibole was not found in the conglomerate matrix of the western facies; it was found in abundance in one sample only from the northern facies; and it was found in all the samples examined from the southern facies. The proportion of various heavy-mineral species in the samples studied, however, varied greatly. Garnet, sphene, and amphibole are generally angular, whereas zircon and tourmaline exhibit both well-formed euhedrons and well-rounded grains.

SANDSTONE

GENERAL DESCRIPTION

Thick beds of gray to tan sandstone crop out as low ledges and isolated exposures in the sandstone facies below the thick quartzite-bearing conglomerates. Excellent exposures of sandstone are seen in the lower member of the Harebell Formation low on the south slopes of Whetstone Mountain and along Blackrock Creek just above its confluence with Buffalo Fork. Good exposures of sandstone in the lower member of the Pinyon Conglomerate as well as in the Harebell Formation are present below the conglomerate north of Upper Slide Lake. Typically the sandstones are medium to coarse grained and may con-

tain conglomerate, tuff, shale, claystone, coal, and sparse limestone lenses. Lenses of conglomerate with numerous pebbles derived from Paleozoic and Mesozoic rocks are known in sandstones of the Harebell Formation along the Gros Ventre drainage (Love, 1956b). Crossbedding is common; some ripple marks and ripple cross-lamination are also present. Mud chips and probable shrinkage cracks were seen at a few localities.

TABLE 7. — *Nonopaque heavy minerals (in percent) in the sandstone matrix of conglomerates in the western facies (Pinyon Conglomerate), the northern facies (Harebell Formation and Pinyon Conglomerate), and the southern facies (Pinyon Conglomerate)*

[0.0625- to 0.125-mm-size fraction, 100 grains counted per slide. Middle of field number corresponds to station number in fig. 2. Tr., trace]

Field No.	Garnet	Zircon	Tourmaline	Sphene	Epidote	Apatite	Rutile	Am.[a]	Am.[b]	Pyroxene
Western facies (Pinyon Conglomerate)										
P–53–h/t	87	5	6	0	0	0	1	0	0	1
54–h/t	92	6	1	0	1	0	Tr.	0	0	0
Average	89.5	5.5	3.5	0	.5	0	.5	0	0	.5
Northern facies (Harebell Formation and Pinyon Conglomerate)										
H–15–h	39	9	7	41	4	0	0	0	0	0
17–h	42	31	2	16	5	3	0	0	Tr.	1
34–h1	49	27	17	3	3	0	1	Tr.	0	0
34–h2	91	4	3	2	0	0	0	0	0	0
35–h/t	62	26	6	5	1	0	0	0	0	0
41–t/h	30	9	1	21	0	0	0	7	30	2
P–50–h	62	13	10	9	2	4	0	0	0	0
H–77–t/h2	58	15	8	8	4	6	0	1	0	0
78–t/h	52	15	5	21	2	4	1	0	0	0
Average	53.9	16.6	6.6	14.0	2.3	1.9	.2	.9	3.3	.3
Southern facies (Pinyon Conglomerate)										
P–4–h	55	17	6	16	0	0	0	4	0	2
4–t	43	11	10	20	7	3	Tr.	3	3	Tr.
64–t/h	56	2	Tr.	18	Tr.	0	0	3	21	0
95–h/t	33	6	5	15	4	2	1	5	29	0
95–h/t1	25	4	1	9	4	1	0	4	52	0
Average	42.4	8.0	4.4	15.6	3.0	1.2	.2	3.8	21.0	.4

[a]Colorless and light-blue-green amphibole.
[b]Pleochroic brown amphibole.

PETROGRAPHY

Most of the sandstones consist of poorly rounded, moderately sorted sand set in either calcite cement or fine-grained argillic matrix. The sandstones are of two types: nontuffaceous and tuffaceous (figs. 17 and 18). The nontuffaceous sandstones are similar in texture and composition to the sandstone matrix of the conglomerate facies, containing as they do abundant angular quartz, feldspar, altered rock fragments, and chert, and lesser amounts of quartzite, mica, and heavy minerals (table 8). The tuffaceous sandstones are very distinctive under the microscope. They contain abundant euhedral quartz, zoned plagioclase, and brown biotite, and lesser amounts of volcanic rock fragments, altered rock fragments, chert, quartzite, and heavy minerals (fig. 17*A* and *B*). Mixing with nontuffaceous detritus is obvious in many of the tuffaceous sandstones (fig. 17*A* and *B*). Chemical analyses of a few samples show that the tuffaceous sandstones have higher Na_2O/K_2O and Al_2O_3/SiO_2 ratios than their nontuffaceous counterparts (table 9); the chemical differences probably reflect the larger quantity of plagioclase found in the tuffaceous sandstones.

TABLE 8. — *Modal composition (in percent) of the tuffaceous and nontuffaceous sandstones of the lower member of the Harebell Formation*

[300 grains counted per slide. Field numbers correspond to station numbers in fig. 2. Leaders (.....) indicate not present]

Field No.	Quartz	Potassium feldspar	Plagioclase	Volcanic rock fragments	Altered fragments	Chert	Quartzite	Mica[1]	Fine-grained altered matrix	Calcite cement	Heavy minerals
Tuffaceous sandstone											
W–368	11.0	2.7	25.0	6.7	6.0	0.7	1.0	6.7	[2]32.0	6.3	2.0
377	23.3	1.7	27.3	13.0	6.7	1.3	1.7	1.7	21.0	2.0	.3
378	15.7	3.3	23.7	15.7	6.7	3.3	4.0	2.7	24.0	.....	1.0
379	21.7	2.3	22.0	1.3	5.7	4.3	.3	.3	[2]41.7	.....	.3
380	23.3	4.0	49.3	2.7	2.3	1.3	.....	5.0	[2]12.0	.....	.....
382	29.0	1.7	39.0	1.7	6.0	.....	10.3	3.3	8.7	.....	.3
383	31.6	.7	52.0	1.0	2.7	.3	1.7	2.3	7.0	.3	.3
384	16.3	1.7	31.7	1.0	3.7	.....	1.0	12.3	30.0	.....	2.3
H–36–t/h	38.3	2.7	35.7	.....	4.3	2.0	1.7	2.7	12.7	.....	....
39–t3	20.3	5.7	11.7	2.7	11.7	4.0	2.0	1.3	.....	40.0	.7
41–t2	35.0	2.3	30.3	.....	5.0	.....	.....	4.3	16.3	.....	6.7
41–t3	21.6	1.7	14.0	1.7	5.3	3.7	2.0	.3	.3	42.7	6.7
251–t/h	25.0	2.7	42.3	1.0	3.0	.3	.....	4.3	20.7	.....	.7
261–t1	27.7	1.0	42.3	.3	4.7	.....	1.0	2.0	19.7	.7	.7
262–t2	44.0	1.3	31.3	.....	3.7	.3	1.0	1.3	1.0	16.0	....
Nontuffaceous sandstone											
L66–5–5	23.0	3.0	6.7	0.3	9.0	3.0	3.3	2.7	.....	48.3	0.3
5–24A	50.6	3.7	1.3	.....	8.7	15.3	4.0	.3	16.0	.....	....
H–52–t/h2	50.3	1.7	3.7	.3	6.0	12.7	4.3	.3	20.7	.....	....
244–t1	28.3	.7	1.3	.....	8.0	2.0	.....	.7	6.0	52.3	.7
246–t2	48.4	1.3	2.3	.....	11.7	7.7	.7	.7	20.7	[3]6.0	.7
253–t/h	39.0	3.0	5.7	.....	7.3	7.0	2.0	3.0	24.7	8.0	.3
257–t	42.6	4.7	7.7	.....	5.3	1.7	.7	.7	15.3	21.3	....
261–t	49.7	2.3	9.7	.....	8.7	11.3	2.7	.....	14.7	1.0	....
280–t	36.0	5.7	7.3	.....	7.3	2.7	.3	1.7	38.0	.....	1.0

[1]Tuffaceous sandstones have biotite only.
[2]Includes chert cement.
[3]Includes some detrital(?) carbonate.

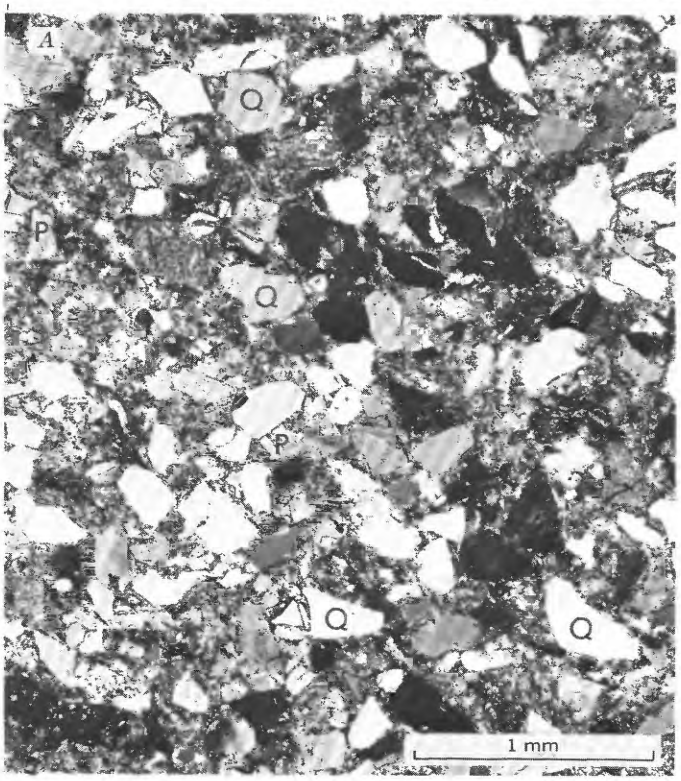

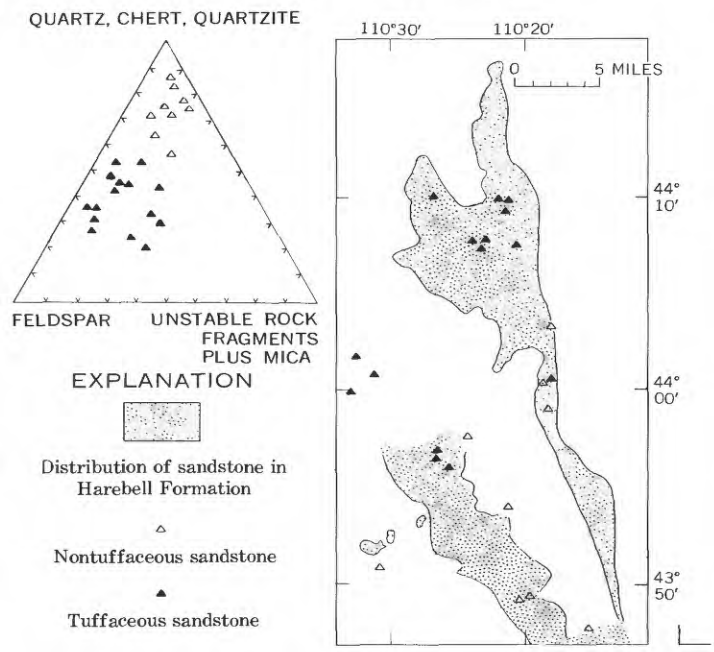

FIGURE 18. — Composition of clastic constituents and distribution of tuffaceous and nontuffaceous sandstones in the lower member of the Harebell Formation.

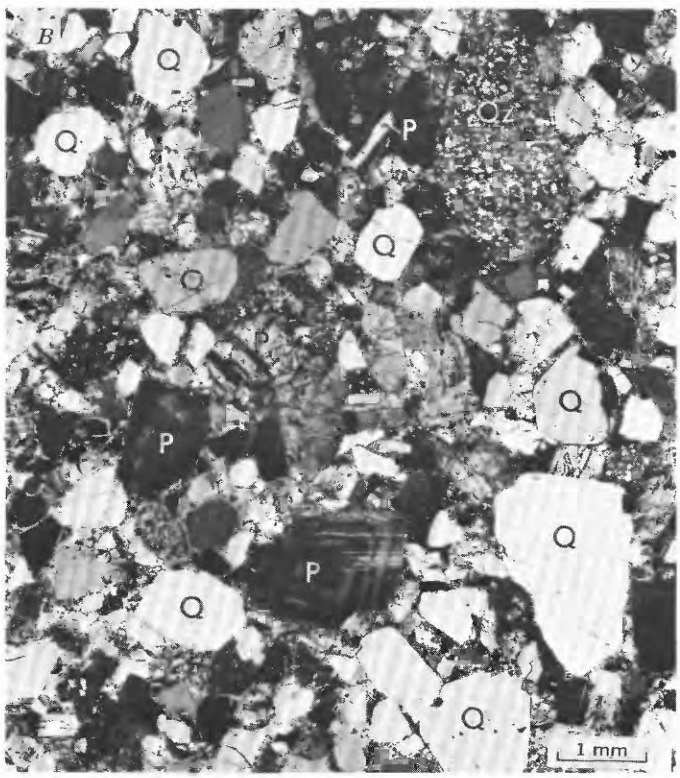

FIGURE 17. — Photomicrographs of sandstone and tuffaceous rocks in the lower member of the Harebell Formation. *A*, Calcite-cemented tuffaceous arenite with admixed nonvolcanic detritus; station 39 on Pilgrim Creek; crossed nicols. *B*, Calcite-cemented coarse-grained tuffaceous arenite with quartz euhedrons, plagioclase with oscillatory zoning, and quartzite fragment; station 262 on the south slope of Whetstone Mountain; crossed nicols. *C*, Crystal tuff composed of quartz and plagioclase euhedrons cemented by chert; type section of the Harebell, station W379 in Snake River Canyon; crossed nicols. qz, quartzite; Q, quartz; P, plagioclase.

TABLE 9. — *Rapid rock analyses (in percent) of nontuffaceous and tuffaceous sandstones from the lower member of the Harebell Formation*

[Middle of field number corresponds to station number in fig. 2. Analysts: Leonard Shapiro, P. L. D. Elmore, G. W. Chloe, H. Smith, J. L. Glenn, and Lowell Artis]

	Nontuffaceous sandstone					Tuffaceous sandstone				
Sample No.	1	2	3	4	5	6	7	8	9	10
SiO_2	43.6	84.5	77.8	81.5	73.5	73.3	48.7	63.3	67.7	64.2
Al_2O_3	5.5	7.1	8.2	7.1	8.7	14.4	8.3	13.7	15.0	10.8
Fe^2O^3	.73	.44	1.2	1.2	4.0	1.4	1.1	4.5	3.5	.83
FeO	.88	.28	.72	.56	3.2	.44	.88	2.7	1.3	.52
MgO	.90	.70	1.1	.93	1.8	.60	.90	2.5	1.7	.46
CaO	24.1	1.5	2.2	.89	.81	3.3	18.7	5.0	2.6	10.6
Na_2O	1.1	.34	1.0	.89	.85	2.6	1.6	2.7	3.3	2.2
K_2O	1.4	1.2	1.9	1.6	1.7	1.8	1.5	1.0	1.5	1.1
H_2O-	.38	.74	1.6	1.4	.93	.67	.82	1.7	.68	.54
H_2O+	1.3	1.3	1.9	2.7	3.6	.93	1.6	.80	1.7	2.1
TiO_2	.27	.24	.35	.35	.59	.33	.47	1.8	.64	.26
P_2O_5	.17	.09	.09	.09	.14	.05	.09	.28	.13	.04
MnO	.41	.00	.00	.04	.05	.02	.67	.06	.07	.17
CO_2	19.1	1.2	1.1	.54	.17	.08	14.5	.05	.08	6.1
Sum	100	100	99	100	100	100	100	100	100	100

SAMPLE DESCRIPTIONS

Sample No.	Field No.	Description
1	L66–5–5	Calcite-cemented lithic arenite.
2	H–246–t2	Subfeldspathic wacke.
3	H–253–t/h	Lithic wacke.
4	H–261–t	Feldspathic wacke.
5	H–280–t	Do.
6	H–36–t/h	Tuffaceous wacke.
7	H–39–t3	Calcite-cemented tuffaceous arenite.
8	H–41–t2	Tuffaceous wacke.
9	H–251–t/h	Do.
10	H–262–t2	Calcite-cemented tuffaceous arenite.

All the tuffaceous sandstones studied occur in the lower member of the Harebell Formation at or below the base of the northern conglomerate facies (fig. 18), whereas nontuffaceous sandstones are interbedded with both the northern and the southern conglomerate facies and also occur below both of the facies. Thin sections, supplied by J. D. Love, from the lower part of the type Harebell section along the south edge of Yellowstone National Park are all of tuffaceous sandstone. One sample (fig. 17*C*) from the type Harebell contains numerous perfect quartz and plagioclase euhedrons in a silicified matrix and might more appropriately be termed a crystal tuff.

Quartz euhedrons in the tuffaceous sandstones show straight extinction and commonly exhibit resorption cavities identical with those seen in the quartz phenocrysts of many volcanic flows. Both quartz with straight extinction (and angular outlines) and quartz with undulose extinction are common in the nontuffaceous sandstones, an observation which raises the possibility of an unrecognized volcanic contribution to them also. Feldspars in the nontuffaceous sandstones are orthoclase, microcline, perthite, and plagioclase; plagioclase is by far the most abundant feldspar in the tuffaceous sandstones. The volcanic plagioclase consists of both fresh and altered grains, and many whole and broken euhedrons exhibit either normal or oscillatory zoning. Most of the plagioclase shows polysynthetic albite twinning, and determinations by the Michel-Lévy method indicate calcic compositions as high as An_{54}. Most of the volcanic rock fragments are distinguished by small laths and microlites of plagioclase set in an altered matrix. Altered rock fragments, chert grains composed of microcrystalline and chalcedonic quartz and quartzite fragments are common in both tuffaceous and nontuffaceous sandstones, emphasizing the mixing of detritus from different sources. Large brown biotite flakes are abundant in some tuffaceous sandstones, whereas both muscovite and biotite are present in nontuffaceous sandstones.

Sparry calcite is the most common cement in both tuffaceous and nontuffaceous sandstones. In sandstones where calcite is minimal, a brown fine-grained matrix consisting of clay minerals, microcrystalline quartz, disseminated opaque minerals, and possibly other unidentified minerals is abundant.

Heavy-mineral separates of the 0.0625- to 0.125-mm fraction of 11 selected sandstone samples showed wide variation (table 10). Three tuffaceous sandstone samples contain floods of angular grains of either dark-brown clinoamphibole or sphene and lesser amounts of garnet, zircon, and tourmaline. The eight nontuffaceous sandstone samples examined contain mainly garnet, zircon, and tourmaline, and only small amounts of sphene and amphibole. As in the conglomerate matrix, both nontuffaceous and tuffaceous sandstones contain rounded and euhedral zircon and tourmaline. Tourmaline, including the only grains observed of the variety indicolite, is especially abundant in the Harebell sandstones of the Gros Ventre drainage.

MINOR LITHOLOGIES

Thin shale and claystone beds occur both in the conglomerate facies and, with coal and sparse lime-

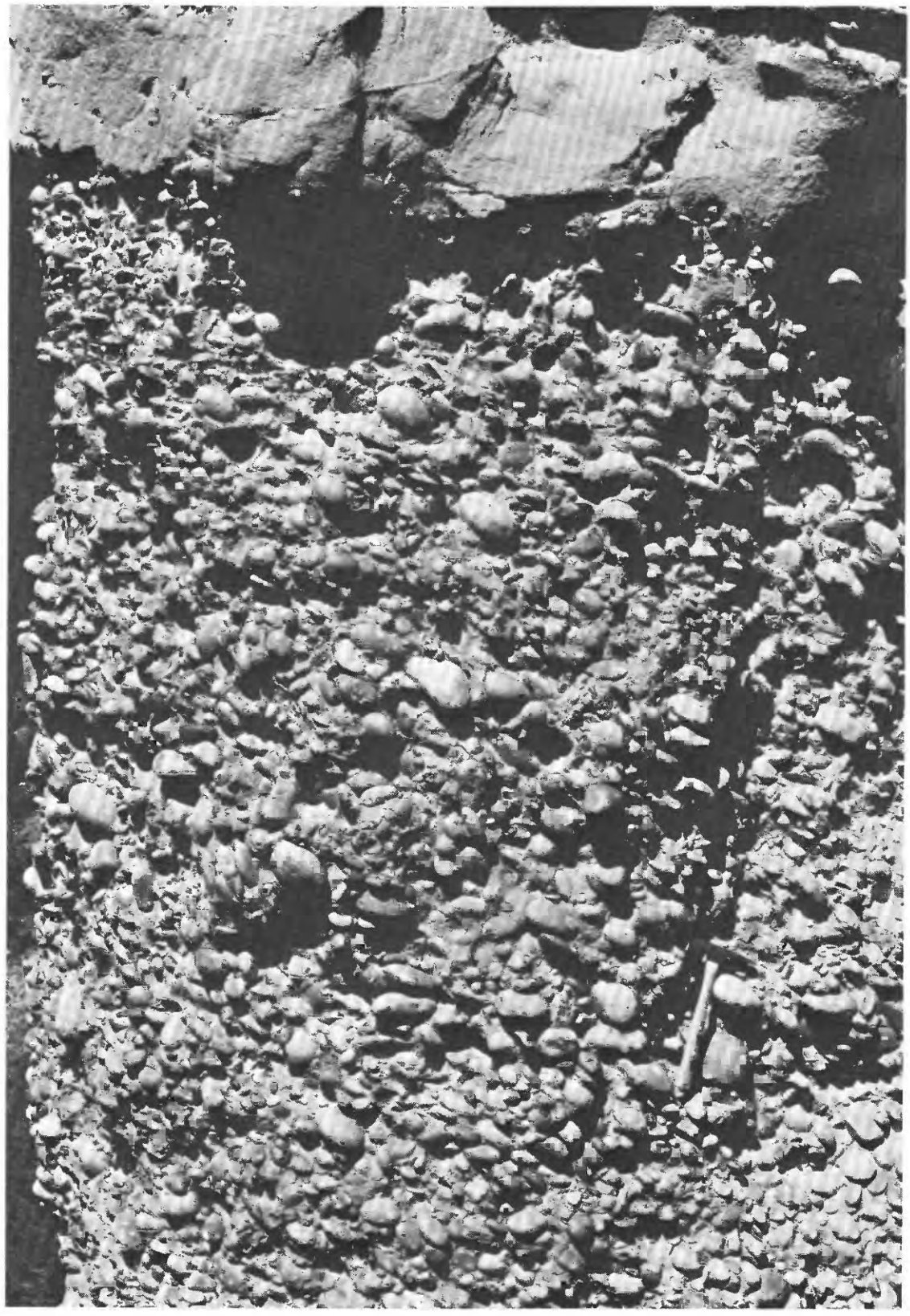

FIGURE 19. — Imbrication in the Pinyon Conglomerate along the South Fork of Fish Creek. Sandstone lens defines bedding; current flowed from right to left. Note pick for scale, lower right.

stone beds, in the sandstone facies. X-ray diffraction patterns of six shale and claystone samples showed quartz (abundant in all samples), montmorillonite(?) (all samples), chlorite(?) (five samples), biotite (three samples), and calcite (one sample). Three limestone samples examined in thin section consist of fine-grained dusty calcite. Silt-sized quartz grains and tiny microflakes of biotite were observed in the limestone samples. Insoluble residues of four limestone samples ranged from 15 to 51 percent, and X-ray diffraction patterns of the residues showed quartz (all samples), biotite (all samples), chlorite(?) (three samples), and montmorillonite(?) (one sample).

TABLE 10. — *Nonopaque heavy minerals (in percent) in sandstones of the Harebell Formation*

[0.0625- to 0.125-mm-size fraction, 100 grains counted per slide. Middle of field number corresponds to station number in fig. 2. Tr., trace]

Field No.	Garnet	Zircon	Tourmaline	Sphene	Epidote	Apatite	Rutile	Am$_1$[a]	Am$_2$[b]	Andalusite
Tuffaceous sandstones in lower member north of Spread Creek										
H–36–t/h	3	Tr.	14	82	0	0	0	Tr.	1	0
41–t2	1	5	3	8	0	0	0	2	81	0
251–t/h	1	0	24	73	0	0	0	0	2	0
Average	1.7	1.7	13.7	54.3	0	0	0	.7	28.0	0
Nontuffaceous sandstones in lower member north of Spread Creek										
H–27–h	73	5	6	15	Tr.	Tr.	1	0	0	0
52–t/h	18	65	14	1	2	0	0	0	0	Tr.
52–t/h–4	82	12	4	0	0	0	2	0	0	0
70–20	35	54	10	1	0	0	0	0	0	0
Average	52	34	8.5	4.3	.5	0	.8	0	0	0
Nontuffaceous sandstones in the Gros Ventre drainage										
H–9–t	42	8	[c]32	9	4	0	4	1	0	0
26–t/h	4	86	[c]7	3	0	0	0	0	0	0
24–t1	1	45	[c]50	1	0	0	3	0	0	0
24–t2	15	55	[c]18	8	2	0	0	2	0	0
Average	15.5	48.5	26.8	5.3	1.5	0	1.8	.8	0	0

[a]Colorless and light-blue-green amphibole.
[b]Pleochroic brown amphibole.
[c]Tourmaline includes small amounts of the variety indicolite.

SEDIMENTARY STRUCTURES AND PALEOCURRENTS

IMBRICATION

DESCRIPTION

Imbrication, or shingling, is defined by the subparallel arrangement of oblate, or flat, stones inclined to the bedding (fig. 19). In the Harebell Formation and the Pinyon Conglomerate the stones are inclined upstream, as indicated by crossbedding and by regional variation in roundstone size. Recognition and measurement of imbrication depend first on precise determination of the bedding attitude as a reference plane. The bedding attitude is usually defined by sand lenses and by variations in sorting and in roundstone size. If the bedding is inclined, as it is in most places, the imbrication orientation must be restored to its original position by rotating the bedding plane to horizontal. Imbrication orientation was used for paleocurrent studies in the conglomerates because imbrication is widespread and well defined and because generally it is the only paleocurrent indicator present. Although imbrication orientation can be roughly estimated for a quick knowledge of paleocurrent direction, I chose to determine the orientation by measuring the fabric of stones in each outcrop. This is time consuming, but it does provide statistical information necessary for precise description of imbrication and for comparisons leading to environmental interpretations.

MEASUREMENT AND STATISTICAL ANALYSIS

Each determination was made by measuring the *c*-axis orientation (both azimuth and inclination) of 50 oblate stones in part of an outcrop, usually limited to several square feet. Generally at least two determinations of 50 *c*-axis orientations each were made at each outcrop. Measurement was facilitated by orienting a pencil perpendicular to the *ab* plane of each stone and measuring the pencil orientation. Orientations measured in inclined strata were restored to their original position by rotating the bedding plane to horizontal (computer program of McIntyre, 1963). The resulting orientations of 50 *c*-axes may be plotted on a stereographic projection (fig. 20) but are more easily analyzed statistically by computer.

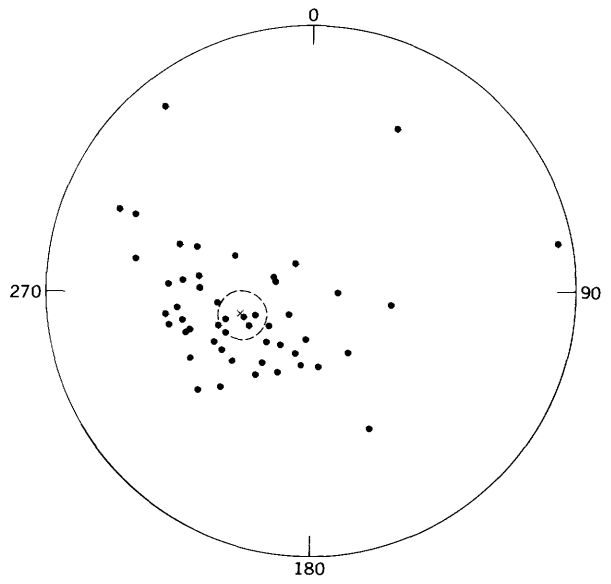

FIGURE 20. — Lower hemisphere stereographic projection of 50 *c*-axis orientations of oblate roundstones. Calculated statistics based on the spherical normal distribution model are: $\bar{\theta} = 252.5°$; $\bar{\phi} = 60.4°$; $\bar{R} = 40.8$ (81.6 percent); $k = 5.3$; $c_{0.95} = 9.6°$; $\chi^2_{(\hat{\psi})} = 20.7$ with 13 degrees of freedom; $\chi^2_{(\hat{\chi})} = 23.3$ with 15 degrees of freedom. "×" marks position of vector mean; the dashed circle outlines $c_{0.95}$, the spherical circle of confidence (95-percent level).

TABLE 11. — *Imbrication statistics at stations in the western facies (Pinyon Conglomerate), the northern facies (Harebell Formation and Pinyon Conglomerate), and the southern facies (Pinyon Conglomerate)*

[Each determination was calculated by averaging 50 *c*-axis orientations. Stations are located in fig. 2. $\bar{\theta}$=vector mean azimuth; $\bar{\phi}$=vector mean inclination; R=vector magnitude; $c_{0.95}$=radius of spherical circle of confidence; k=an indicator of dispersion; $\chi^2_{(\hat{\phi})}$=chi square for angular dispersion about the vector mean; df=degrees of freedom for $\chi^2_{(\hat{\phi})}$; and $\chi^2_{(\hat{\theta})}$=chi square for azimuthal dispersion about the vector mean (with 15 degrees of freedom)]

Station No.	$\bar{\theta}$ (degrees)	$\bar{\phi}$ (degrees)	R (absolute value)	$c_{0.95}$ (degrees)	k	$\chi^2_{(\hat{\phi})}$	df	$\chi^2_{(\hat{\theta})}$ (15df)
Western facies (Pinyon Conglomerate)								
53	147.9	47.0	37.8	11.5	4.0	8.1	15	20.5
54A	160.2	59.6	43.5	7.8	7.6	6.9	10	17.6
54B	139.6	68.8	36.4	12.4	3.6	24.8	15	24.8
56	121.7	68.4	43.5	7.8	7.6	16.8	10	21.2
Northern facies (Pinyon Conglomerate and Harebell Formation)								
15	41.3	61.5	40.2	10.0	5.0	17.1	13	18.3
16	84.6	55.4	40.6	9.7	5.2	19.4	13	17.6
17A	105.9	53.5	45.5	6.3	11.0	18.0	7	19.0
17B	90.4	54.4	44.4	7.1	8.8	16.2	10	24.8
34A	57.9	58.8	38.4	11.1	4.2	27.3	14	13.3
34B	39.5	58.8	43.8	7.5	8.0	13.2	8	16.9
35	36.0	63.1	41.1	9.4	5.5	24.5	12	43.4
37	309.1	61.1	40.2	10.0	5.0	16.8	13	6.8
38	55.6	44.2	42.3	8.6	6.4	6.8	11	17.6
39	73.0	75.9	44.0	7.4	8.2	7.3	10	15.4
40	63.3	64.4	42.0	8.8	6.1	21.3	12	8.2
41	88.1	62.5	38.1	11.3	4.1	17.3	14	15.4
43	71.7	49.4	40.2	10.0	5.0	17.5	13	17.6
44A	105.6	60.6	42.3	8.6	6.3	16.8	12	21.2
44B	89.4	57.3	40.7	9.7	5.2	19.4	12	24.0
46	71.0	59.3	39.5	10.4	4.6	17.0	14	16.9
47	92.3	52.7	45.6	6.2	11.3	1.8	6	57.8
48	71.1	64.1	43.4	7.8	7.5	12.0	11	11.8
49	91.0	67.4	43.3	7.9	7.4	12.7	10	16.1
50	92.9	57.5	39.2	10.6	4.5	6.5	14	13.3
51	78.9	52.2	40.2	10.0	5.0	19.1	13	17.6
52	322.0	81.4	43.9	7.5	8.0	13.3	10	11.8
57	111.9	52.3	46.0	5.9	12.4	19.0	8	21.9
58	111.3	58.9	42.4	8.5	6.5	30.8	11	29.8
59	142.6	57.9	43.4	7.9	7.4	8.4	11	13.3
60	113.7	55.9	42.2	8.7	6.3	38.1	12	21.2
61	83.0	52.2	43.1	8.0	7.2	9.0	11	8.2
62A	34.2	69.0	43.8	7.6	7.9	31.0	10	16.9
62B	136.6	54.0	41.8	8.9	6.0	25.9	12	25.5
73	95.6	67.7	44.8	6.8	9.5	9.3	9	26.2
75	131.2	55.2	43.9	7.5	8.0	6.3	9	18.3
76	82.9	52.3	45.7	6.1	11.5	13.3	8	6.8
77A	90.4	72.9	40.1	10.0	4.9	30.6	13	16.9
77B	39.7	74.0	38.7	10.9	4.3	15.4	14	19.0
78A	324.3	80.4	41.3	9.2	5.6	16.7	11	14.7
78B	154.8	74.3	41.9	8.9	6.0	8.5	12	16.1
247A	32.3	71.0	39.1	10.7	4.5	27.3	14	15.4
247B	44.0	57.3	41.6	9.1	5.8	29.0	12	19.0
248A	15.9	78.6	43.8	7.6	7.9	16.3	9	7.5
248B	106.9	68.6	43.9	7.5	8.0	12.0	10	21.2
256A	348.0	66.2	44.5	7.1	8.9	28.2	10	26.9
256B	120.8	67.8	43.8	7.6	7.9	17.1	10	31.2
256C	96.3	63.8	46.2	5.7	13.1	3.8	6	16.9
259A	104.0	51.4	42.9	8.2	6.9	11.6	11	16.1
259B	110.6	53.1	42.8	8.3	6.8	8.5	11	25.5
259C	85.5	50.5	43.4	7.8	7.5	20.1	11	13.3
260	46.5	75.4	44.6	7.0	9.2	16.3	9	16.1
265	116.6	64.3	41.0	9.5	5.4	33.5	13	17.6
268A	69.7	56.5	43.3	7.9	7.3	7.3	11	12.6
268B	46.2	54.6	43.6	7.7	7.6	8.9	10	17.6
268C	67.5	60.7	45.1	6.6	10.0	11.9	9	14.7
268D	7.5	59.3	45.4	6.4	10.8	16.4	9	20.5
269A	118.1	67.5	42.2	8.7	6.2	19.3	12	29.8
269B	111.3	73.9	43.0	8.1	7.0	7.8	11	16.9
270A	84.4	61.5	43.0	8.2	7.0	13.6	10	19.0
270B	89.7	60.0	45.7	6.2	11.5	10.2	8	14.0
270C	137.1	61.8	42.5	8.5	6.5	14.5	11	24.0
271A	81.9	58.2	43.8	7.6	7.9	25.1	10	9.0
271B	56.7	54.3	45.0	6.7	9.8	4.4	9	12.6
272A	59.1	58.2	44.9	6.8	9.7	19.9	9	39.8
272B	72.2	66.3	45.3	6.5	10.4	16.8	8	22.6
273	109.0	60.8	43.6	7.7	7.7	7.5	10	18.3
274A	86.0	52.8	43.9	7.5	8.0	24.3	10	16.9
274B	105.6	53.3	42.6	8.4	6.7	13.0	11	14.7
274C	52.1	65.0	42.0	8.8	6.1	27.0	12	21.2
275A	41.7	59.1	44.4	7.2	8.7	11.0	10	9.0
275B	37.8	61.3	44.7	6.9	9.3	10.9	9	21.2
277A	1.2	52.6	43.6	7.7	7.7	23.9	10	25.5
277B	116.8	54.7	42.5	8.5	6.5	17.6	11	23.3
278	111.2	63.9	45.1	6.6	10.0	25.2	9	13.3
Southern facies (Pinyon Conglomerate)								
1	234.4	66.2	44.3	7.2	8.6	12.4	10	12.6
2A	239.6	71.6	46.6	5.4	14.6	28.8	7	33.4
2B	221.3	78.0	43.7	7.6	7.8	43.8	10	14.7
4	199.0	67.2	45.2	6.6	10.2	14.5	9	22.6
9	168.4	84.7	41.6	9.1	5.8	13.6	12	18.3
Southern facies (Pinyon Conglomerate)—Continued								
10A	194.8	59.7	43.4	7.9	7.4	11.5	11	16.1
10B	198.2	60.6	42.5	8.5	6.5	22.0	11	21.2
11A	252.5	60.4	40.8	9.6	5.3	20.7	13	23.3
11	246.4	46.2	43.7	7.7	7.7	8.7	10	14.0
12	216.0	64.1	41.9	8.9	6.0	10.0	12	18.3
14	149.1	80.8	40.3	9.9	5.0	26.0	13	8.2
21	290.3	67.0	44.2	7.3	8.4	18.0	10	20.5
22	16.6	65.9	40.2	9.9	5.0	14.3	12	20.5
26A	91.9	69.4	35.6	12.9	3.4	18.9	16	30.5
26B	155.9	73.7	43.6	7.7	7.7	6.5	10	42.7
64A	150.9	62.3	40.5	9.8	5.1	27.2	13	27.6
64B	133.2	52.1	46.2	5.7	13.0	10.9	5	68.6
71A	148.0	48.9	42.5	8.5	6.5	17.9	11	20.5
71B	165.9	53.4	45.4	6.4	10.7	14.3	9	18.3
71C	192.1	54.1	43.2	8.0	7.2	10.4	11	26.2
72A	130.1	63.3	39.8	10.2	4.8	21.0	13	10.4
72B	186.5	58.2	43.5	7.8	7.6	7.0	10	23.3
87A	168.8	68.2	45.4	6.4	10.7	11.0	7	26.9
87B	109.0	66.4	44.0	7.5	8.1	39.1	10	15.4
88A	131.4	56.7	40.1	10.0	4.9	15.1	11	17.6
88B	89.6	53.4	44.4	7.1	8.8	14.7	10	18.3
89A	124.8	59.6	44.5	7.0	9.0	13.7	10	65.0
89B	204.2	61.7	37.9	11.5	4.0	22.5	15	34.1
90A	53.7	68.3	43.0	8.1	7.0	20.7	11	12.6
90B	194.0	49.8	44.8	6.9	9.4	6.6	9	14.7
92A	167.4	56.4	43.2	8.0	7.2	14.1	11	6.1
92B	152.2	59.0	42.9	8.2	6.9	12.0	11	16.9
93	180.9	50.6	43.1	8.0	7.1	7.1	11	17.6
95A	201.3	60.0	42.1	8.7	6.2	10.4	12	26.9
95B	202.8	57.9	45.2	6.6	10.2	20.3	9	19.0
96A	179.8	64.7	43.6	7.7	7.7	12.1	10	16.9
96B	196.4	59.4	45.6	6.2	11.3	9.6	8	14.7
96C	209.1	56.4	44.5	7.1	8.9	8.7	8	21.9
97A	167.2	52.7	43.7	7.7	7.8	11.1	10	17.6
97B	163.0	53.0	43.6	7.7	7.7	5.3	10	17.6
172A	173.1	59.4	43.0	8.1	7.0	20.0	11	19.0
172B	130.5	72.1	42.0	8.8	6.1	8.8	12	11.8
173A	176.3	60.8	45.4	6.4	10.8	8.2	9	16.9
173B	212.8	62.8	42.7	8.4	6.7	9.6	11	14.7
180	121.7	58.4	44.4	7.1	8.8	10.8	10	36.3
181A	131.1	58.8	42.6	8.4	6.6	28.3	11	21.2
181B	102.0	55.6	41.0	9.4	5.4	15.3	12	14.0
183A	142.7	60.8	42.8	8.3	6.8	19.8	11	24.8
183B	116.4	66.7	41.7	9.0	5.9	15.3	12	9.7
183C	145.5	60.3	43.8	7.6	7.9	5.3	10	26.2
185A	184.5	69.4	44.0	7.4	8.2	15.8	10	16.9
185B	126.5	56.1	42.1	8.7	6.2	15.9	12	19.0
189A	115.8	62.4	39.3	10.5	4.6	9.1	14	19.0
189B	169.0	60.9	40.8	9.6	5.3	18.6	13	16.1
189C	233.8	65.3	39.3	10.6	4.5	20.0	14	14.0
191A	139.9	61.5	41.8	8.9	6.0	9.3	12	20.5
191B	187.8	57.7	42.5	8.5	6.5	17.8	11	19.7
193A	170.2	52.7	41.8	8.9	6.0	39.1	12	17.6
193B	162.7	72.1	40.9	9.5	5.4	14.2	13	11.8
194	132.7	51.1	43.3	7.9	7.3	17.0	11	7.5
195	171.9	61.6	42.0	8.8	6.1	14.4	12	10.4
203	212.6	67.4	45.9	6.0	12.0	8.7	8	13.3
204A	192.7	56.6	43.3	7.9	7.3	19.3	11	9.7
204B	175.9	62.8	43.5	7.8	7.6	17.6	10	12.6
206A	116.0	67.9	41.8	9.0	5.9	7.9	12	6.8
206B	154.0	68.3	40.2	10.0	5.0	24.7	13	18.3
210A	50.2	74.0	42.2	8.6	6.3	14.0	12	15.4
210B	115.4	58.6	42.8	8.3	6.8	28.3	11	20.5
212A	135.3	53.0	40.3	9.9	5.0	33.8	13	27.6
212B	156.9	61.9	42.3	8.6	6.4	21.6	11	22.6
213A	144.9	61.7	38.3	11.2	4.2	10.9	14	11.1
213B	174.4	55.6	42.5	8.5	6.5	9.0	11	14.7
214A	59.8	73.8	44.1	7.4	8.3	16.5	10	10.4
214B	80.2	50.9	41.8	8.9	6.0	22.3	12	14.7
215A	250.1	65.4	42.9	8.2	6.9	14.3	11	11.8
215B	262.2	70.1	38.2	11.2	4.1	10.1	14	31.2
219A	159.0	52.2	45.5	6.3	11.0	8.8	8	8.2
219B	148.0	61.5	44.3	7.2	8.6	12.2	10	9.7
222A	113.4	66.6	43.3	7.9	7.4	31.7	11	16.1
222B	118.8	68.8	42.6	8.4	6.6	15.7	11	18.3
223A	149.5	66.7	45.4	6.4	10.6	5.8	9	15.4
223B	182.6	65.6	45.2	6.6	10.2	8.7	8	20.5

Plots of a few determinations suggested that the spherical normal distribution (Fisher, 1953) might be an appropriate model; hence, statistical computations for each determination (50 measurements) were made utilizing this model. The resulting statistics are given in table 11. Computational details were discussed by Andrews and Shimizu (1966), McElhinny (1967), Steinmetz (1962), and Watson and Irving (1957), and they are summarized in the following paragraph.

Each c-axis orientation is expressed as a vector with an azimuth θ (measured in degrees clockwise from north) and an inclination ϕ (measured in degrees from horizontal); each may also be expressed as a direction cosine. The sum of the direction cosines (X, Y, Z) for each set of $n = 50$ vectors is given by

$$\sum_{i=1}^{50} \cos\phi \cos\theta = Y,$$

$$\sum_{i=1}^{50} \cos\phi \sin\theta = X, \text{ and}$$

$$\sum_{i=1}^{50} \sin\phi = Z.$$

The following statistics are defined in terms of direction cosines:

(1) R, the magnitude of the vector mean (resultant vector), is calculated by

$$R=(X^2+Y^2+Z^2)^{1/2}.$$

The direction cosines of the vector mean are

$$X/R, \ Y/R, \text{ and } Z/R.$$

(2) $\bar{\theta}$, the azimuth of the vector mean (and also of the interpreted paleocurrent orientation), is given by

$$\bar{\theta}=\sin^{-1}(X/R)/[1-(Z/R)^2]^{1/2}.$$

(3) $\bar{\phi}$, the inclination of the vector mean, is given by

$$\bar{\phi}=\sin^{-1}(Z/R).$$

(4) $c_{0.95}$, the radius of the spherical circle of confidence about the vector mean, is given by

$$c_{0.95}=\cos^{-1}\left[1-(n-R)(20^{\frac{1}{n-1}}-1)/R\right].$$

(5) k, an indicator of dispersion for the spherical normal distribution model, is given by

$$k=(n-1)/(n-R).$$

(6) $\chi^2(\hat{\psi})$, the chi-square for angular dispersion of 50 c-axis orientations about the vector mean, is given by

$$\chi^2=\sum_{j=1}^{p} \frac{(f_{\text{obs}_j}-f_{\text{exp}_j})^2}{f_{\text{exp}_j}}$$

where

f_{obs_j} = observed frequency of $\hat{\psi}$ in the jth class,

f_{exp_j} = expected frequency of $\hat{\psi}$ in the jth class, and

p = number of observed 5° classes, $1 \leq p \leq 72$.

The observed frequency of $\hat{\psi}$, f_{obs_j}, is calculated as follows. First, $\hat{\psi}_i$, the angular dispersion between the vector mean and each c-axis orientation, is calculated by

$$\hat{\psi}_i=(X/R)\ X_i+(Y/R)\ Y_i+(Z/R)\ Z_i$$

where

X_i, Y_i, and Z_i = the direction cosines for each orientation, and

X/R, Y/R, and Z/R = the direction cosines of the vector mean.

The resulting $\hat{\psi}_i$ values are summarized into p 5° classes to give f_{obs_j}. The expected frequency of $\hat{\psi}$, f_{exp_j}, is calculated by

$$f_{\text{exp}_j}=n\cdot[e^{(-p\cdot a)}-e^{(-p\cdot b)}]$$

where

n=50, the number of c-axis orientations,

a=1−cos [(j−1)·5], and

b=1−cos·(j·5)

and where (j·5) and [(j−1)·5] are the class limits. Then df, the number of degrees of freedom, is given by

$$df=p-1-2$$

(7) $\chi^2(\hat{\chi})$, the chi-square for azimuthal dispersion of 50 c-axis orientations about the vector mean, is given by

$$\chi^2(\hat{\chi})=\sum_{m=1}^{18} \frac{(f_{\text{obs}_m}-n/18)^2}{n/18}$$

where

f_{obs_m} = observed frequency of χ in the mth class,

n = 50, the number of c-axis orientations, and

18 = number of observed 20° classes.

The c axes are rotated (McIntyre, 1963) so that R, the resultant vector, is alined vertically, and the new values for χ_i are determined. The χ_i are then partitioned into eighteen 20° classes (from 0° to 350°) where the observed frequency is f_{obs_m} in class m and the expected frequency is always $n/18=50/18=2.78$. The number of degrees of freedom (df) is then always 18−3=15.

Chi-square tests for angular dispersion and azimuthal dispersion about the vector mean confirm the appropriateness of the spherical normal model. The chi-square values for angular dispersion ($\chi^2(\hat{\psi})$) of 74.4 percent of the 156 determinations made on the conglomerates do not vary significantly (0.05 level) from a spherical normal distribution, nor do the chi-square values for azimuthal disperson ($\chi^2(\hat{\chi})$) of 84.0 percent.

The consistency of each determination (50 *c*-axis orientations) is shown by the value of R, the vector magnitude (fig. 21*A*). The vector magnitudes of the 156 determinations in the conglomerates range from 35 (70 percent) to 47 (94 percent) and average 42.8 (85.6 percent). The values for R are much larger than the significance point (0.05 level) of $R=11.4$ calculated by Watson's (1956) method for testing randomness of direction; in other words, none of the 156 determinations of 50 *c*-axis orientations each used in this study comes close to being randomly oriented.

The precision of each determination is measured by the radius of the spherical circle of confidence and can be calculated from R and from n, the number of *c*-axis measurements per determination (fig. 21*B*). For the 156 determinations in the conglomerates, the radii of the circles of confidence (95 percent) range from 5° to 13° and average 8.3°. In other words, both azimuth and inclination of each vector mean can be expected to be within ±5° to ±13° (95-percent confidence).

COMPARISON OF IMBRICATION IN CONGLOMERATES WITH THAT IN MODERN STREAMS

Imbrication is well developed in streambeds of Jackson Hole, where quartzite roundstones derived from the Harebell and Pinyon conglomerates are abundant (fig. 22). At each of 24 stations in the streambeds, 50 *c*-axis orientations were measured, and the statistics were summarized by use of the spherical normal distribution (table 12). The imbri-

TABLE 12. — *Imbrication statistics for 24 determinations of 50 c-axis orientations each in modern streams of Jackson Hole*

[Each determination was calculated by averaging 50 *c*-axis orientations. Stations are located in fig. 2. $\bar{\theta}$=vector mean azimuth; $\bar{\phi}$=vector mean inclination; R=vector magnitude; $c_{0.95}$=radius of spherical circle of confidence; k=an indicator of dispersion; $\chi^2_{(\hat{\phi})}$=chi square for angular dispersion about the vector mean; df=degrees of freedom for $\chi^2_{(\hat{\phi})}$; and $\chi^2_{(\hat{\alpha})}$=chi square for azimuthal dispersion about the vector mean (with 15 degrees of freedom)]

Station No.	$\bar{\theta}$ (degrees)	$\bar{\phi}$ (degrees)	R (absolute value)	$c_{0.95}$ (degrees)	k	$\chi^2_{(\hat{\phi})}$	df	$\chi^2_{(\hat{\alpha})}$ ($15df$)
171	267.2	61.4	45.8	6.1	11.7	8.8	8	11.1
174	279.5	68.2	43.3	7.9	7.3	21.7	11	14.0
175	209.9	59.9	39.8	10.2	4.8	14.4	13	24.8
176	238.8	63.4	44.4	7.1	8.8	16.1	10	15.4
177	189.0	59.8	44.2	7.3	8.5	16.2	10	19.0
178	143.4	56.7	44.9	6.8	9.6	5.5	9	29.1
179	262.7	67.2	45.9	6.0	12.1	9.5	8	15.4
184	11.9	62.3	42.3	8.6	6.4	7.8	11	16.1
186	258.4	57.5	45.2	6.6	10.2	29.3	9	22.6
187	261.7	63.9	45.4	6.4	10.6	7.8	9	16.9
188	214.9	60.5	44.7	6.9	9.3	13.7	9	31.9
198A	198.8	66.1	45.5	6.3	10.9	5.7	9	7.5
198B	259.3	65.3	44.3	7.2	8.6	11.1	10	16.9
199	129.2	52.3	43.1	8.1	7.1	11.1	11	16.9
202A	125.2	62.5	45.4	6.4	10.8	10.2	9	11.8
202B	169.7	58.6	44.2	7.3	8.4	14.8	10	16.1
237	254.5	61.4	45.1	6.6	10.0	9.1	9	11.8
238	2.6	58.3	44.2	7.3	8.4	14.7	10	19.0
239A	357.0	63.3	46.6	5.4	14.4	5.5	7	17.6
239B	16.1	66.2	44.7	6.9	9.2	7.9	9	11.8
240	335.2	64.8	45.4	6.4	10.7	6.8	9	13.3
241	351.0	69.2	43.8	7.5	8.0	6.4	10	10.4
242	308.2	59.6	44.6	7.0	9.1	4.7	8	17.6
243	309.9	62.7	46.0	5.9	12.4	9.8	8	21.2

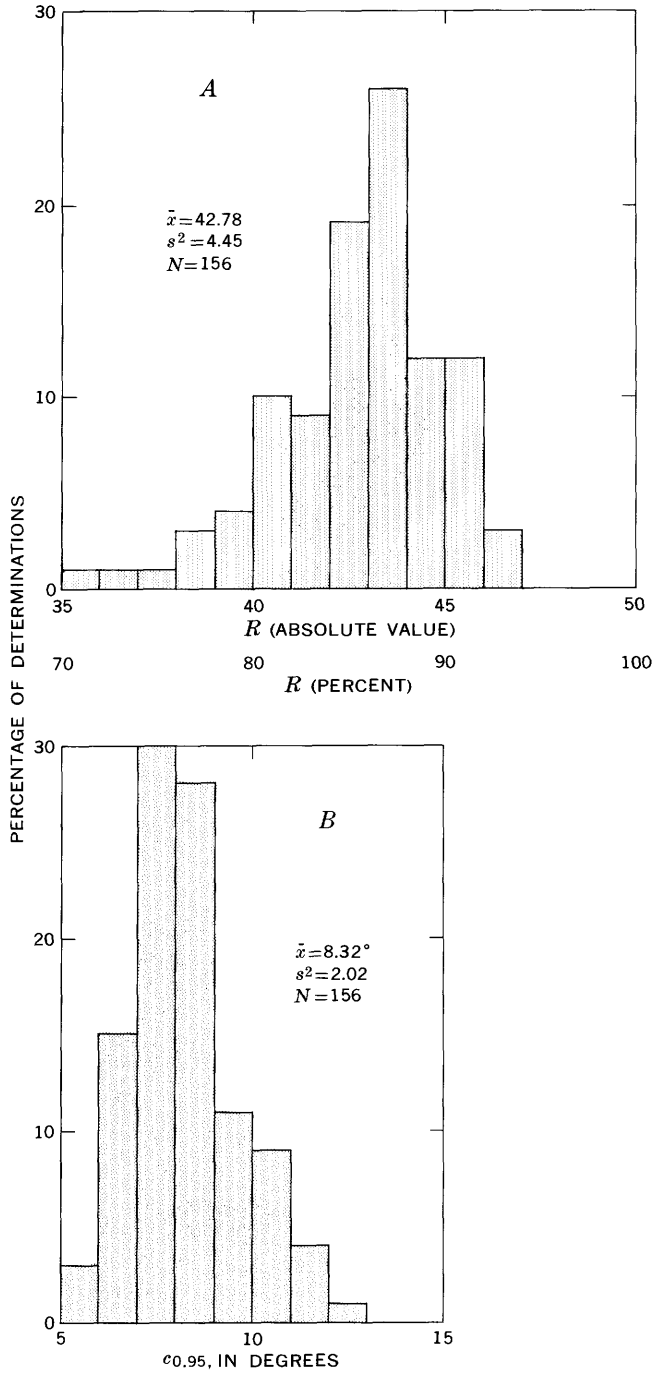

FIGURE 21. — Frequency distribution of the vector magnitudes (R) and of the radii of the spherical circles of confidence ($c_{0.95}$) for 156 determinations consisting of 50 *c*-axis orientations each. *A*, Vector magnitudes; *B*, radii of spherical circles of confidence. $\bar{x}$, arithmetic mean; s^2, variance; N, number of determinations. All determinations are from the Harebell Formation and the Pinyon Conglomerate. For a sample of 50 *c*-axis orientations to have a probability of $\geq$0.05 of being drawn from a randomly oriented population, R must be $\leq$11.4 (22.74 percent).

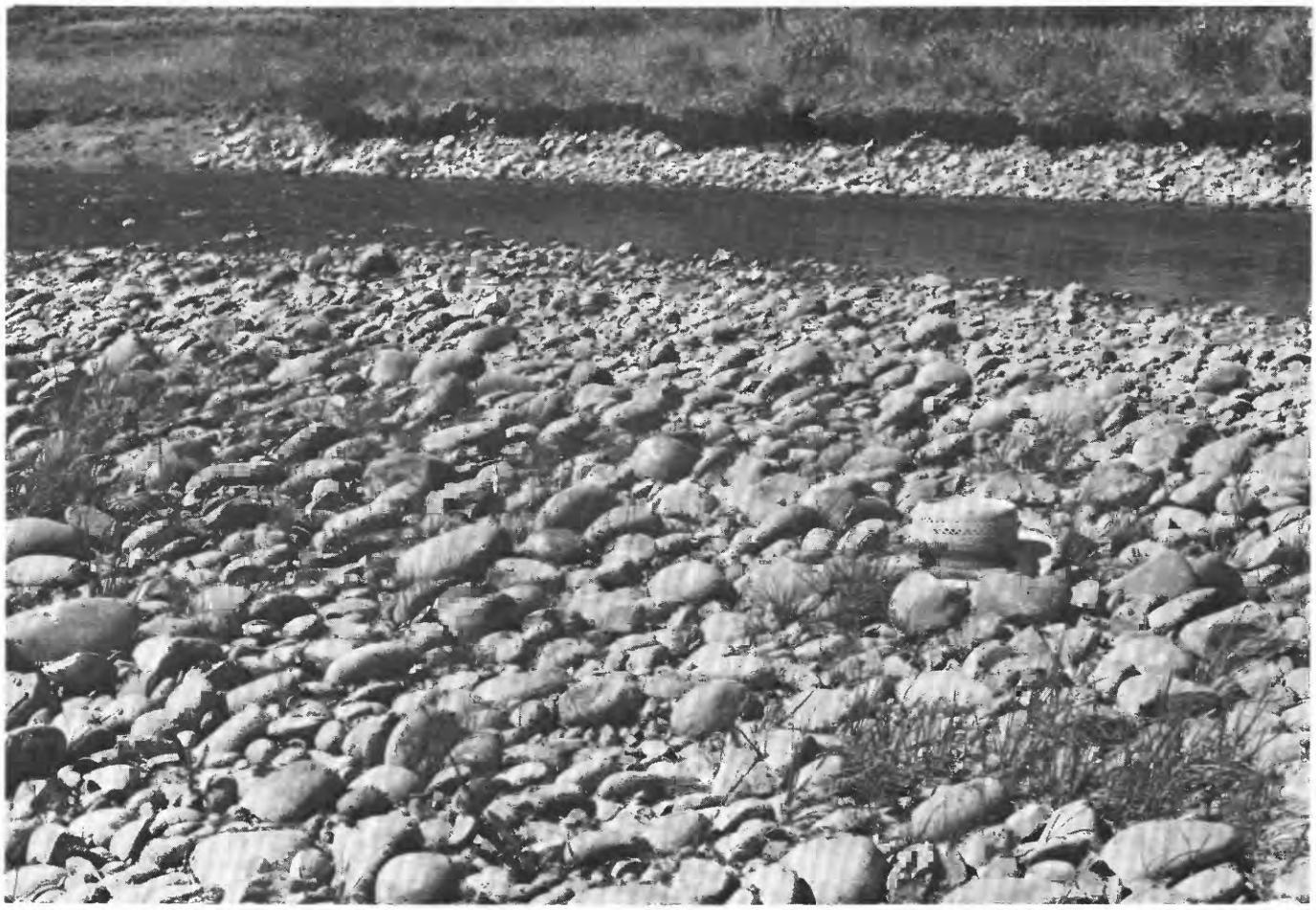

FIGURE 22. — Imbrication of quartzite roundstones derived from the Pinyon Conglomerate on the North Fork of Fish Creek. Stream in background flows from left to right.

cation dips upstream at all the stations studied, which is in general agreement with the dips observed for other fluvial deposits (Pettijohn, 1957, p. 250–251). Hence, the vector mean azimuth for *c*-axis orientations points downstream in all the streambeds studied and also in the conglomerates.

The inclinations of *c*-axis vector means computed for imbrication in the Jackson Hole region (fig. 23) average 61.6° for conglomerate roundstones and 62.2° for stream roundstones. These figures correspond to an upstream inclination (*ab* plane) of about 28°–29°, the general range for fluvial deposits that Cailleux (1945) reported, and they contrast with his very low inclinations for marine imbrication. In a brief survey of the literature on imbrication, Pettijohn (1957, p. 250–251) noted disagreement among the findings of Cailleux and those of Krumbein (1939, 1940, 1942; see also calculations of inclination on Krumbein's data by White, 1952). Krumbein's imbrication data are difficult to compare with those from the Harebell and Pinyon conglomerates because (a) pebble long axes instead of short axes were measured at San Gabriel Canyon, Calif. (1940), and Arroyo Seco, Calif. (1942), and (b) both these deposits and the glacial outwash studied (Krumbein, 1939) consisted of poorly sorted and poorly rounded stones in comparison with the conglomerates of Jackson Hole. Later studies have reported upstream inclinations of 20°–25° (Sedimentary Petrology Seminar, 1965) and 14°–25° (Schlee, 1957a) for fluvial gravels, somewhat less than the inclination observed in the conglomerates. In summary, it seems best to compare the inclination of roundstone imbrication in the conglomerates with that in modern streams of Jackson Hole, inasmuch as the same quartzite stones dominate both. The similarity of the degree of roundstone inclination in conglomerates to that in streams supports the interpretation of a fluvial environment of deposition for the conglomerates.

The variance of *c*-axis inclinations for roundstones is much less in modern streams than in the conglom-

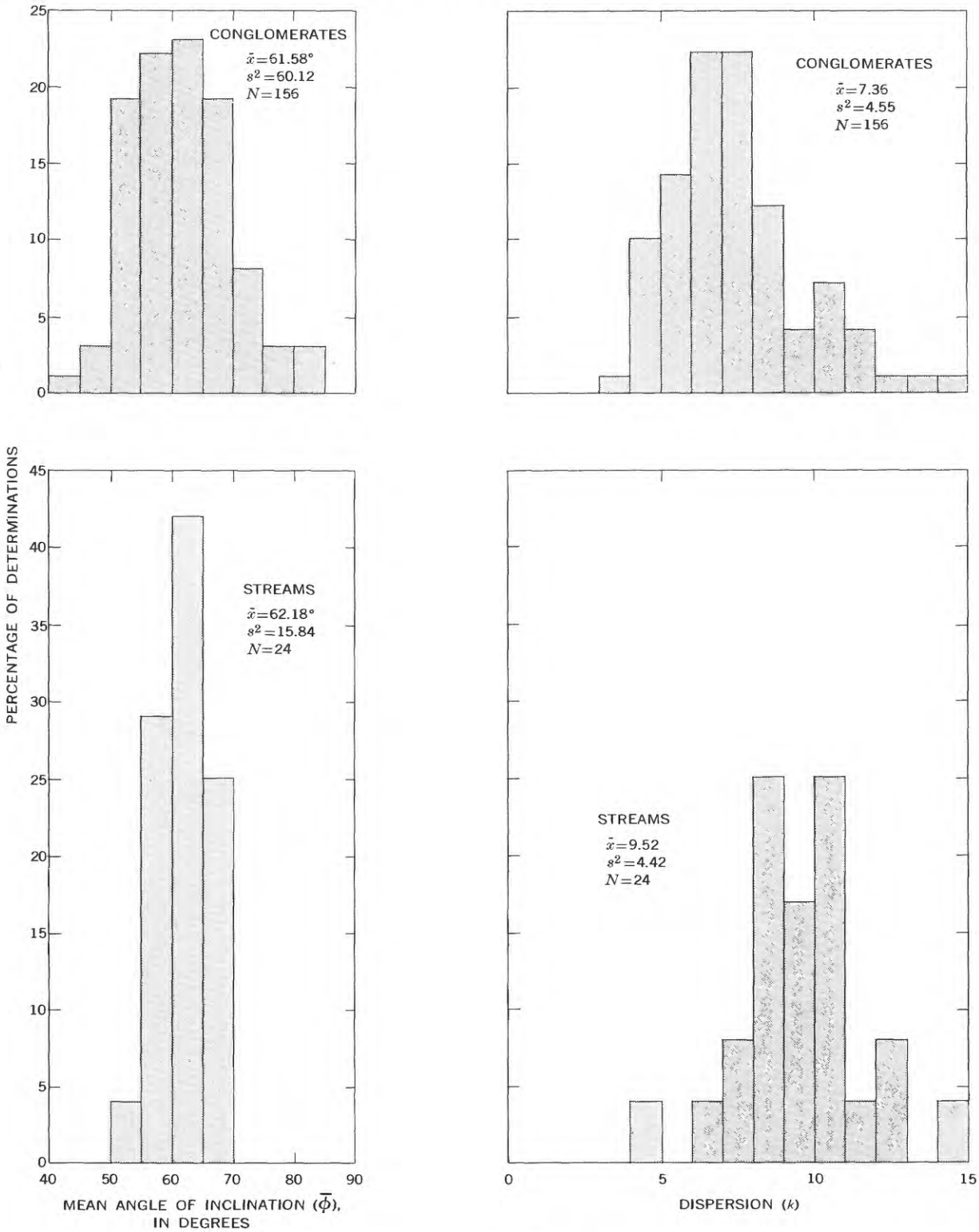

FIGURE 23. — Comparison of mean angle of inclination ($\bar{\phi}$) and dispersion (k) of c-axis orientations between roundstones from the Harebell Formation and the Pinyon Conglomerate and roundstones from modern streams in Jackson Hole. The average of the mean inclination angles for conglomerates is not significantly different from that for streams at any acceptable level. The average dispersion for the conglomerates is significantly different from that for streams at the 0.01 level. $\bar{x}$, arithmetic mean; s^2, variance; N, number of determinations.

erates. The difference may result from two factors: (a) orientation of stones in the conglomerates may be affected by compaction or tectonism, and (b) *c*-axis measurements may be rotated by an incorrect amount when bedding is restored to horizontal. Bedding in the conglomerate is difficult to measure precisely, and errors in measurement may lead to undercompensation or overcompensation when the data are rotated, especially if bedding strike and imbrication azimuth intersect at a large angle.

Dispersion of orientations in roundstone imbrication in Jackson Hole (fig. 23) is significantly greater in the conglomerates (average k=7.4) than in modern streams (average k=9.5). (The computed indicator of dispersion (k) becomes larger as dispersion decreases.) The greater dispersion noted for the conglomerates may be due to two causes: (a) different original orientation related to differences in size, shape, or sorting, and (b) compaction or tectonic deformation causing reorientation of the conglomerate stones. The effects of the latter are commonly visible in outcrop, but differences in size, shape, or sorting between the conglomerate roundstones and the stream sediments appear minimal. Therefore compaction or tectonic deformation is viewed as the most likely explanation for the differences in orientation dispersion.

PALEOCURRENTS

Paleocurrent directions as interpreted from the azimuth of the *c*-axis vector mean for each determination are shown in figure 24. In general, imbrication-orientation data show that paleocurrents flowed east-northeasterly (mean direction=78.2°) in the northern facies and south-southeasterly (mean direction=163.9°) in the southern facies. Imbrication azimuths in figure 24 likewise define two distinct paleocurrent systems: one associated with the northern facies and one with the southern facies. Within the northern facies, no differences in imbrication orientation are apparent between the Pinyon Conglomerate and the Harebell Formation. The small standard deviations of ±42.6° and ±49.6° for the northern and southern facies respectively indicate that arithmetic averaging of vector azimuths will produce reliable approximations in further computations.

Maps of moving-average vector azimuths for the northern and southern facies were prepared by computer (fig. 25). The azimuthal data were gridded by computing a weighted moving-average direction at each grid intersection (grid cell=2 miles square, oriented north-south). Each grid value was computed from the eight nearest vector azimuths by weighting each azimuth inversely with respect to its distance from the grid intersection and then taking the arithmetic average of the weighted azimuths. In the northern facies this involved subtracting azimuths in the northwest quadrant from 360° and changing the sign to negative in order to average the data properly with the predominantly east-northeast paleocurrents. The gridded azimuth values were then plotted as vectors.

In addition to smoothing the directional data by the moving-average method, it was desired to determine what, if any, local trends are present within each facies. Generally, more than one imbrication determination was made at each station, thus allowing computation of the precision of the station vector means. The 152 determinations from both facies are readily grouped at two additional levels: 82 stations (42 in the northern facies and 40 in the southern facies) and two facies (northern and southern). Analysis of variance (Krumbein and Graybill, 1965, p. 191–221) showed highly significant differences between facies, as might be expected, but not between stations (table 13). The largest variance component exists at the facies level, the next largest at the determination level, and the smallest at the station level (table 13). Comparison of the variance component at the determination level with that at the station level suggests that a minimum of 10–20 determinations per station are required to detect significant differences between stations. Because only about two determinations per station were made, the precision of the station vector means is very poor, and the moving-average map is not likely to show real variation within each facies.

TABLE 13. — *Analysis of variance and estimates of variance components for imbrication azimuths (three-level nested design)*

[Computed from data in table 11]

ANALYSIS OF VARIANCE

Level	Degrees of freedom	Sum of squares	Mean square	*F* value	Significance
Total	150	602,810			
Between facies	1	285,660	285,660.0	121.87	<0.0001
Between stations within facies	80	187,520	2,344.0	1.25	None
Between determinations within stations	69	129,630	1,878.7		

ESTIMATES OF VARIANCE COMPONENTS

Level	Variance component	Unit size
Facies	3,771.5	2
Station	253.6	82
Determination	1,878.7	151

CROSSBEDDING AND RIPPLE CROSS-LAMINATION

HAREBELL AND PINYON PALEOCURRENTS

In the sandstones of the Harebell Formation and the Pinyon Conglomerate, festoon crossbedding is common, and ripple cross-lamination is present locally. Crossbedding is not common in the conglomerates but does occur locally in sandstone lenses (fig. 26). As many measurements as possible (one to 15)

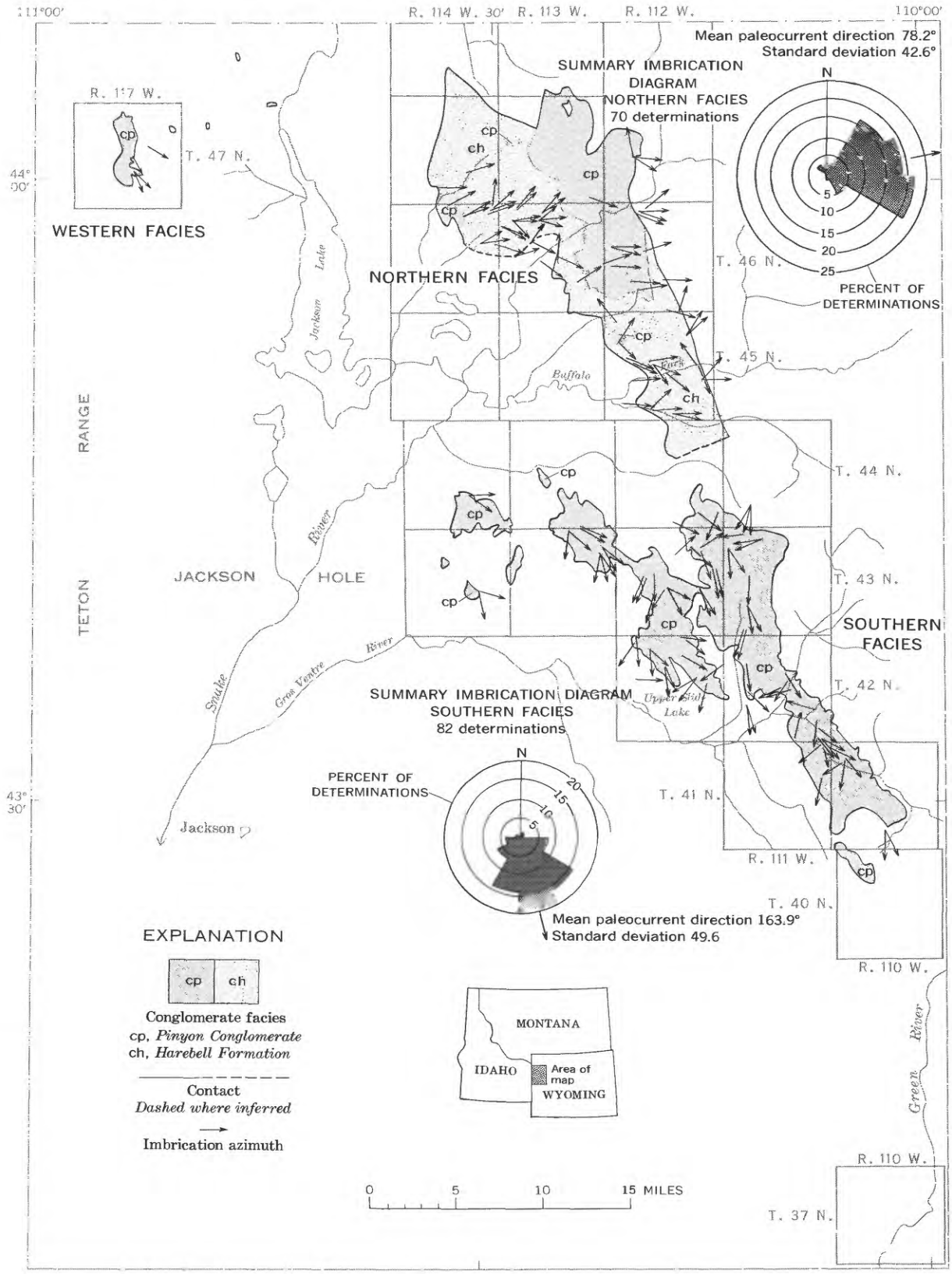

FIGURE 24. — Paleocurrent directions as interpreted from imbrication azimuths in the Harebell Formation and the Pinyon Conglomerate. Each arrow is the azimuthal result of 50 *c*-axis orientations (one determination).

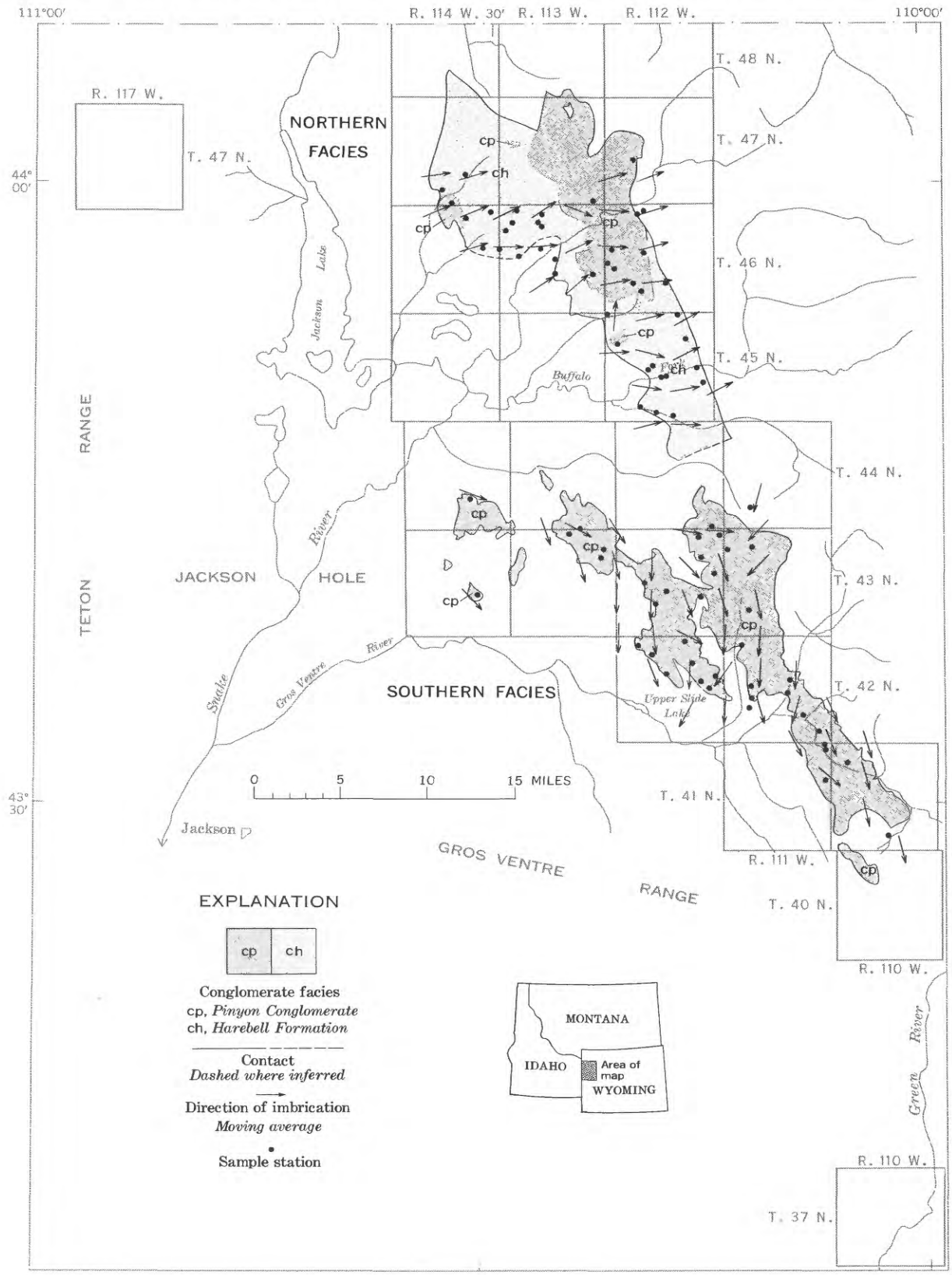

FIGURE 25. — Moving-average directions based on imbrication in the Harebell Formation and the Pinyon Conglomerate.

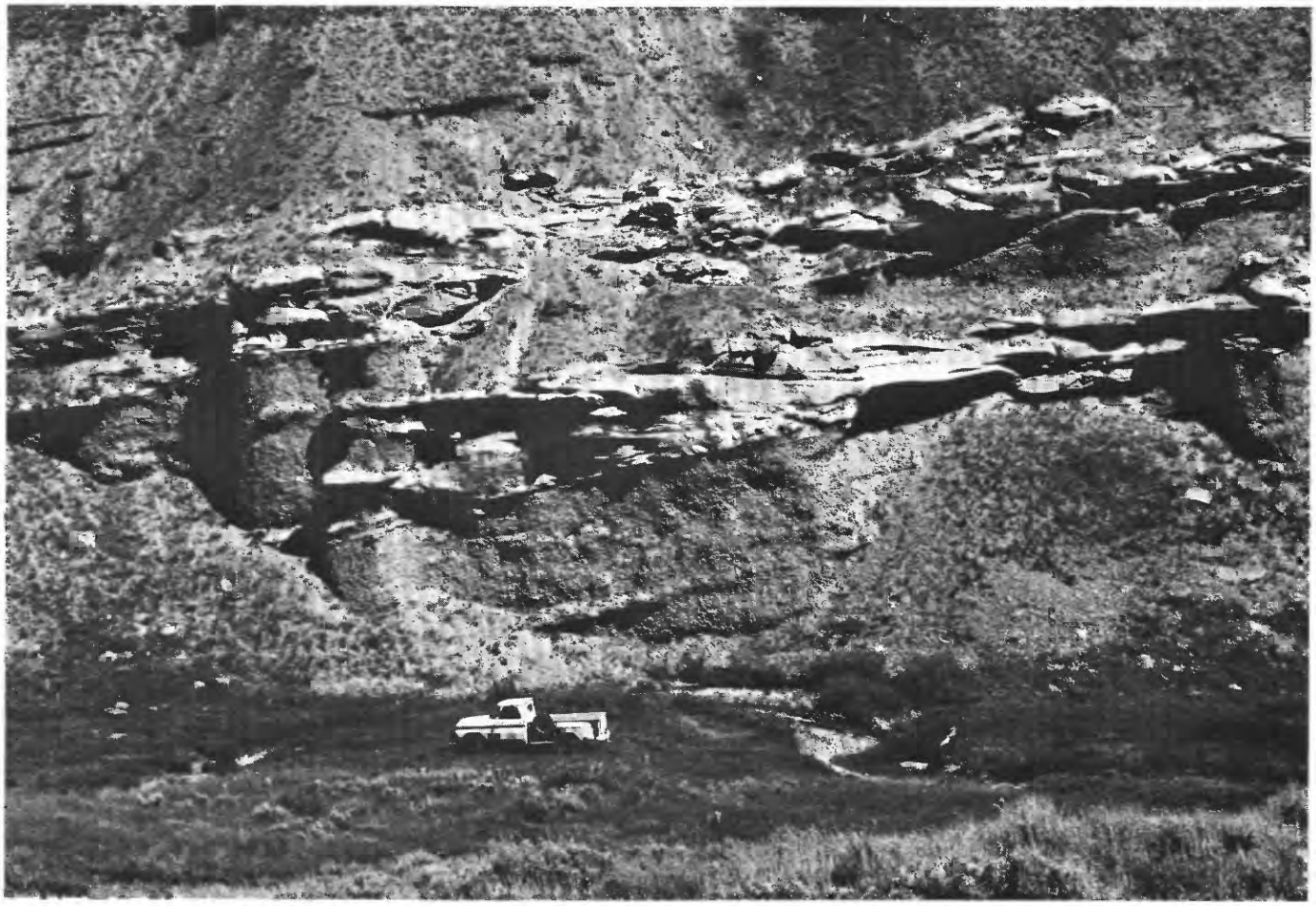

FIGURE 26. — Large-scale festoon crossbedding in sandstone lenses near the top of the Pinyon Conglomerate on Purdy Creek, a tributary to the South Fork of Fish Creek.

were taken at each outcrop to determine paleocurrents in the sandstones and to check conglomerate paleocurrents deduced from roundstone imbrication. Crossbedding orientations were restored to original orientations by rotating the bedding planes to horizontal; vector mean azimuth and vector magnitude were computed for each station (fig. 27). Crossbedding dip azimuths in both the northern conglomerate facies (95.4°) and the underlying Harebell sandstones (63.8°) were found to be easterly and northeasterly, in close agreement with imbrication data from the conglomerates. Crossbedding dip azimuths in the southern conglomerate facies are south-southeasterly (163.5°), also in close agreement with imbrication data. Harebell crossbedding in the south was too variable and sparse to yield clearly a preferred orientation. Crossbedding orientation confirms the upcurrent inclination of imbricated roundstones in the conglomerates and agrees well with the paleocurrent directions determined from imbrication orientation.

UPPER CRETACEOUS AND PALEOCENE PALEOCURRENTS COMPARED

Most of the Harebell and Pinyon paleocurrent systems are strongly unidirectional, a feature consistent with fossil evidence for a continental alluvial environment. The underlying Upper Cretaceous sandstones and shales contain both marine and continental strata, and fossil evidence suggests the proximity of a marine environment for parts of the Harebell Formation. Crossbedding orientation in strata above and below the Harebell and Pinyon south of Buffalo Fork was studied briefly to assess marine influence on paleocurrent orientation and to determine what, if any, information might be gained concerning the source of these sediments. The crossbedding azimuths exhibited two distinct types of distribution (fig. 28): (1) bimodal symmetrical distribution for the mixed marine and continental sandstones (the Bacon Ridge Sandstone, the lenticular sandstone and shale sequence, and the Mesaverde Formation), and (2) unimodal distribution for the

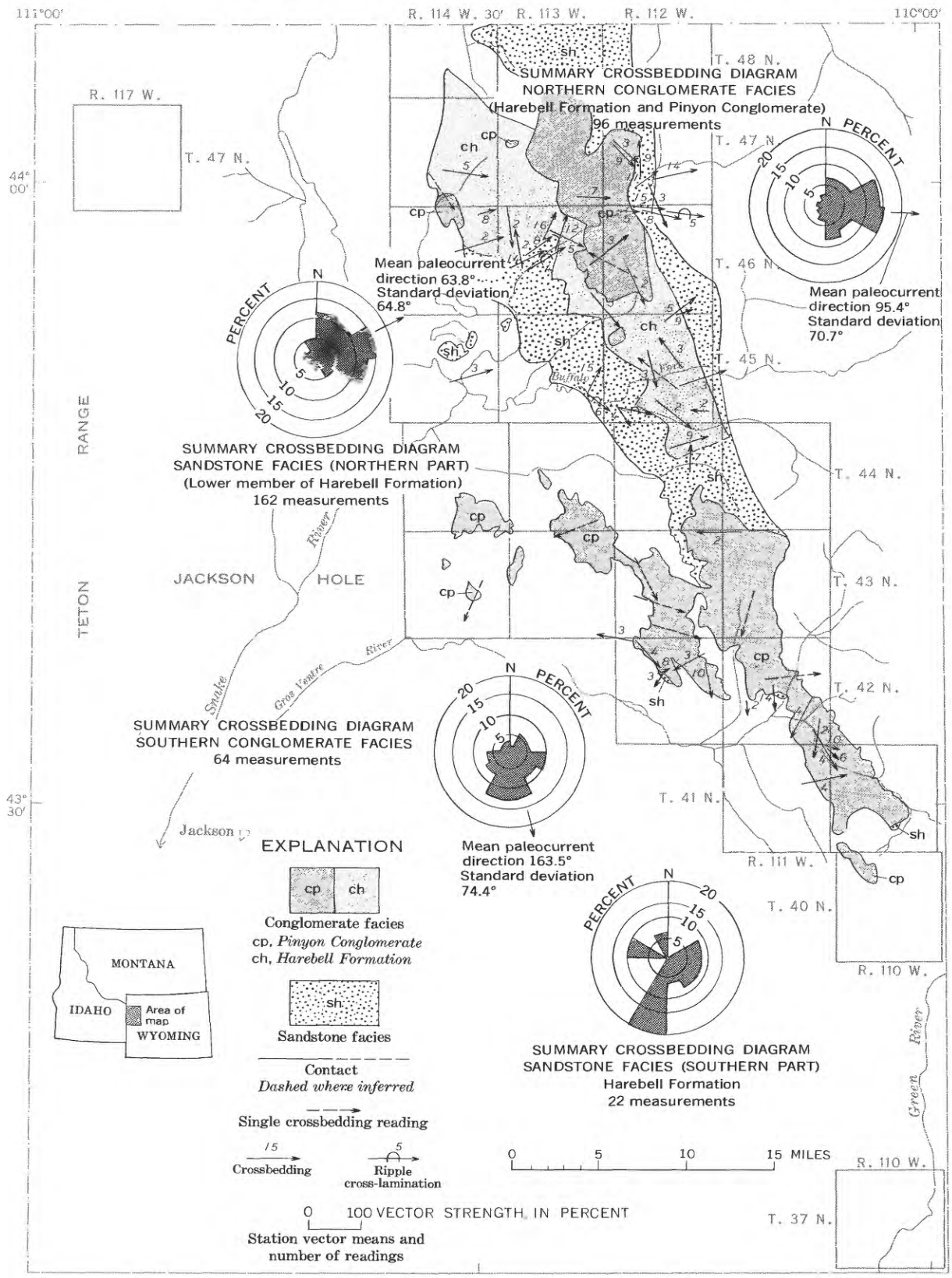

FIGURE 27. — Crossbedding orientation in the Harebell Formation and the Pinyon Conglomerate.

overlying continental clastics (Harebell Formation, Pinyon Conglomerate, and unnamed sandstone and claystone sequence). In the Upper Cretaceous and Paleocene of Jackson Hole, a clear distinction is apparent between marine-continental and continental paleocurrent systems, and both the Harebell Formation and the Pinyon Conglomerate bear the stamp of a continental system. The bimodality of the continental-marine paleocurrents probably reflects the alternation of these two environments, whereas the unimodality of the continental clastics reflects fluvial transport from western and northwestern sources.

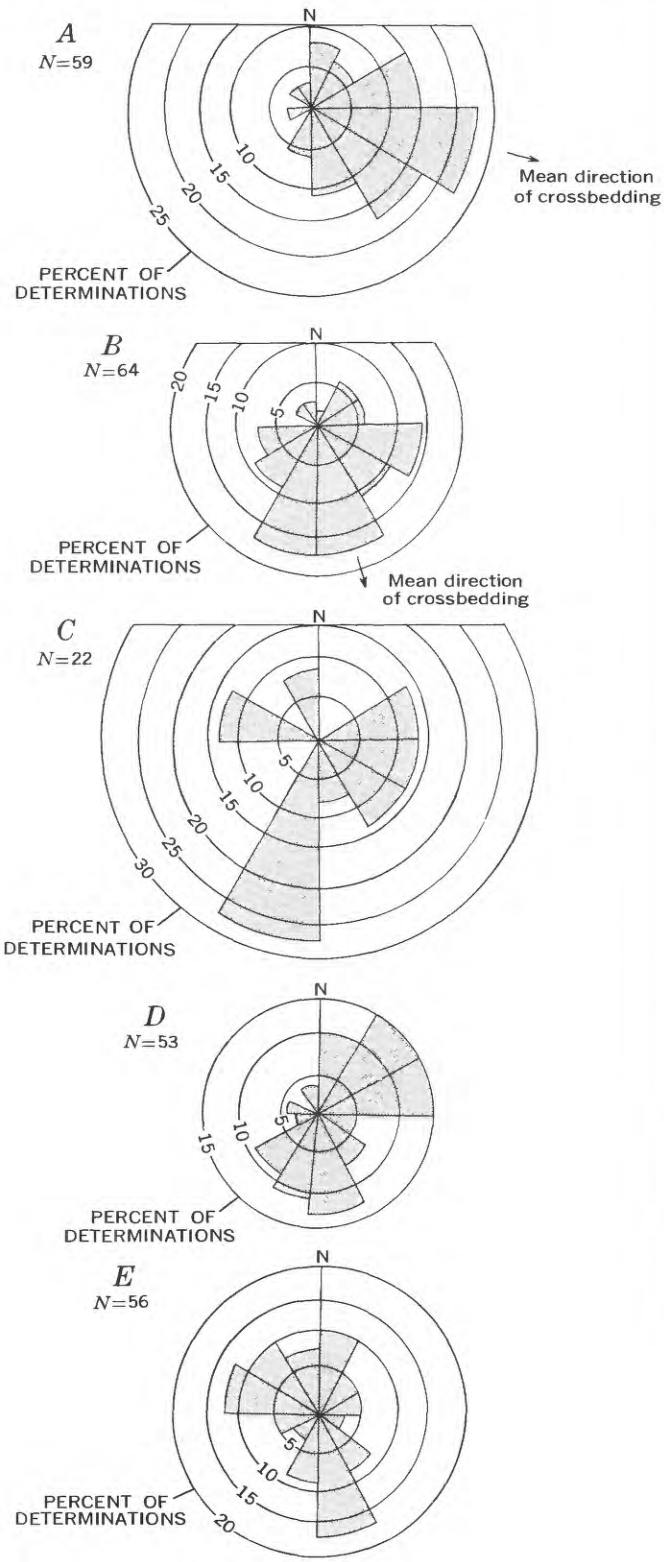

FIGURE 28. — Paleocurrent directions as interpreted from crossbedding orientations in Upper Cretaceous and Paleocene rocks between the Gros Ventre River and Buffalo Fork. *A*, Unnamed sandstone and claystone sequence; *B*, Pinyon Conglomerate; *C*, Harebell Formation; *D*, Mesaverde Formation and underlying lenticular sandstone and shale sequence; *E*, Bacon Ridge Sandstone. *N*, number of measurements.

REGIONAL VARIATION OF QUARTZITE ROUNDSTONE SIZE

Grain size is an indicator of paleostream competency in clastic deposits and is commonly used to determine source, paleocurrent directions, and location of paleostreams (Potter and Pettijohn, 1963, p. 202–205). Grain-size distributions in very coarse conglomeratic sediments are impractical to analyze in the large numbers necessary to evaluate regional trends; therefore, the standard practice of measuring the 10 largest particle sizes at each outcrop was applied. In the conglomerate facies, the maximum dimension (length) of 973 roundstones was measured (table 14) at a total of 98 stations: three stations in the western facies, 46 in the northern facies, and 49 in the southern facies. At each station, the 10 largest roundstones seen were measured, except at two stations where only eight roundstones were measured and at one station where only five were measured. North of the Teton Range (western facies), maximum quartzite roundstone length (the longest of the 10 largest stones for each station) ranges from 14 to 50 inches, and the mean maximum length (the average length of the 10 largest stones for each station) ranges from 12 to 22 inches. In the northern facies, maximum quartzite roundstone length ranges from 9 to 19 inches, and mean maximum length ranges from 8 to 14 inches. In the southern facies, maximum length ranges from 12 to 21 inches, and mean maximum length ranges from 9 to 17 inches. Frequency distributions of mean maximum lengths show that roundstones are significantly longer in the southern facies than in the northern facies (fig. 29; table 15).

Before the regional variation of roundstone length was studied further, the data were examined for stratigraphic variation. Love (1972, table 1) suggested that roundstones are generally smaller in the Harebell Formation than in the Pinyon Conglomerate. If this stratigraphic distinction applies also

TABLE 14. — *Length of largest quartzite roundstones at stations in the western facies (Pinyon Conglomerate), the northern facies (Harebell Formation and Pinyon Conglomerate), and the southern facies (Pinyon Conglomerate)*

[Station localities are shown in fig. 2]

Western facies (Pinyon Conglomerate)

Sta. No.	Length (in.)	Sta. No.	Length (in.)	Sta. No.	Length (in.)	Sta. No.	Length (in.)
53	11.5	53	10.0	54	12.0	56	16.0
	9.0		10.0		13.0		18.0
	12.0		14.0		12.5		14.0
	12.5	54	13.0		13.5		15.0
	14.0		12.5		14.0		13.0
	12.0		13.0		12.0		15.0
	11.5		11.0	56	50.0		15.0

Northern facies (Harebell Formation and Pinyon Conglomerate)

15	10.0	40	9.5	48	11.0	62	12.0
	10.0		10.0		12.0		12.0
	11.0		12.0		13.0		
	9.0		11.0				12.0
	9.0				11.0		13.0
			13.5		10.5		14.0
	10.0		10.5		12.0		18.0
	10.0		11.0		12.0		17.0
	10.0		12.0		11.0		
	10.0					73	12.0
	10.0	41	7.0	49	10.0		10.5
			8.0		10.0		9.5
17	10.0		8.0		11.0		10.0
	11.0		9.0		9.0		9.0
	11.0		9.0		9.5		
	11.0						10.0
	10.0		9.0		10.0		11.5
			7.5		11.0		13.0
	11.0		8.0		9.0		9.5
	11.0		8.0		10.0		10.0
	12.0		9.0		10.0	75	10.0
	10.0						9.5
	12.0	43	10.0	50	11.0		10.0
			12.0		11.0		11.0
18	7.5		12.0		11.0		11.0
	8.0		12.0		10.0		
	8.0		10.0		12.0		11.5
	7.5						10.5
	9.5		13.0		10.0		12.0
			10.0		11.5		9.5
	10.0		11.0		10.0		9.5
	8.0		10.0		11.5		
	8.0		12.0		10.0	76	11.0
	8.0						9.0
	7.5	44	9.0	51	10.5		10.0
			9.0		12.0		10.0
29	7.0		9.0		13.0		11.0
	9.0		9.0		10.0		
	8.0		12.0		13.5		10.0
	8.0						9.5
			10.0		10.0		10.0
	8.0		10.0		12.0		11.0
	8.0		11.0		10.5		12.0
	10.0		9.0		10.5		
	8.0		9.0		11.0	77	11.5
							11.5
34	10.0	45	10.0	57	10.5		12.0
	10.0		11.0		11.0		11.5
	11.0		12.0		12.0		13.0
	10.0		12.0		9.0		
	10.0		12.0		9.5		11.0
							11.0
	9.0		13.0		12.0		12 0
	10.0		10.5		10.0		13.5
	10.0		11.0		11.0		13.5
	10.0		12.0		12.5		
	11.0		10.0		13.0	78	9.5
							11.0
38	9.0	46	9.0	58	14.0		12.0
	9.0		9.5		11.0		10.5
	11.0		10.5		9.0		9.5
	8.0		10.0		10.0		
	9.0		9.0		10.5		10.0
							10.0
	10.0		8.0		10.5		9.5
	11.0		9.5		11.5		11.0
	9.0		14.0		10.5		12.0
	10.0		9.0		9.0		
	9.0		9.0		9.0	245	9.0
							8.0
				59	15.5		8.5
39	7.5	47	12.5		10.0		10.0
	7.5		19.0		10.5		8.5
	9.0		12.0		13.0		
	9.0		12.0		12.0		7.5
	7.5		12.0				8.0
					12.0		9.0
	8.0		15.0		12.0		10.5
	8.0		13.0		12.0		10.0
	10.0		15.0		10.0		
	7.5		13.0		10.0	83B	12.0
	9.0		13.0				10.5
				62	12.5		14.0
40	10.0	48	11.0		12.0		9.5
	11.0		12.5		13.0		10.0

Northernn facies—Continued

83B	10.5	259	12.0	269	12.0	274	10.5
	9.5		12.0		11.5		11.0
	12.0				16.0		
	9.5	260	9.5		12.0		14.0
	9.5		10.0		12.0		12.0
			10.5				12.0
247	12.0		9.5		12.0		11.5
	10.5		12.0		12.5		12.5
	11.0				12.0		
	16.0		9.5		13.0	31	10.0
	17.0		10.0		16.0		11.0
			11.0				10.0
	13.0		10.5	270	12.0		10.0
	12.5		9.5		13.0		11.0
	12.0				13.0		
	11.5	265	11.0		12.0		10.0
	11.0		11.0		12.0		9.0
			12.5				9.0
248	11.0		13.5		12.0		9.0
	11.0		12.0		12.0		9.0
	11.0				12.0		
	11.5				12.5	279	12.0
	11.0		12.0		16.0		12.0
			11.0				11.0
	12.0		13.0	271	15.5		11.0
	12.0		13.0		12.0		12.0
	11.0		12.5		14.5		
	14.0				11.5		13.0
	14.0	266	14.5		13.5		12.0
			12.0				12.0
256	10.5		12.0		11.5		12.5
	13.0		12.0		13.0		12.0
	10.0		13.0		13.5		
	10.5				12.0	260	9.5
	11.0		12.0		12.0		10.0
			12.5				10.5
	12.5		15.0	272	15.0		9.5
	11.0		13.5		13.0		12.0
	11.5		14.0		13.0		
	12.5				15.5		9.5
	14.0	268	12.0		13.0		10.0
			14.0				11.0
259	10.0		14.0		14.0		10.5
	10.5		14.0		13.5		9.5
	11.0		13.0		15.0		
	11.5				13.0	277	11.5
	10.0		14.5		14.0		10.5
			12.5				10.5
	10.5		12.0	274	12.5		14.0
	10.0		12.5		11.5		13.0
	11.5		16.5		12.5		

Southern facies (Pinyon Conglomerate)

1	8.5	9	10.0	71	13.5	88	15.0
	8.5		10.5		13.0		14.5
	10.3		9.5		13.5		12.5
	8.0		10.5		15.0		13.0
	10.7		9.5		13.5		
						89	13.5
	10.7	10	11.0		13.0		14.5
	11.5		10.5		16.0		14.0
	12.9		11.0		13.0		16.0
	10.3		13.0		13.5		13.5
	8.5		12.0		15.0		
							14.0
2	17.0		12.0	72	14.5		14.0
	13.0		12.0		17.0		14.0
	12.0		12.0		15.0		17.0
	12.0		11.0		14.5		19.0
	12.0		12.0		15.5		
						90	11.0
					16.5		10.5
	11.0	20	10.0		15.0		12.5
	11.0		10.0		15.0		12.5
	11.0		11.0		14.5		12.0
	11.0		10.0		16.5		
	11.0		11.0				11.5
				87	15.0		13.0
4	16.0		10.0		15.0		10.5
	12.0		9.0		13.5		11.0
	11.0		12.0		13.0		11.0
	11.0		11.0		13.0		
	10.0		10.0			91	12.0
					13.0		10.0
	10.0	64	14.0		16.5		10.5
	10.0		14.0		14.0		11.0
	10.0		16.0		14.5		11.5
	10.0		15.5		18.0		
	10.0		14.5	88	13.5		10.5
					15.0		10.0
9	11.5		14.0		13.0		12.0
	9.5		15.5		13.0		13.0
	11.0		13.5		15.5		17.0
	10.0		14.5				
	12.0		15.5		15.0	92	12.5

TABLE 14. — *Length of largest quartzite roundstones at stations in the western facies (Pinyon Conglomerate), the northern facies (Harebell Formation and Pinyon Conglomerate), and the southern facies (Pinyon Conglomerate)*—Continued

Sta. No.	Length (in.)	Sta. No.	Length (in.)	Sta. No.	Length (in.)	Sta. No.	Length (in.)
Southern facies—Continued							
92	12.5	97	14.5	172	13.0	183	12.5
	15.0				13.5		15.5
	11.5		15.0				13.5
	14.0		17.0	173	14.5		12.5
			16.0		16.0		
	14.5		15.0		14.5		14.0
	13.5		15.0		14.0		12.5
	15.0				14.5		12.5
	11.5	137	10.0				15.0
	13.5		9.0		15.0		14.5
			8.5		14.5		
94	13.0		8.5		14.5	185	12.5
	14.0		9.0		14.5		13.5
	16.0				19.5		11.5
	16.0		10.5				11.5
	15.0		12.0	180	11.0		11.0
			9.5		10.5		
			10.0		14.0		15.0
	13.0		10.5		10.5		11.5
	13.0				12.0		15.0
	14.0	138	14.0				11.0
	14.0		10.5				11.5
	15.0		10.0		12.0		
			10.0		11.0		
95	12.5		10.0		11.0	189	15.0
	14.0				11.0		13.0
	12.5		10.0		13.5		15.0
	19.0		13.5				15.0
	20.0		12.0	181	17.5		13.0
			10.0		12.5		
			12.0		11.5		15.5
	13.5				13.0		14.0
	13.0	139	10.0		13.5		14.0
	13.0		10.5				14.0
	14.0		11.5		11.5		14.5
	21.0		10.0		13.0		
			11.0		12.0	191	12.5
96	13.0				13.5		14.0
	14.0		10.5		12.5		11.5
	12.5		15.5				11.5
	15.0		13.0	182	12.5		12.0
	13.0		11.5		12.0		
			10.0		12.0		14.0
	14.5				12.5		14.5
	12.5	172	13.0		13.0		13.0
	14.0		13.0				13.5
	12.0		13.0		15.0		13.5
	12.5		13.5		13.0		
			13.0		12.0	193	16.0
97	13.5				12.5		13.0
	14.0		13.0		13.5		12.5
	13.5		18.0				14.0
	15.0		17.0	183	13.0		14.0

Sta. No.	Length (in.)	Sta. No.	Length (in.)	Sta. No.	Length (in.)	Sta. No.	Length (in.)
Southern facies—Continued							
193	15.0	204	10.5	212	15.0	219	12.0
	12.0				12.0		12.5
	13.5	205	15.0		13.0		13.0
	13.0		13.5				12.0
	14.0		13.5		13.5		
			13.5		13.0	222	15.0
194	13.5		13.0		12.5		15.0
	11.0				14.0		14.5
	12.0		13.0		13.0		15.0
	11.5		13.5				14.5
	16.0		14.0	213	14.0		
			17.0		16.5		14.5
	13.0		15.5		15.0		16.5
	13.0				13.0		16.0
	12.0	209	14.0		13.0		14.0
	12.0		15.0				15.0
	12.5		15.0		13.0		
			14.0		13.5	223	12.0
195	15.5		17.0		17.5		11.5
	11.5				15.5		14.0
	16.0		17.0		13.5		12.5
	12.5		15.0				11.5
	15.0		15.5	214	17.0		
			14.5		14.0		12.5
	15.5		14.5		14.5		11.5
	12.0				12.5		12.5
	13.0	210	16.0		16.0		13.5
	11.0		21.0				12.0
	12.0		14.5		13.5		
			19.5		14.0	11A–11	13.0
203	14.0		14.0		18.0		11.0
	11.5				14.0		11.0
	12.5		14.5		15.0		13.0
	12.5		13.5				11.0
	14.5		14.0	215	12.0		
			14.5		11.0		12.0
	14.0		17.5		11.0		11.0
	13.0				15.0		11.0
	13.5	211	16.0		12.0		11.0
	13.0		18.0				11.0
	13.0		17.0		18.0		
			17.0		15.0		
204	11.0		16.0		11.0	12–14	12.0
	12.5				12.5		12.0
	12.0		16.0		12.5		11.0
	12.0		17.0	219	16.5		12.0
	11.0		16.0		13.5		15.0
			20.0		12.5		
	10.5		15.0		13.0		11.0
	10.5				12.0		11.0
	11.0	212	12.5				14.0
	11.0		13.0		12.0		11.0

TABLE 15. — *Student's* t *tests for significant differences in mean maximum roundstone length between the northern and southern facies and between the Harebell Formation and the Pinyon Conglomerate within the northern facies*

[$\bar{x}$, arithmetic mean; s^2, variance]

	Number of stations	Maximum roundstone length (inches)		Student's t value	Degrees of freedom	Significance
		$\bar{x}$	s^2			
Northern and southern facies						
Northern facies	46	11.10	2.16	6.42	93	0.01
Southern facies	49	13.16	2.74			
Harebell Formation and Pinyon Conglomerate within northern facies						
Harebell Formation	32	10.93	2.21	1.13	44	None
Pinyon Conglomerate	14	11.47	2.00			

TABLE 16. — *Analysis of variance and estimates of variance components for measurements of mean maximum quartzite roundstone length (three-level nested design)*

[Computed from data in table 14]

ANALYSIS OF VARIANCE

Level	Degrees of freedom	Sum of squares	Mean square	F value	Significance
Total	942	4,856.5			
Between facies	1	1,049.2	1,049.20	42.62	<0.0001
Between stations within facies	93	2,289.7	24.62	13.76	<0.0001
Between measurements within stations	848	1,517.6	1.79		

ESTIMATES OF VARIANCE COMPONENTS

Level	Variance component	Unit size
Facies	2.1763	2
Station	2.3002	95
Measurement	1.7896	943

to the distribution of mean maximum roundstone length, then data from the northern facies must be subdivided into that from the Harebell Formation and that from the Pinyon Conglomerate before regional variation is analyzed. Accordingly, the data for the northern facies were subdivided and summarized statistically, and the t test was applied to detect stratigraphic variation (table 15). No significant difference in roundstone length was found, and therefore, combination of the data from the Harebell and the Pinyon of the northern facies seems justified.

Weighted-moving-average maps of mean maximum and maximum quartzite roundstone lengths

(figs. 30 and 31) were prepared by computer following the procedure described for imbrication vector maps. Quartzite roundstone length shows a general downstream decrease in both the northern and the southern facies (when downstream is defined by paleocurrent direction). In addition to downstream decrease, roundstone size in both facies also shows marked regional differences, including several lobate features near the upstream ends. These lobate features are of special interest inasmuch as they represent regions of maximum competency which may be interpreted as paleostream courses.

To evaluate the confidence to be placed on any interpretation of regional patterns, it is desirable to examine the precision of station values upon which the regional patterns are based. Therefore an analysis of variance (three-level nested model) similar to that made on imbrication data was performed (table 16). The analysis shows highly significant differences between facies and between stations; hence, the method used to sample for mean maximum roundstone length was adequate for distinguishing real differences in length between stations. The moving-average maps of roundstone length probably depict real variations within facies. Roundstone length at each station is known within ±1.3 inches (95-percent confidence interval), suggesting that contour intervals of about 1 inch are appropriate for the moving-average maps.

The regional variation of mean maximum quartzite length was further investigated by fitting trend surfaces of degree 1 through 5 to the data for each facies (computer program of Miesch and Connor, 1968). Total reduction of the sum of squares exceeds 50 percent for each facies (table 17). Analysis of variance of the trend-surface data was used to select surfaces which showed a significant fit over the preceding surfaces (table 18; Krumbein and Graybill, 1965, p. 333–337). The highest degree trend surfaces showing a more significant fit ($\geqslant$90-percent confidence level) over the preceding surface for both the northern and the southern facies were selected for contouring (fig. 32). These surfaces confirm the downstream decrease in roundstone size shown by the moving-average maps. The lobate features defined by the moving-average map of the northern facies are seen to coalesce in the cubic trend of that facies; this may be an overgeneralization to the trend-surface method, inasmuch as between-station differences in roundstone length were shown to be highly significant.

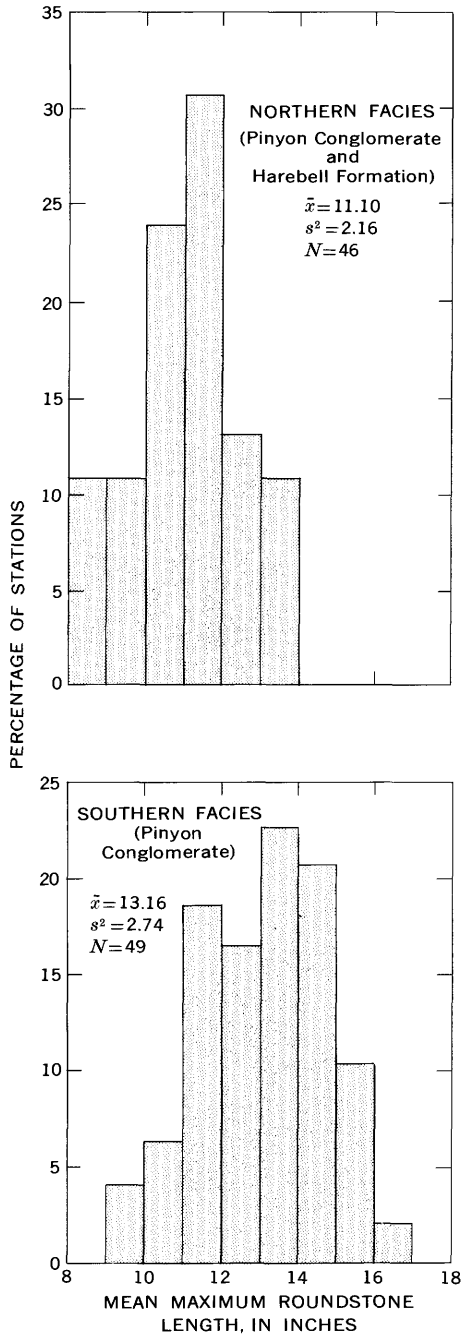

FIGURE 29. — Frequency distributions of mean maximum (average of 10 largest) quartzite roundstone lengths for stations in the northern and southern conglomerate facies, Harebell Formation and Pinyon Conglomerate. $\bar{x}$, arithmetic mean; s^2, variance; N, number of stations.

SYNTHESIS OF INFORMATION ON SEDIMENT DISPERSAL

Data on paleocurrent directions and regional variation in roundstone size were used to identify the position and trend of major paleostreams responsible for depositing the conglomerates (fig. 33). As interpreted by me, the data outline three distinct stream courses and, in the southern facies, possibly two other stream courses.

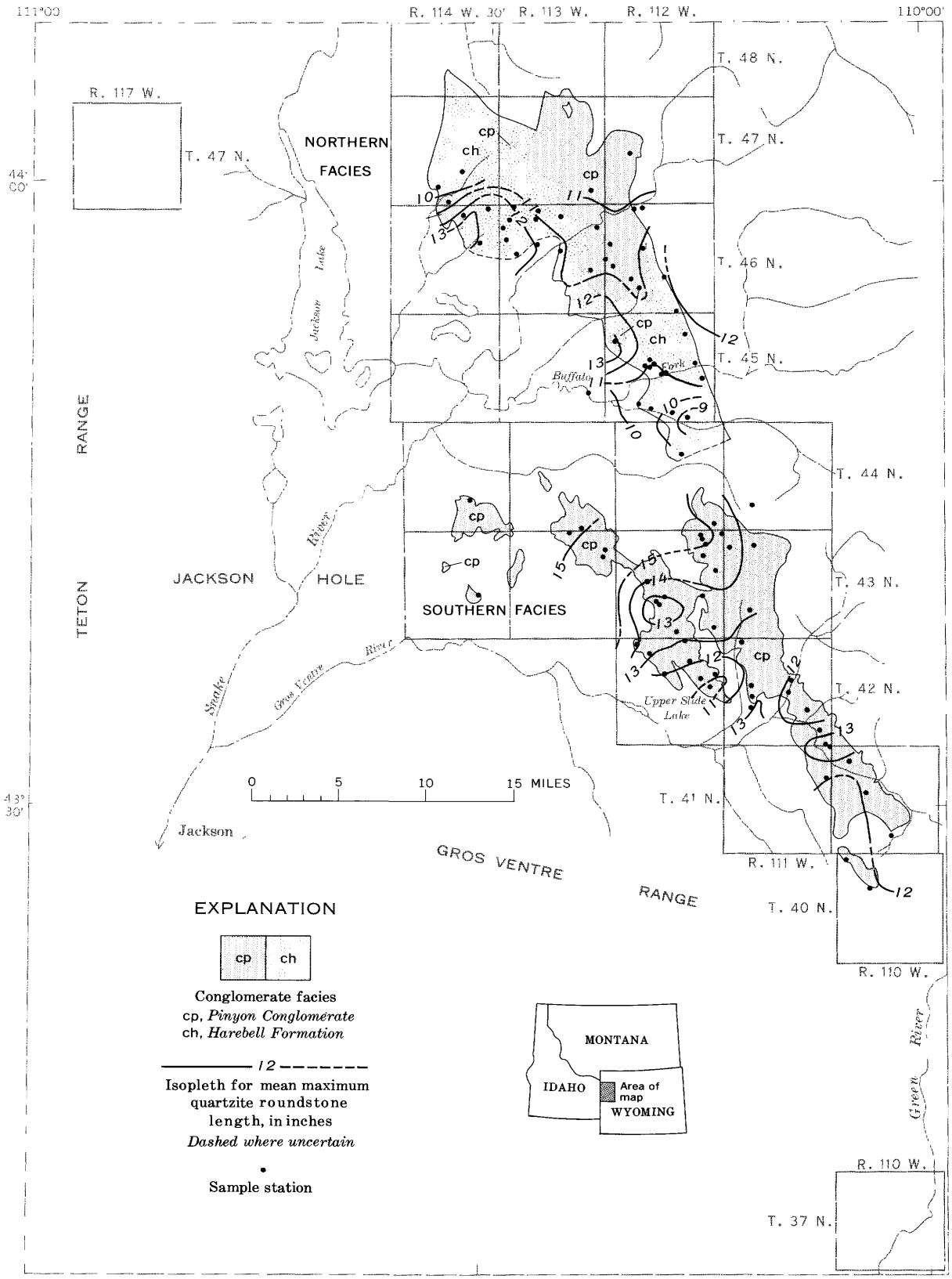

FIGURE 30. — Moving-average isopleth map of mean maximum quartzite roundstone lengths at stations in the Harebell Formation and the Pinyon Conglomerate.

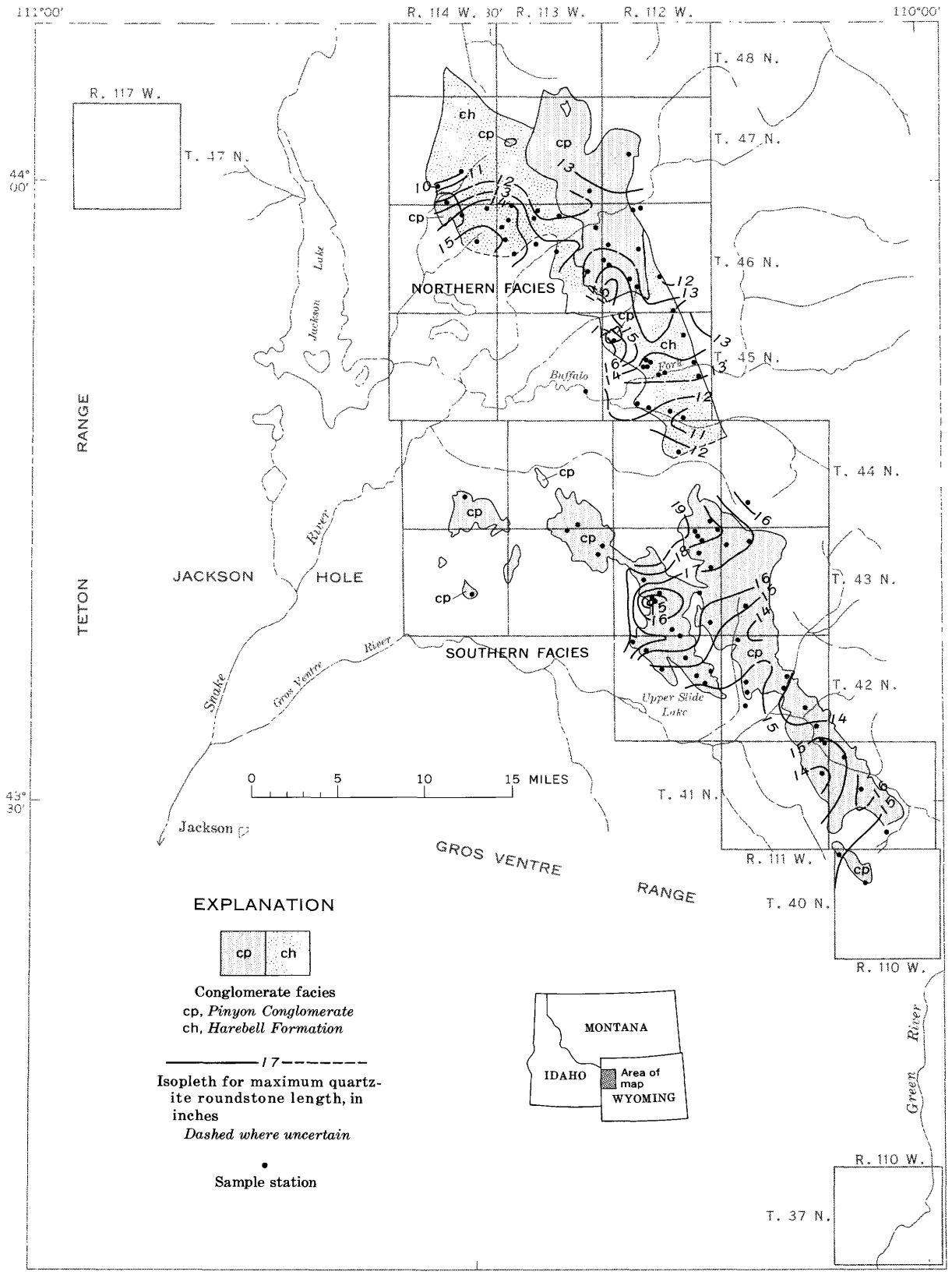

FIGURE 31. — Moving-average isopleth map of maximum quartzite roundstone lengths at stations in the Harebell Formation and the Pinyon Conglomerate.

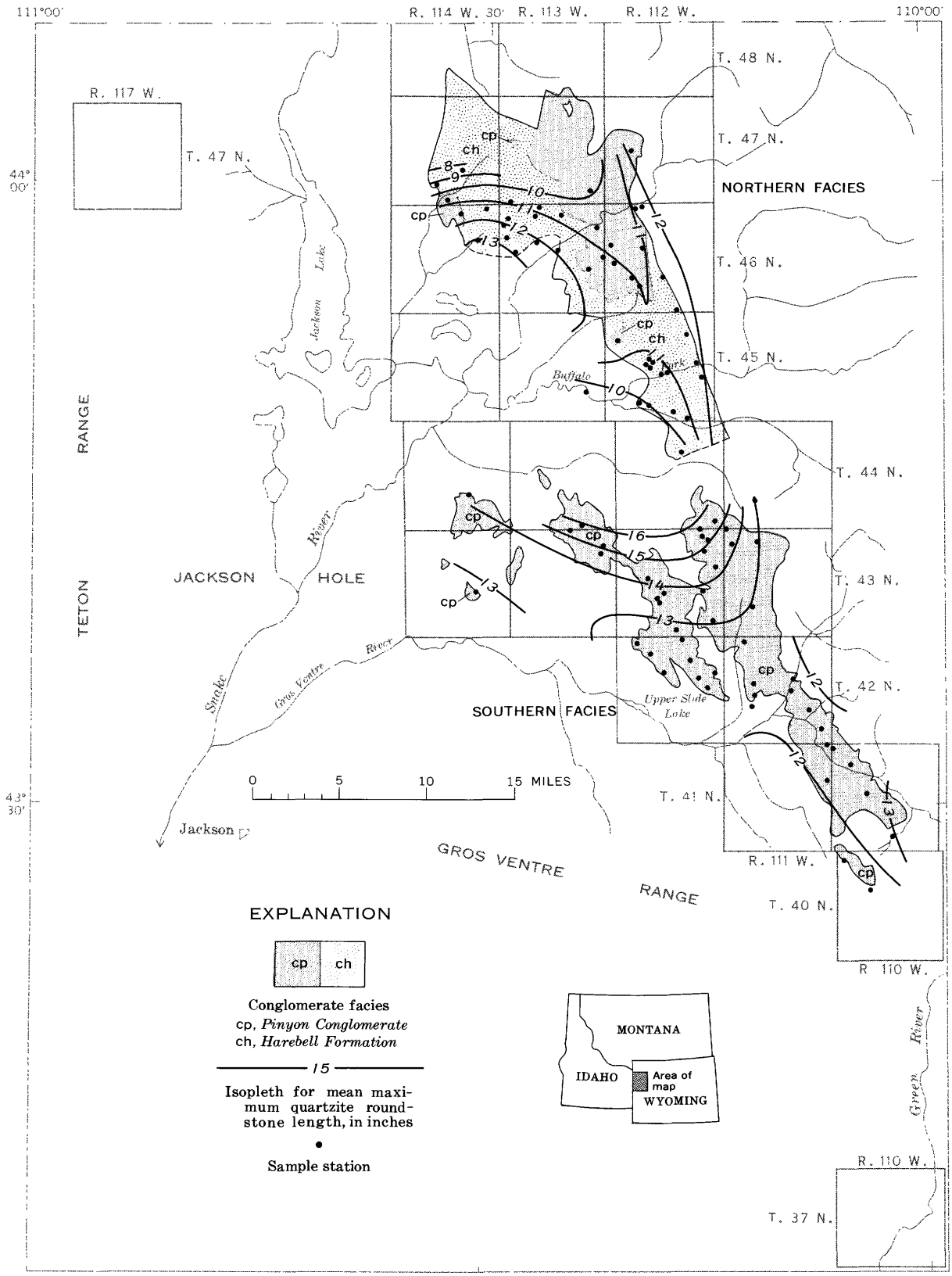

FIGURE 32. — Highest degree significant (≥90-percent confidence level) surfaces fitted to mean maximum quartzite roundstone length at stations in the Harebell Formation and the Pinyon Conglomerate. Each surface is cubic, and each is fitted separately to stations in the northern and southern facies.

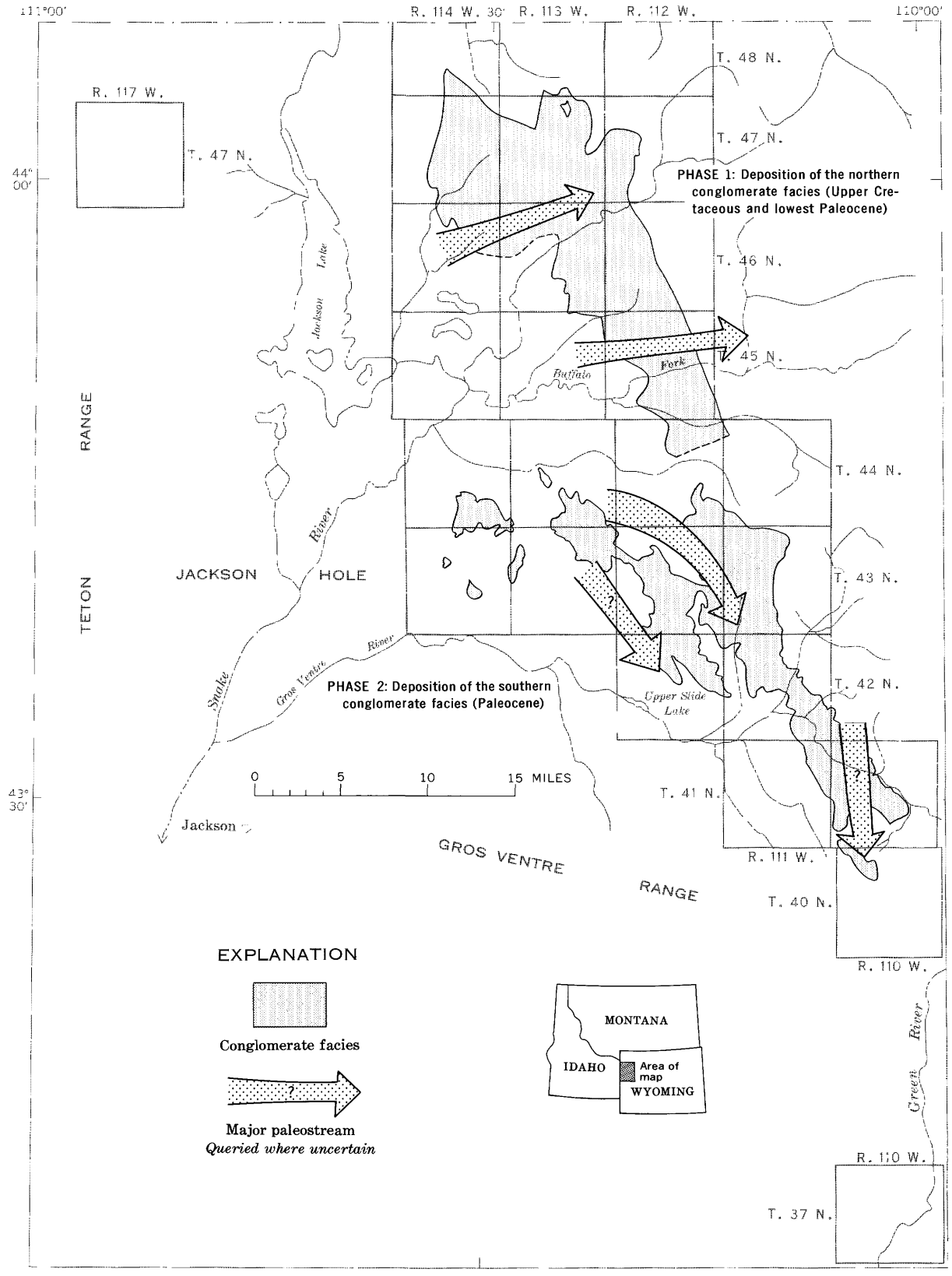

FIGURE 33. — Interpreted positions and orientations of major paleostreams responsible for deposition of the Harebell Formation and the Pinyon Conglomerate.

TABLE 17. — *Percent reduction of the sum of squares for trend surfaces fitted to mean maximum quartzite roundstone length in the northern and southern conglomerate facies*

	Added reduction	Cumulative reduction
Northern facies		
Reduction due to linear surface	2.912	2.912
Added reduction due to:		
Quadratic surface	10.523	13.435
Cubic surface	22.317	35.752
Quartic surface	6.183	41.935
Quintic surface	15.228	57.163
Southern facies		
Reduction due to linear surface	38.796	38.796
Added reduction due to:		
Quadratic surface	5.279	44.075
Cubic surface	11.850	55.925
Quartic surface	.949	56.874
Quintic surface	1.912	58.786

TABLE 18. — *Analysis of variance of data from trend surfaces fitted to mean maximum quartzite roundstone length in the northern and southern conglomerate facies*

Source	Sum of squares	Degrees of freedom	Mean square	*F* value	Confidence (percent)
Northern facies					
Total	5762.820	45			
Due to linear	167.813	2	83.907	0.645	25+
Deviations from linear	5595.007	43	130.116		
Due to quadratic	606.422	3	202.141	1.621	75+
Deviations from quadratic	4988.585	40	124.715		
Due to cubic	1286.089	4	321.522	3.126	95+
Deviations from cubic	3702.497	36	102.847		
Due to quartic	356.315	5	71.263	.660	25+
Deviations from quartic	3346.182	31	107.941		
Due to quintic	877.562	6	146.260	1.481	75+
Deviations from quintic	2468.619	25	98.745		
Southern facies					
Total	8521.233	47			
Due to linear	3305.897	2	1652.949	14.263	99.99+
Deviations from linear	5215.335	45	115.896		
Due to quadratic	449.836	3	149.945	1.322	50+
Deviations from quadratic	4765.499	42	113.464		
Due to cubic	1009.766	4	252.442	2.554	90+
Deviations from cubic	3755.733	38	98.835		
Due to quartic	80.867	5	16.173	.145	1+
Deviations from quartic	3674.867	33	111.360		
Due to quintic	162.926	6	27.154	.209	2.25+
Deviations from quintic	3511.941	27	130.072		

The interpreted relationship between the northern and the southern facies must account for the following observations:

1. The southern conglomerate facies is entirely Paleocene age; the northern facies is both Late Cretaceous and Paleocene age (Love, 1972).
2. The paleostream courses in both facies appear to head in the same region, or nearly so.
3. The southern facies contains more volcanic roundstones and larger quartzite roundstones than does the northern facies.

The interpretation that best accounts for these observations is that the conglomerates were deposited in two distinct phases. During Late Cretaceous and early Paleocene time, east-northeastward-flowing streams deposited the northern facies. Somewhat later, during Paleocene time, the streams shifted southward and deposited the southern facies. Although the two facies shared a similar source, additional volcanics were available to streams depositing the southern facies. Cannibalization of the northern facies must be considered as a possible source of quartzite for the southern facies, but larger quartzite roundstones in the southern facies indicate that quartzite was still being brought from elsewhere.

Data on the western conglomerate facies are sparse because of its limited distribution. Its age is not precisely known, but regional relations suggest that it is Paleocene (Love, 1972). Its distinctive petrographic attributes suggest that it may represent yet another phase of conglomerate deposition.

OTHER QUARTZITE-BEARING CONGLOMERATES

BEAVERHEAD FORMATION

Conglomerates which contain quartzite roundstones similar to those of the Harebell and Pinyon

TABLE 19. — *Composition (in percent) of roundstones counted in the Divide quartzite conglomerate lithosome (Ryder, 1967) of the Beaverhead Formation and in the Lance and Fort Union Formations*

[Stations located in figs. 34 and 38; 100 roundstones were identified at each station. $\bar{x}$, arithmetic mean; s, standard deviation; s^2, variance; Tr., trace. Leaders (.....) indicate not present]

Station No.	Quartzite	Vein quartz	Sedimentary rocks					Plutonic[1] rocks	Volcanic rocks		
			Chert	Sandstone	Limestone	Shale	Total		Welded tuff	Porphyritic rocks	Total
Beaverhead Formation (Divide conglomerate lithosome of Ryder, 1967)											
155	66	....	1	11	22	....	34	....	....	8	8
156	76	....	2	10	4	....	16	....	....	8	8
162	79	....	Tr.	13	5	1	19	....	1	1	2
166	83	....	1	13	2	1	17	....	....	....	....
167	71	....	2	12	11	2	27	....	....	2	2
168	83	....	1	4	5	....	10	....	....	7	7
224	85	....	....	4	11	....	15	....	....	....	....
225	85	....	....	6	6	2	14	Tr.	....	1	1
226	80	....	1	7	7	2	17	1	....	2	2
227	74	....	2	9	15	....	26	....	....	....	....
231	80	....	....	3	12	....	15	....	....	5	5
$\bar{x}$	78.36	....	0.91	8.36	9.09	0.73	19.09	0.09	0.09	3.09	3.18
s	6.07	....	.83	3.75	5.84	.90	7.02	....	....	3.27	3.22
s^2	36.85	....	.69	14.05	34.09	.82	49.29	....	....	10.69	10.36
Lance Formation											
66	14	7	78	1	....	....	79	....	....	....	....
Fort Union Formation											
68	67	3	29	1	....	....	30	....	....	....	....
109	63	5	27	3	1	....	31	....	....	....	1

[1]Plutonic refers to granitic and gneissic rocks and their relatives, except for stations 225 and 226, where diabase was recorded.

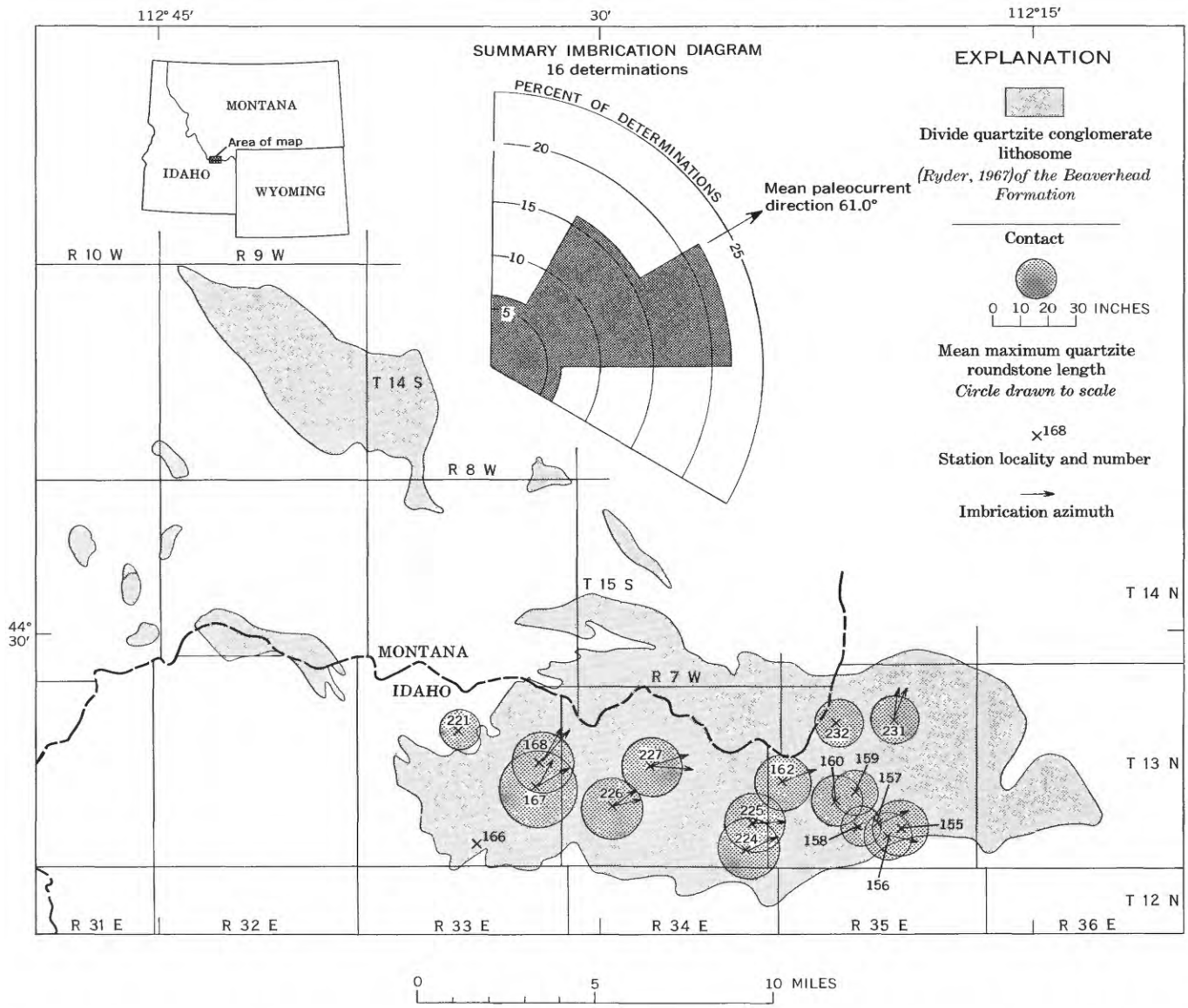

FIGURE 34. — Station localities, imbrication azimuths, and mean maximum quartzite roundstone lengths in the Divide quartzite conglomerate lithosome (Ryder, 1967) of the Beaverhead Formation.

were first described in the Upper Cretaceous, Paleocene, and Eocene Beaverhead Formation of Idaho and Montana by Lowell and Klepper (1953) and by Scholten, Keenmon, and Kupsch (1955). Ryder (1967) defined an extensive lithosome of quartzite cobble conglomerate within the Beaverhead Formation which he termed the Divide quartzite conglomerate lithosome (figs. 1 and 34). Reconnaissance studies of the quartzite conglomerate indicated a southwesterly or southerly source for the Divide (Ryder, 1967; Tanner, 1963). Because the Divide quartzite conglomerate lithosome (figs. 35 and 36) bears a strong resemblance to conglomerates in the Harebell and Pinyon, a petrographic and paleocurrent study was made to determine what, if any, relationship exists between them.

The roundstones in the Divide lithosome closely resemble those of the Harebell and Pinyon (table 19; fig. 37). About 75 percent of the Divide roundstones are quartzite, very similar to those in the Pinyon north of the Teton Range, but the Divide is less quartzite rich than the main body of conglomerates in Jackson Hole. Roundstones derived from sedimentary rocks, mainly Madison Limestone and sandstone of undetermined origin, and from quartz phenocryst-bearing porphyritic volcanic rocks are common; all these lithologies are seen in the Harebell and Pinyon. Hand-specimen and thin-section

FIGURE 35. — Typical outcrop of the Divide quartzite conglomerate lithosome (Ryder, 1967) of the Beaverhead Formation above the West Fork of Indian Creek (sta. 225, fig. 34). Note abundant large quartzite roundstones.

study of quartzite stones from the Divide reveals the same range of colors, textures, and mineralogy as found in the quartzite stones of the Harebell and Pinyon. Clearly the quartzite, other sedimentary rock, and quartz phenocryst-bearing volcanic roundstones of the Divide and of the Harebell and Pinyon conglomerates were derived from the same or a similar source.

Imbrication orientations and maximum quartzite roundstone lengths were measured in the Divide lithosome (table 20; fig. 34). The imbrication is very similar to that observed in the Harebell Formation and the Pinyon Conglomerate; 16 determinations of 50 measurements each showed a strong predominance of northeasterly azimuths, about 30°–60° more easterly (depending on location) than in the findings of Ryder (1967). Mean maximum length of quartzite roundstones at 14 stations showed a northeasterly decrease, in agreement with imbrication data. It is noteworthy that mean maximum quartzite length ranges from 14 to 27 inches in the Divide, generally well above the sizes noted farther east in the Harebell and Pinyon. The largest quartzite boulder seen in the Divide measured 34 inches in long dimension.

In summary, the Divide quartzite conglomerate lithosome shared similar source terranes with the Harebell and Pinyon, and paleocurrent evidence indicates that the source of the Divide lay to the southwest. This conclusion is in agreement with that of Ryder (1967, 1968) and of Scholten (1968, p. 117) that the source of the Divide quartzite conglomerate was the Belt quartzite terrane along the eastern flank of the Idaho batholith.

FORT UNION FORMATION

Quartzite-bearing conglomerates in the Paleocene Fort Union Formation are known in several areas along the west flank of the Bighorn Basin (figs. 1 and 38). Two areas are discussed in the present report: (1) the Grass Creek and Left Hand synclines (Hewett, 1926, p. 30–40; Rohrer, 1966b, p. 16–17) and (2) the Heart Mountain area north of Cody (figs. 38, 39, and 40) (Pierce, 1966). That

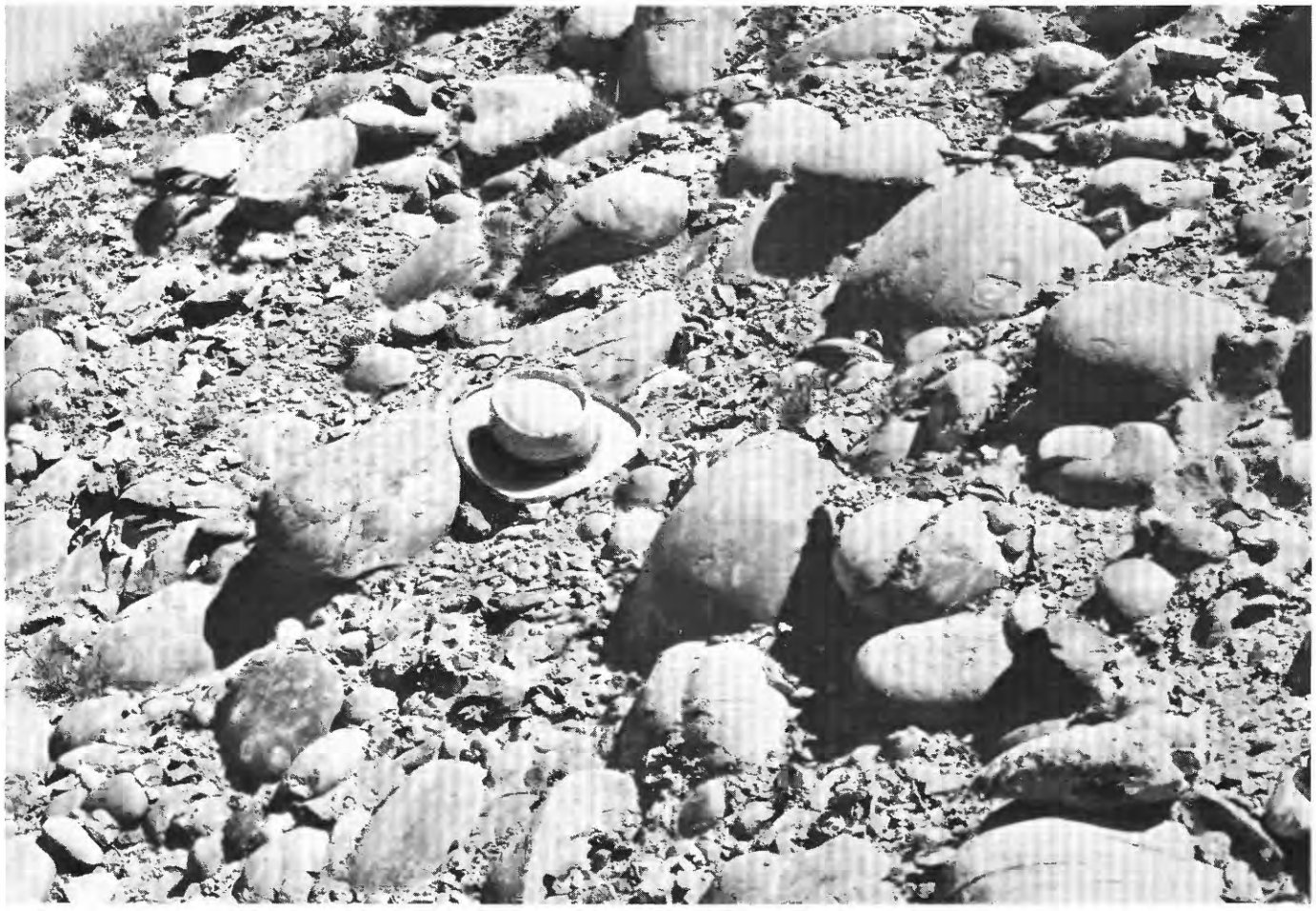

FIGURE 36. — Large quartzite roundstones in the Divide quartzite conglomerate lithosome (Ryder, 1967) of the Beaverhead Formation above Edie Creek (sta. 167, fig. 34).

TABLE 20. — *Imbrication statistics for 17 determinations of 50 c-axis orientations each in the Divide quartzite conglomerate lithosome (Ryder, 1967) of the Beaverhead Formation*

[Each determination was calculated by averaging 50 *c*-axis orientations. Stations are located in fig. 34. $\bar{\theta}$=vector mean azimuth; $\bar{\phi}$=vector mean inclination; R=vector magnitude; $c_{0.95}$=radius of spherical circle of confidence; k=an indicator of dispersion; $\chi^2_{(\hat{\phi})}$=chi square for angular dispersion about the vector mean; df=degrees of freedom for $\chi^2_{(\hat{\phi})}$; and $\chi^2_{(\hat{\alpha})}$=chi square for azimuthal dispersion about the vector mean (with 15 degrees of freedom)]

Station No.	$\bar{\theta}$ (degrees)	$\bar{\phi}$ (degrees)	R (absolute value)	$c_{0.95}$ (degrees)	k	$\chi^2_{(\hat{\phi})}$	df	$\chi^2_{(\hat{\alpha})}$ (15df)
156	98.5	50.7	35.6	12.9	3.4	28.4	16	21.2
157	63.8	64.5	43.6	7.7	7.6	22.1	10	21.9
162	66.8	55.1	42.0	8.8	6.1	17.9	12	21.2
167A	27.5	65.4	39.5	10.4	4.6	19.7	14	19.0
B	58.0	68.5	39.7	10.3	4.7	19.4	13	29.8
168A	37.4	56.7	40.2	10.0	5.0	12.6	13	19.7
B	31.3	58.7	39.8	10.2	4.8	16.1	13	30.5
224	64.3	70.7	43.3	8.0	7.3	18.0	10	12.6
225A	86.8	59.9	43.0	8.1	7.0	9.1	11	26.2
B	78.1	64.8	42.1	8.7	6.2	21.6	12	15.4
226A	75.2	64.4	41.1	9.4	5.5	19.1	12	21.9
B	51.3	64.8	45.4	6.4	10.8	6.2	9	25.5
227A	92.5	52.4	42.0	8.8	6.2	11.5	12	12.6
B	70.2	55.8	40.0	10.1	4.9	15.5	13	16.1
231A	5.5	61.2	40.6	9.7	5.2	22.9	13	24.0
B	22.7	59.9	45.2	6.5	10.3	16.7	9	23.3

these conglomerates were derived from the same source as those of the Harebell Formation and the Pinyon Conglomerate of Jackson Hole was suggested by Love and Reed (1968, fig. 46). To test their hypothesis, I studied quartzite roundstone petrography and paleocurrents in parts of the Fort Union, and I studied paleocurrents in the underlying Upper Cretaceous Lance Formation. Heavy minerals from Fort Union and a few Lance sandstones were also examined for comparison with those from Paleocene and Cretaceous Pinyon and Upper Cretaceous Harebell rocks studied in Jackson Hole.

The Fort Union conglomerates of the Grass Creek and Left Hand synclines were not examined by me, but their pebble lithology was thoroughly studied by Hewett (1926, p. 30–34), who found that quartzite roundstones were dominant and that chert, silicified wood, quartz, sandstone, and coal were common. He reported that the chert pebbles, as shown by the fossils in them, were probably derived from strata of Mississippian to Permian age, and that the quartzite roundstones were probably derived from strata of the Belt Supergroup. Hewett suggested a south-

westerly source for the conglomerates, and the conglomerates that he pictured (his pls. 12 and 15) strongly resemble the Harebell and Pinyon conglomerates of Jackson Hole.

Pebble counts that I made in the conglomerates of the Heart Mountain area showed abundant quartzite accompanied by sandstone, chert, and white vein quartz (table 19; fig. 37). Sandstone and chert are more abundant in these conglomerates than in the Harebell and Pinyon Formations, and the vein quartz is unique to the Fort Union Formation. The quartzite stones in the Fort Union, as shown by detailed examination, do not resemble those in the Harebell and Pinyon. Stones extracted from the Fort Union matrix are much more angular and irregular in shape (fig. 41) than are stones of the Harebell and Pinyon, which are characteristically well rounded and oblate (fig. 4). The Fort Union quartz-

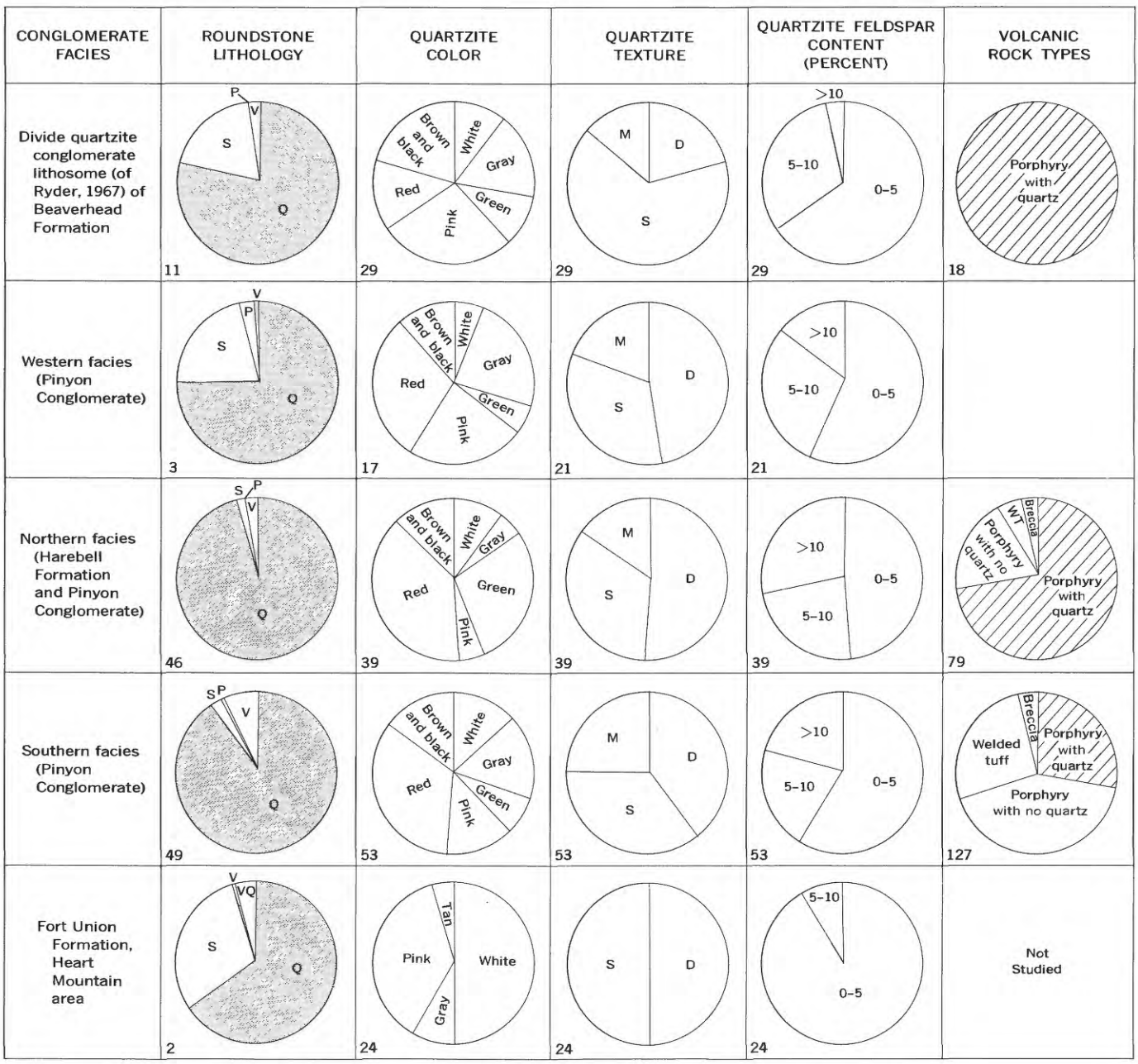

FIGURE 37. — Petrographic affinities of five quartzite-bearing conglomerate facies studied by the author. Roundstone lithology: P, plutonic; V, volcanic; Q, quartzite; S, soft sedimentary rocks; VQ, vein quartz. Quartzite texture: D, detrital; S, solution; M, metamorphic. Volcanic rock types: WT, welded tuff. Number in lower left corner indicates number of roundstones studied.

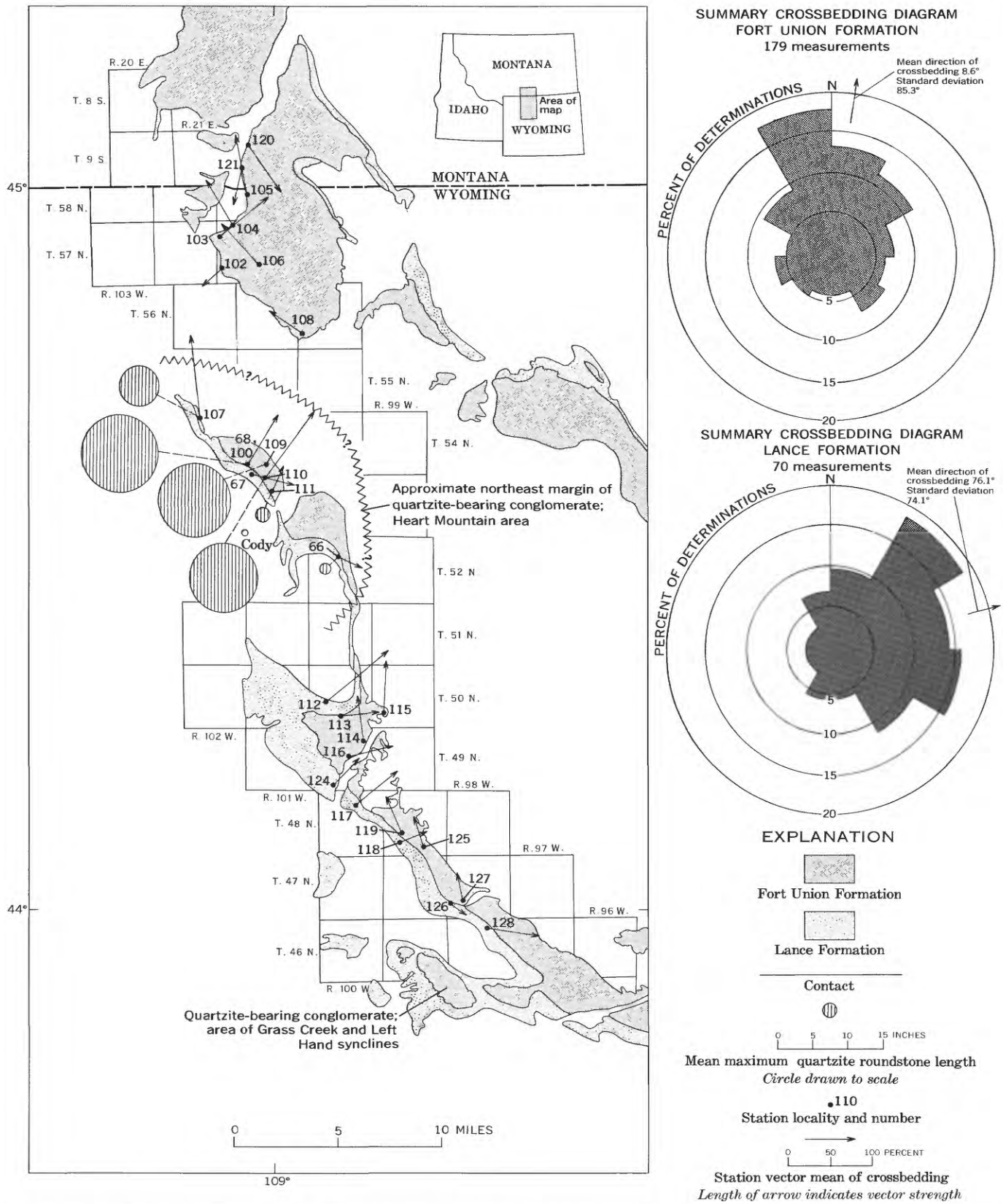

FIGURE 38. — Station localities, crossbedding orientations, and quartzite roundstone lengths in the Lance and Fort Union Formations on the west flank of the Bighorn Basin. Distribution of the Lance and Fort Union Formations from Andrews, Pierce, and Eargle (1947).

FIGURE 39. — Section of conglomerate in Fort Union Formation north of Cody at bench mark "Iron" (sta. 68). ss, sandstone; cgl, conglomerate. View looking north.

ite stones, as seen in thin section, consist of orthoquartzites with detrital and solution textures (figs. 37 and 42), sparse feldspathic quartzites, and no metamorphic quartzites, in contrast to the Harebell and Pinyon quartzite stones, of which 42–51 percent were feldspathic and 15–25 percent were metamorphic quartzites.

To examine further the possibility of a common source for Upper Cretaceous and Paleocene clastics in Jackson Hole and for those in the western flank of the Bighorn Basin, heavy minerals were identified in 12 samples of the Lance and Fort Union Formations (table 21) and were compared with heavy minerals from their respective time equivalents, the Harebell and Pinyon (tables 7 and 10). (Data from Upper Cretaceous and Paleocene rocks were combined for each basin in order to test for major differences between the provenances of the Upper Cretaceous–Paleocene basin fillings. The data are not considered sufficient to test for differences between formations, because for some formations only a few samples were studied and because some of these samples vary considerably in relative abundances of heavy minerals.) Sphene and brown amphibole, as

TABLE 21. — *Nonopaque heavy minerals (in percent) in the Lance and Fort Union Formations, western flank of the Bighorn Basin*

[0.0625- to 0.125-mm-size fraction, 100 grains counted per slide. Middle of field number corresponds to station number in fig. 38. Tr., trace]

Field No.	Garnet	Zircon	Tourmaline	Sphene	Epidote	Apatite	Rutile	Am[1]	Am[2]	Other
Lance Formation										
L–67–h1	23	48	13	5	10	0	0	1	0	[3]tr.
67–h3	79	13	3	5	0	0	0	tr.	0	0
126–t/h	82	15	2	1	0	0	0	0	0	0
Average	61.3	25.3	6.0	3.7	3.3	0	0	.3	0	0
Fort Union Formation										
FU–100–t/h–3	90	5	0	0	1	3	0	0	0	[3]1
100–t/h–5	85	7	4	2	2	0	0	0	0	0
114–t/h	14	59	20	1	1	0	2	2	0	[3]1
116–t/h	5	85	7	3	0	0	0	0	0	0
119–t/h	3	94	1	tr.	tr.	0	2	0	0	0
125–t/h	5	75	16	0	tr.	0	2	0	0	[4]1
121–t/h	32	60	5	0	0	3	0	0	0	0
122–t/h	27	52	18	3	0	0	0	0	0	0
127–t/h	90	5	1	1	3	0	0	0	0	0
Average	39.0	49.1	8.0	1.1	.8	.7	.7	.2	0	.3

[1]Colorless and light-blue-green amphibole.
[2]Pleochroic brown amphibole.
[3]Kyanite.
[4]Pyroxene.

FIGURE 40. — Quartzite pebble and cobble conglomerate in the Fort Union Formation north of Cody (sta. 68). Note poor sorting and abundant subrounded pebble-sized fraction, both typical of the conglomerate.

shown by microscopic examination of the samples, are characteristic of the Jackson Hole suite but not of the Bighorn Basin suite. The nonparametric Mann-Whitney *U* test (Siegel, 1956, p. 116–127) was applied to detect significant differences in relative abundance of each mineral species (table 22); zircon, sphene, and possibly brown amphibole showed different abundances. The work of Stow (1938, 1947) farther north compares generally well with my data on Lance and Fort Union heavy minerals, except that small amounts of staurolite and kyanite that he reported were not seen by me.

Crossbedding orientation in the Lance and Fort Union Formations along the western flank of the Bighorn Basin suggests a westerly or southwesterly source (fig. 38). About 10 measurements were taken at each of eight stations in the Lance and 21 stations in the Fort Union. Orientation of crossbedding proved to be easterly in the Lance (vector mean= 76.1°) and north-northeasterly in the Fort Union (vector mean=8.6°). Crossbedding orientation in the Fort Union conglomerates of the Heart Mountain area, however, is northeasterly.

TABLE 22. — *Mann-Whitney* U *tests for differences between means of Upper Cretaceous and Paleocene heavy mineral suites from Jackson Hole and those from the Bighorn Basin*

[Jackson Hole data are computed from tables 7 and 10; Bighorn Basin data, from table 21. $\bar{x}$, arithmetic mean; s^2, variance. Mean and variance are in percent. Numbers in parentheses are number of samples]

Mineral	Jackson Hole (27)		Bighorn Basin (12)		z (U-test)	Significance
	$\bar{x}$	s^2	$\bar{x}$	s^2		
Garnet	42.6	805.1	44.6	1370.4	—0.030	None
Zircon	19.8	497.5	43.2	1082.5	—2.084	.05
Tourmaline	10.0	119.3	7.5	52.6	.761	None
Sphene	15.0	412.0	1.8	3.5	3.073	.01
Epidote	1.7	4.1	1.4	8.3	.761	None
Apatite	.9	2.7	.5	1.4	.487	None
Rutile	.5	1.0	.5	.8	.091	None
Am₁[1]	1.2	3.7	.3	.4	1.187	None
Am₂[2]	8.1	372.5	0	.....	1.461	.20

[1]Colorless and light-blue-green amphibole.
[2]Pleochroic brown amphibole.

The quartzite-bearing conglomerates and associated sandstones along the western flank of the Bighorn Basin appear to have been derived from the southwest, from the direction of Jackson Hole. Petrographic data suggest that the conglomerates of the

Heart Mountain area were not derived from the same source as those of the Harebell and Pinyon, but perhaps from older Mesozoic and Paleozoic sedimentary rocks in the now-buried Washakie Range, remnants of which are exposed beneath the edge of the Absaroka volcanic field. (See Love, 1939, p. 5, 90–94.) The quartzites may well have been derived from parts of the Flathead Quartzite or from some other quartzose sandstone. Petrographic data are not sufficient to determine the source of the conglomerates of the Grass Creek and Left Hand synclines, but possibly the source was the same as that for the conglomerates of the Harebell Formation and the Pinyon Conglomerate.

FIGURE 41.—Typical quartzite roundstones from conglomerate in the Fort Union Formation north of Cody (sta. 68). Note the subrounded outlines, in contrast to the well-rounded outlines of Harebell and Pinyon cobbles (fig. 4).

CONCLUSIONS

SOURCE OF CONGLOMERATES

EVIDENCE FOR LONG-DISTANCE TRANSPORT

The coarse conglomerate deposits that I studied can be differentiated geographically and petrographically into five distinct deposits: the Divide quartzite conglomerate lithosome of Ryder (1967), the western facies (Pinyon Conglomerate), the northern facies (Harebell Formation and Pinyon Conglomerate), the southern facies (Pinyon Conglomerate), and the conglomerates of the Fort Union Formation at Heart Mountain (figs. 1, 37, and 43). Although

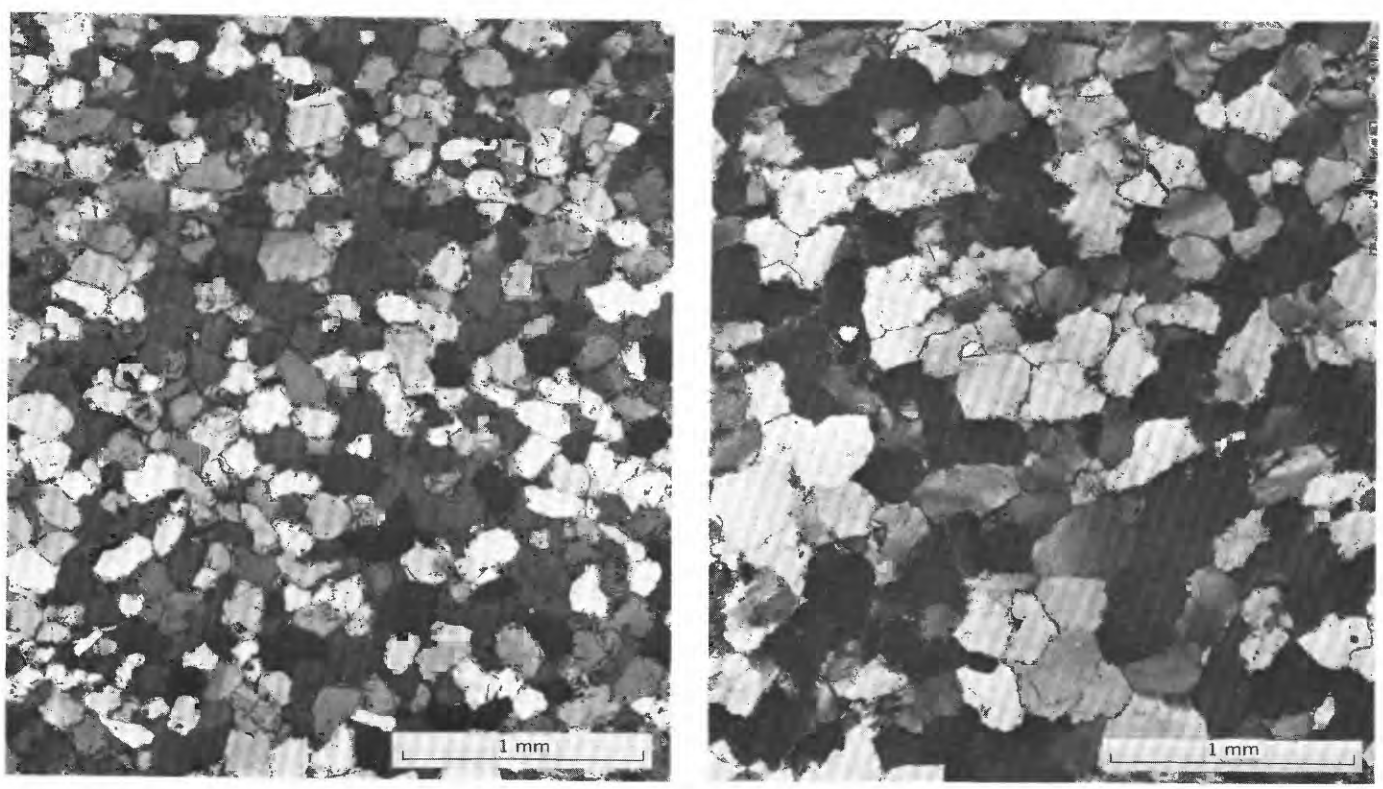

A *B*

FIGURE 42. — Photomicrographs of typical textures and mineralogy of quartzite roundstones found in the Fort Union Formation north of Cody (sta. 68). *A*, Orthoquartzite with well-preserved detrital grain outlines and quartz cement. *B*, Orthoquartzite with indented sutured grain contacts. Crossed nicols.

petrographically distinct, the first four deposits contain similar roundstones of quartzite, volcanic rock, and other sedimentary rock which tie them to the same or a similar source terrane (fig. 37). Roundstones of quartzite from each of the four conglomerates show a similar range of color, microscopic texture, and mineralogy; roundstones of quartz phenocryst-bearing porphyritic volcanic rock are present in the same deposits. Paleocurrent studies show either easterly, northeasterly, or southeasterly sediment transport in all four of these conglomerate deposits and in the associated sandstone facies (fig. 43). Likewise, the length of quartzite roundstones and the abundance of soft sedimentary roundstones decrease from west to east among the first four deposits. The quartzite roundstones and heavy-mineral suites of the Fort Union Formation at Heart Mountain are very different from those of the Harebell and Pinyon conglomerates, and therefore the Fort Union conglomerates were probably derived from a different source.

The distribution of outcrops of potential source rocks for the conglomerates can be related to roundstone lithology (fig. 43). Potential source rocks include the Precambrian quartzites of the Belt Supergroup in Idaho and Montana (Ross, 1947; 1963, pl. 1), the thick sequence of Precambrian and Cambrian quartzites of southeastern Idaho (Crittenden and others, 1971), the Ordovician orthoquartzites of the Kinnikinic and the Swan Peak Quartzites (Ketner, 1966; 1968), the Upper Cretaceous Elkhorn Mountains Volcanics and Livingston Group, and the widespread Paleozoic and Mesozoic sedimentary rocks, including the Flathead and Quadrant Quartzites. The roundstones found in the Harebell Formation and the Pinyon Conglomerate can be grouped into two classes: (1) orthoquartzites and soft sedimentary rocks available nearby, and (2) orthoquartzites, feldspathic quartzites, metamorphic quartzites, and volcanic rock available only at great distances. From the relationship between paleocurrents and possible source rocks shown in figure 43, it is evident that the most likely sources of the latter rock types are the Belt quartzites, the Precambrian and Cambrian quartzites, the Ordovician orthoquartzites, and the Elkhorn Mountains Volcanics and Livingston Group. The suggestion that the quartzite roundstones of the Harebell and Pinyon were derived at great distance (as much as 100–200 airline miles) from Idaho and Montana is not new, having been made by Love (1956c, p. 140–141), Eardley (1960, p. 87; 1962, p. 326), and Scholten (1968, p. 117).

The locations of Late Cretaceous and Paleocene uplifts are also shown in figure 43. These are the Late Cretaceous and Paleocene Idaho batholith and the adjacent southwestern Montana overthrust belt (Scholten, 1968), the Late Cretaceous and Paleocene Blacktail-Snowcrest, Madison-Gravelly, and Madison-Gallatin arches (Scholten, 1967), the "Laramide" Beartooth uplift (Foose and others, 1961), the Late Cretaceous Basin Creek uplift (Love and Keefer, 1969), the Late Cretaceous and Paleocene ancestral Teton-Gros Ventre uplift (Love, in Behrendt and others, 1968, table 1), the Late Cretaceous and Paleocene uplift of the Washakie Range (Love, 1939, p. 5, 90–94, 106; Keefer, 1965, p. 56), and the Late Cretaceous and Paleocene ancestral Wind River Range (Keefer, 1957, p. 207–208; Love, 1970, p. 114). The Blacktail-Snowcrest arch may be early Late Cretaceous in age (Ryder and Ames, 1970), and the Washakie uplift may extend farther northward to join the Madison-Gallatin arch and the Beartooth uplift (H. J. Prostka, oral commun., 1971). In addition, the now-buried hypothetical Late Cretaceous and Paleocene Targhee uplift is shown in figure 43 (Love and Reed, 1968, p. 83–84, 89–90). Some of these uplifts may have provided the driving mechanism for moving the far-traveled quartzite and volcanic roundstones great distances. For example, the transport of the conglomerates may have proceeded something like the following (fig. 44): (1) Beginning early in Late Cretaceous time, uplift of the Idaho batholith and attendant eastward thrusting of the northern Rocky Mountains caused stripping off of Belt and Ordovician quartzites, as well as other detritus, and ensuing deposition of the Beaverhead Formation, including the Divide quartzite conglomerate lithosome (Ryder, 1967; Ryder and Ames, 1970; Scholten, 1968). Cretaceous thrusting in southeastern Idaho (Armstrong and Oriel, 1965) may have initiated erosion and eastward transport of Precambrian and Cambrian quartzites and the overlying Ordovician orthoquartzites. Quartzite detritus probably traveled eastward and accumulated at the present location of the Teton Range; more detritus was deposited north and west of the present Teton Range (fig. 44*A*). (2) Subsequent (Late Cretaceous) rise of an ancestral Teton Range (roughly corresponding to the ancestral Teton–Gros Ventre uplift and the Targhee uplift) shed the quartzite detritus farther eastward into Jackson Hole (fig. 44*B*). (3) During Paleocene time a vast region north of the ancestral Teton Range rose, and quartzite detritus as well as welded tuff and andesitic volcanic rock from the Elkhorn Mountains Volcanics and the Livingston Group poured into Jackson Hole (fig. 44*C*). (4) Also during Late Cretaceous and Paleocene time the Washakie Range rose, causing coarse

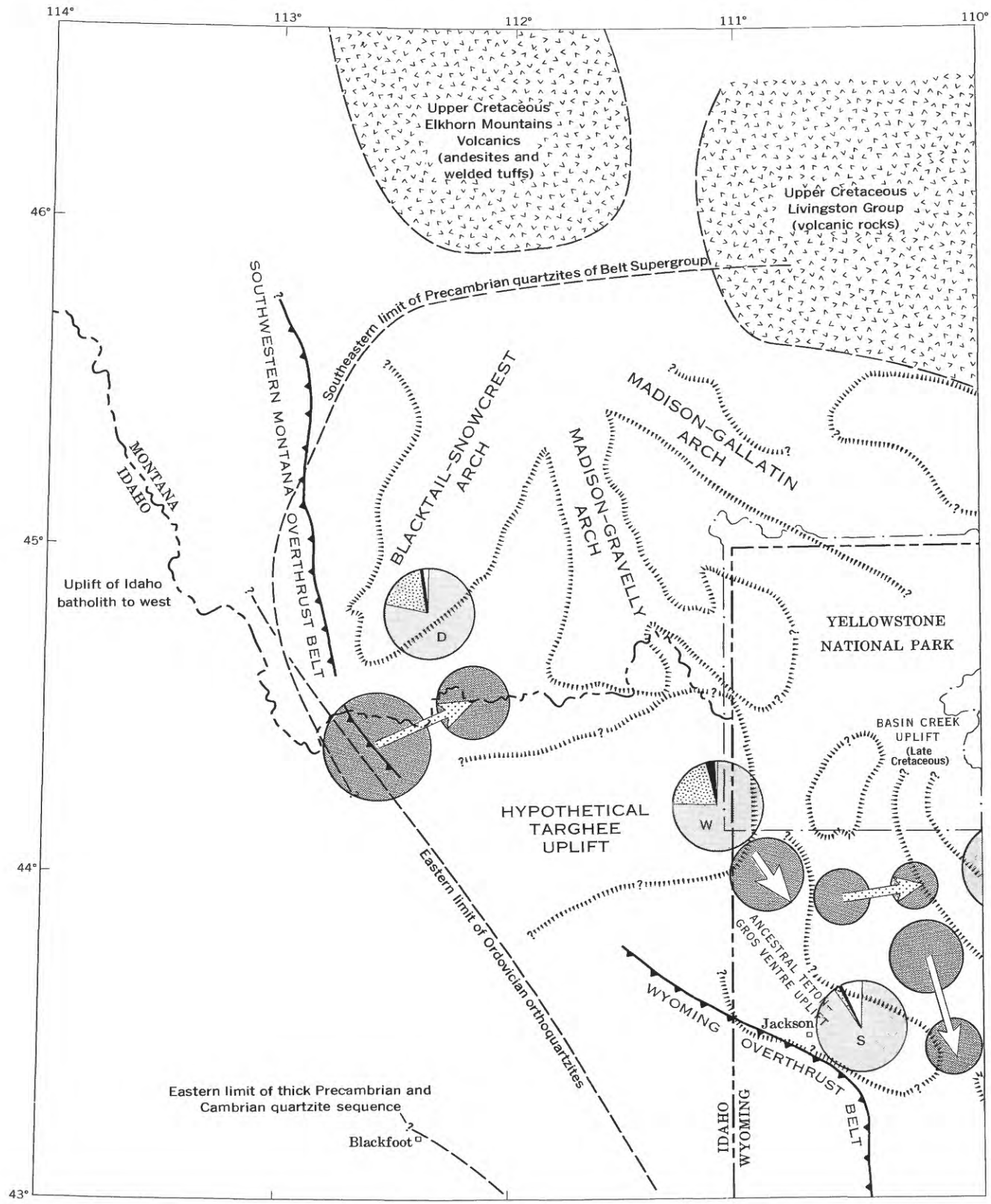

FIGURE 43. — Integration of petrographic and paleocurrent evidence into the geologic setting of the quartzite-bearing
included is the location of the hypothetical

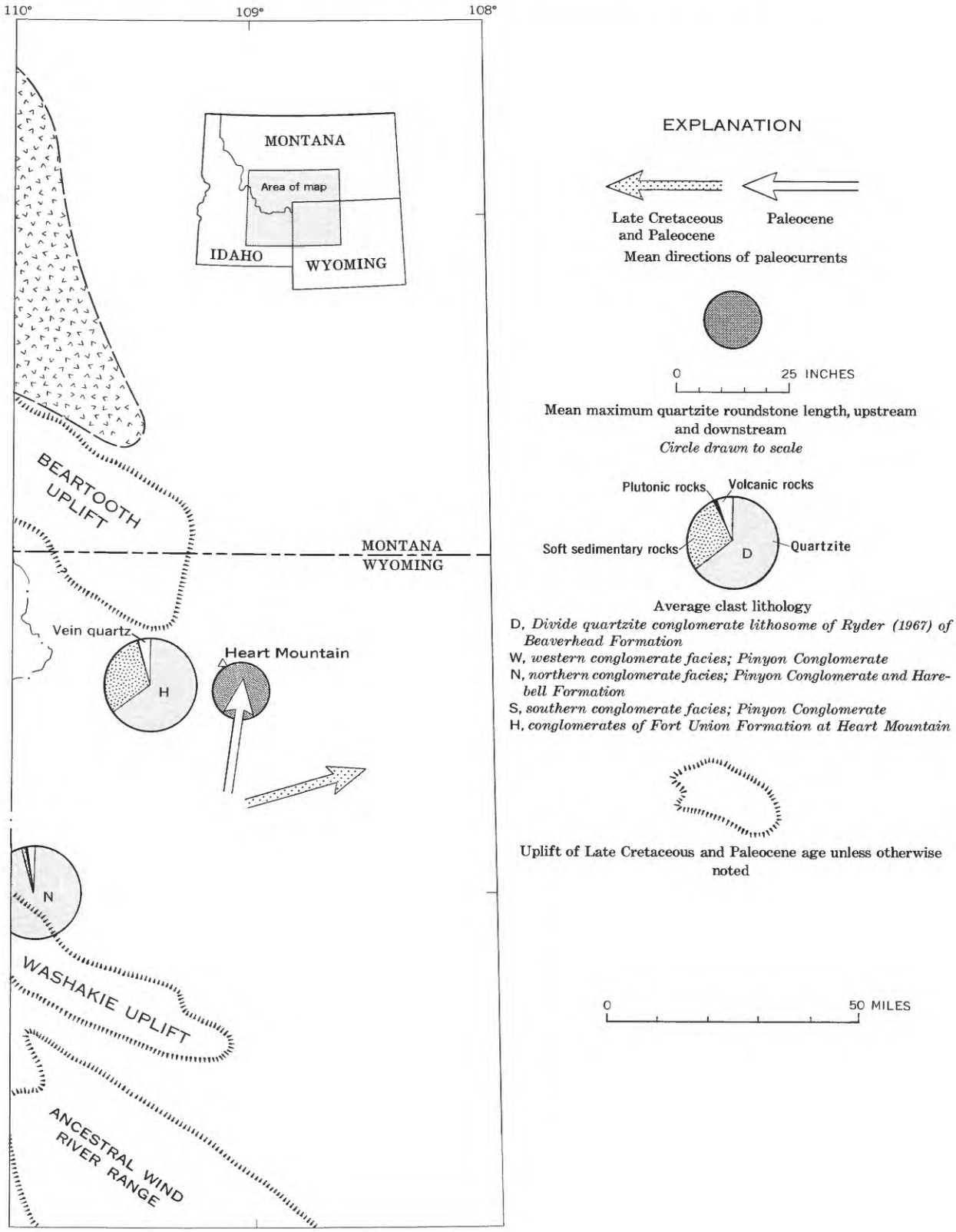

conglomerates. Distribution of possible source rocks and Late Cretaceous and Paleocene uplifts is shown. Also Targhee uplift of Love and Reed (1968).

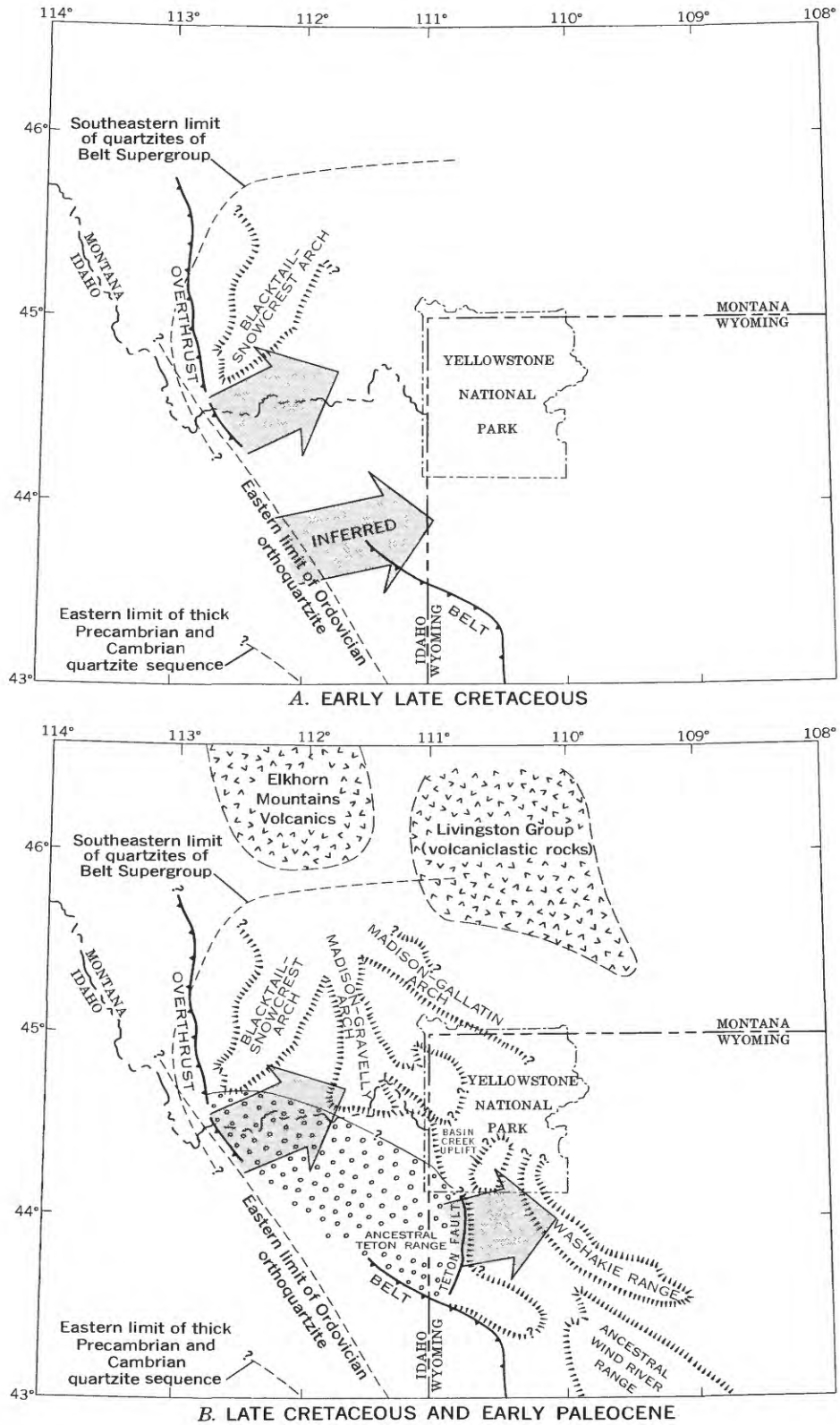

FIGURE 44. — Suggested interpretation according to the long-distance-transport bearing conglomerates

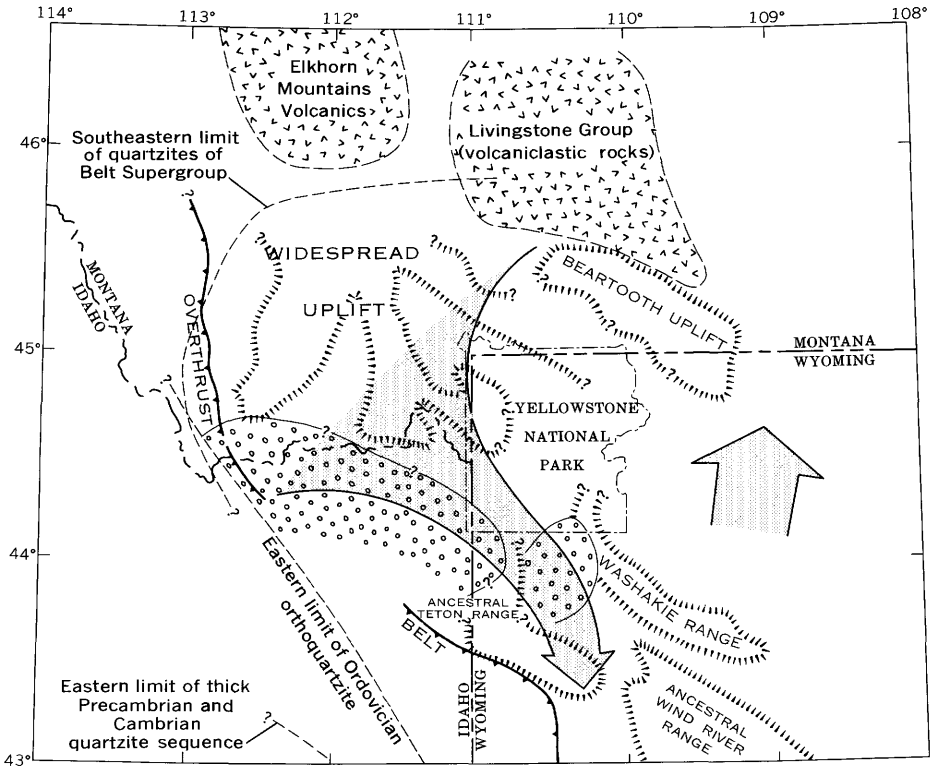

C. PALEOCENE

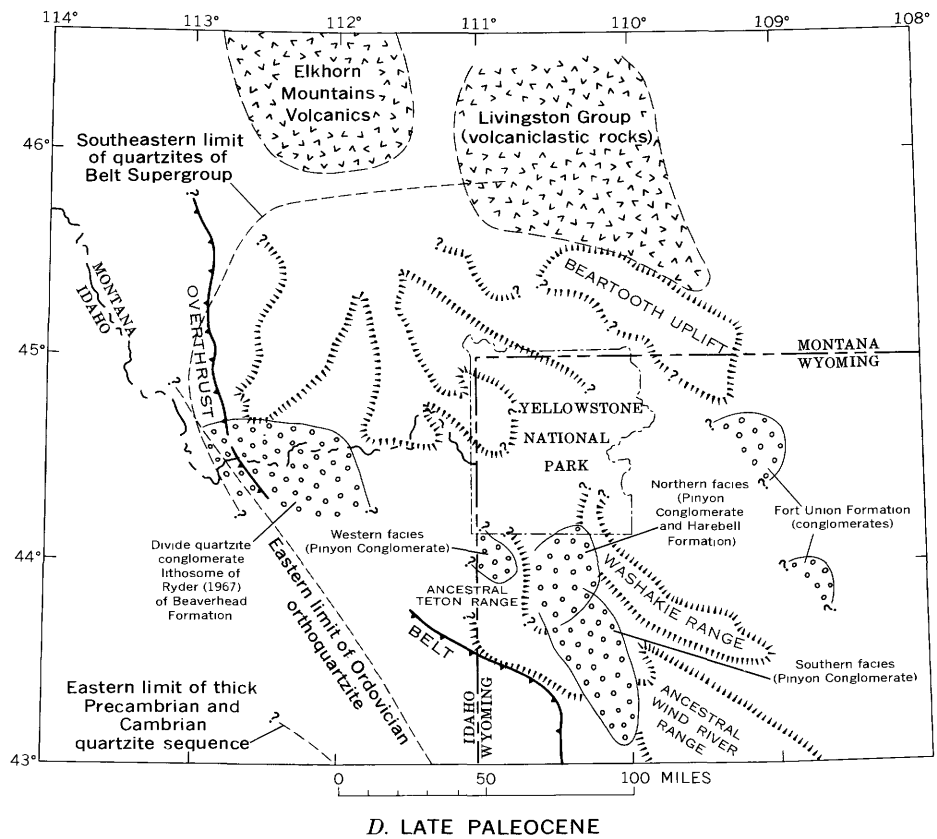

D. LATE PALEOCENE

hypothesis of the sources, dispersal routes, and depositional areas of the quartzite-(circle pattern).

Paleozoic orthoquartzite and chert detritus to be deposited along the western flank of the Bighorn Basin (fig. 44*C*). Thus, quartzite roundstones and other detritus were transported eastward from the eastern flanks of the Idaho batholith to Jackson Hole by successive uplift and reworking of conglomerate deposits (fig. 44*D*).

OBJECTIONS TO LONG-DISTANCE TRANSPORT

Objections to the hypothesis of long-distance transport of the conglomerates may be briefly summarized under three categories: mechanics, lack of evidence for reworking, and gold distribution.

The problem of mechanics arises from the immense volume of roundstones (perhaps 560 cu mi, of which 75 cu mi remains, according to Love, 1972) which must be moved a total distance of at least 100 miles (from the nearest extensive quartzite terrane) to perhaps 280 miles (from the eastern edge of the Idaho batholith). It must be emphasized that the task of roundstone transport was aided considerably by humid conditions (and hence abundant runoff), by steep gradients that probably existed, and by a time span of probably millions of years. All these requirements are consistent with fossil evidence and the physical characteristics of the conglomerates. A few calculations are presented below to illustrate the range of physical conditions required to transport the roundstones found in the conglomerates. It can be shown that the long-distance-transport hypothesis is consistent with estimates of stream velocities, depths, and slopes and that these parameters yield reasonable estimates of the total relief required to move the roundstones.

The velocities and depths necessary to transport the roundstones are not so great as might be generally supposed. They can be calculated according to the sixth-power law and the Manning equation:

$$V_b = 9d^{1/2}, \quad \text{(sixth-power law)}$$

where V_b is the bottom velocity, in feet per second, and d is roundstone diameter, in feet; and

$$V = 1.49\frac{R^{2/3}\, s^{1/2}}{n}, \quad \text{(Manning equation)}$$

where R is the hydraulic radius, in feet (depth in very wide streams), s is the slope, and n is a roughness factor. Details of the sixth-power law were discussed by Malde (1968, p. 46–47), and details of the Manning equation, by Leopold, Wolman, and Miller (1964, p. 156–158). The velocity can be calculated directly from roundstone diameter (approximated by length) by the sixth-power law. Alternatively, one may also use the Nevin-Hjulstrom formula (Fahnestock, 1963, p. 29–30) to compute V_t, the traction velocity, but the results obtained are only slightly different for the particle sizes under consideration. The depth (R, the hydraulic radius) can next be calculated from the Manning equation by using the velocity obtained from the sixth-power law, by assuming slope values ranging from 0.01 to 0.10, known to be common on larger alluvial fans (Denny, 1965, table 7; Riccio, 1962, p. 28), and by assuming a roughness factor of 0.04–0.06 for alluvial channels with coarse detritus (Barnes, 1967; Leopold and others, 1964, p. 158). The results are shown in figure 45. According to these calculations, a typical maximum roundstone size of 1 foot suggests a bottom velocity of 9 feet per second and a possible depth of less than 7 feet; the 4.2-foot boulder at the north end of the Teton Range (fig. 6*A*) could be moved by currents traveling 18 feet per second in water 2–20 feet deep. The work of Fahnestock (1963) on the White River, Mount Rainier, Wash., provides additional insight into the conditions necessary for the transport of coarse detritus. He observed that in the White River the velocities were as much as about 10 feet per second in water about 2 feet deep (Fahnestock, 1963, fig. 8), and the largest particles seen in transit were 1.8 feet in diameter (p. 29). Hence, the computed velocities and depths based on roundstone size in the Harebell and Pinyon are probably generous.

The range of slopes used in the above calculations leads to realistic estimates of the total relief involved in the transport of the conglomerates. The range of slopes is taken from modern alluvial fans, which, as will be shown later, constitute the closest modern analogs to the conglomerates of the Harebell Formation and the Pinyon Conglomerate. A slope of 1 percent (52.8 ft per mi) would project to a total relief of 5,280 feet in 100 miles and 14,800 feet in 280 miles, the range of total distances that the roundstones may have moved. Under these conditions, streams flowing 9 feet per second and having depths of 4–7 feet are capable of transporting roundstones 1 foot in diameter (fig. 45). A further projection of total relief in 100 miles and in 280 miles follows: A 2-percent slope (105.6 ft/mi), 10,560 and 29,600 feet, respectively; 5-percent slope (264 ft/mi), 26,400 and 74,000 feet; and a 10-percent slope (528 ft/mi), 52,800 and 148,000 feet. Assuming that the quartzite roundstones moved the maximum distance of 280 miles, that the total relief involved slopes averaging 10 percent, and that the relief was distributed among three stages of uplift and roundstone transport as shown in figure 44, then the relief involved in each erosion epoch would have averaged nearly 50,000 feet. At 5-percent slope, the relief per erosion epoch would be reduced to about 25,000 feet, and so on. Thus only the slope values above 5 percent yield unreasonable estimates of

relief. As shown earlier, slopes of 5 percent or less also yield reasonable estimates of velocity and depth.

The lack of evidence for reworking of the conglomerates is a result of the general paucity of fine-grained facies in the conglomerates. Long-distance transport through reworking of successive conglomerates would be expected to produce an abundant supply of fine-grained detritus. In considering this problem one must not overlook the sandstone matrix, seen everywhere in the conglomerates. The roundstones are closely packed and probably have a porosity of about 25 percent, comparable to that produced by "closest," or rhombohedral, packing of spheres (Pettijohn, 1957, p. 83–85). If the original volume of the conglomerates approached 560 cubic miles (Love, 1972), then approximately 25 percent, or 140 cubic miles, of sand was contained between the roundstones. Based on the 75 cubic miles of conglomerates remaining, as estimated by Love (1972), 19 cubic miles of sand is still present. In addition to the great volume of sand produced, the high degree of rounding of the quartzite stones themselves attests to prolonged transport and perhaps reworking.

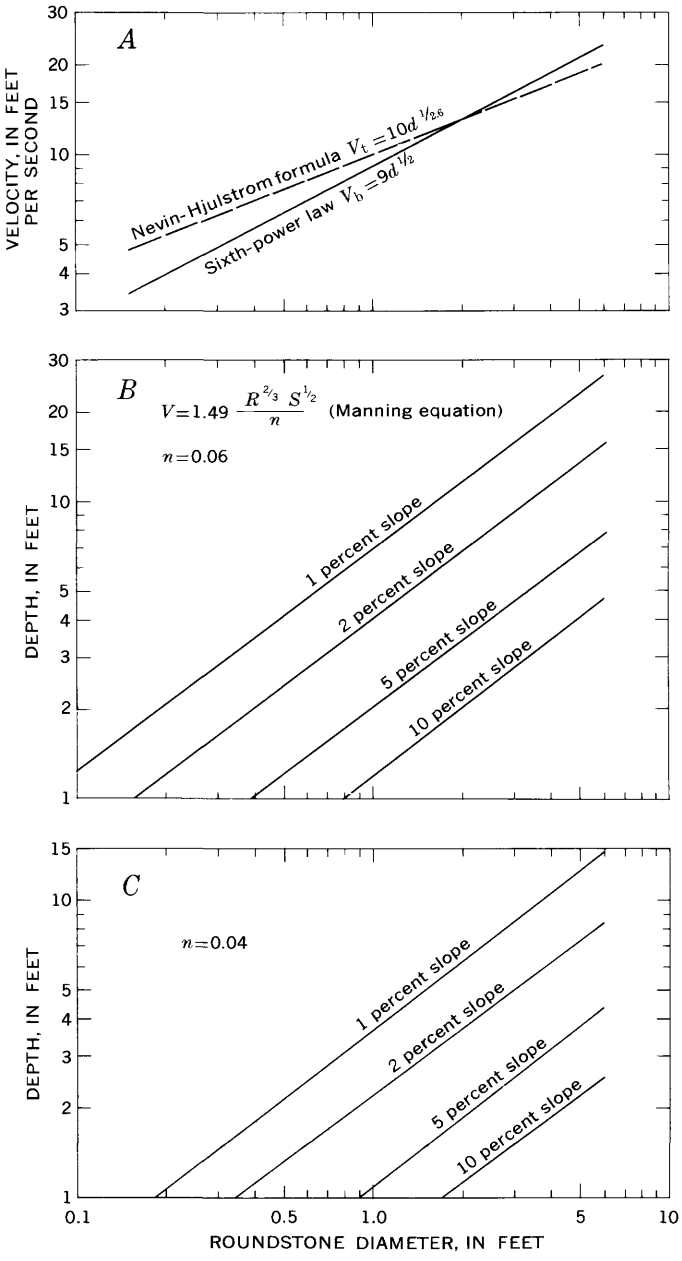

FIGURE 45. — Velocities and depths of streams necessary to transport roundstones found in the Harebell Formation and the Pinyon Conglomerate. *A*, Velocity required to move roundstones of various diameters according to the sixth-power law and the Nevin-Hjulstrom formula. *B*, Depth of water predicted from roundstone diameter using the sixth-power law to derive velocity and the Manning equation to compute depth (approximated by *R*, the hydraulic radius), assuming a roughness of $n=0.06$ and a range in slope of 1–10 percent. *C*, Same as *B* except a roughness of $n=0.04$ is assumed.

The gold distribution in the conglomerates presents a third problem regarding long-distance transport. The Divide quartzite conglomerate lithosome of Ryder (1967) and the western facies of the Pinyon Conglomerate contain only very small quantities of fine-grained gold, whereas the sandstone facies, northern conglomerate facies, and southern conglomerate facies all contain considerably more gold (J. C. Antweiler, unpub. data). If the conglomerates were all derived from the same source and were cycled through comparable depositional episodes, then they might be expected to contain comparable amounts of gold. Here it is important to distinguish between the sources of various components of the conglomerates, such as quartzite or volcanic roundstones. As mentioned earlier, the quartzite roundstones probably had a source terrane different from that of some of the volcanic roundstones, and the sedimentary roundstones may have had yet a third source. The first two (quartzite and volcanics) are probably far traveled, whereas the sedimentary rocks may have come from a wide area nearby, to the northwest of Jackson Hole. The source of the gold may have been any one or more of the several sources suggested for the coarser detritus. Also not evaluated is the possibility of concentrating the gold by successive cycles of reworking, so that the conglomerates (and sandstones) farthest downstream, or youngest in age, may contain the most gold.

ALTERNATIVE EXPLANATIONS

Although I favor long-distance transport of the conglomerates to explain their source, at least three alternative hypotheses were considered and rejected. These, in decreasing order of likelihood, are: (1) Derivation from the Targhee uplift, a now-buried

hypothetical source beneath the Snake River Plain northwest of the Teton Range; (2) derivation from far-thrusted quartzites to the west; and (3) derivation from local quartzite terranes.

Derivation from the hypothetical Targhee uplift was proposed by Love (Antweiler and Love, 1967, p. 2; Love, 1968, 1972; Love and Reed, 1968, p. 83–84). The Targhee uplift hypothesis is in harmony with known transport directions in the Harebell and Pinyon and accounts for the large boulders found in the Pinyon Conglomerate north of the Teton Range. Love (1972) suggested that the absence of Upper Cretaceous strata and the presence of easterly dips in pre-Pinyon rocks north of the Teton Range are further evidence of an uplift nearby. The main objections to the Targhee uplift hypothesis are three: (1) It appeals to an undetected, now-buried source; geophysical studies did not reveal any evidence for a buried uplift (Pakiser and Baldwin, 1961; LaFehr and Pakiser, 1962; Mabey, 1966). (2) The present distribution of terranes containing thick quartzite sequences suggests that much of the proposed Targhee uplift region did not contain abundant quartzite during Cretaceous time (figs. 1 and 43). (3) The location and southwestern or western source of the Divide quartzite conglomerate lithosome of Ryder (1967) is not easily reconciled with the proposed location of the Targhee uplift, to the south and southeast of the Divide.

The hypothesis of quartzite derivation from far-traveled thrust plates near Jackson Hole is not supported by the present distribution of quartzites in the overthrust belt of southwestern Montana, Idaho, and southwestern Wyoming (fig. 43). Paleocene, Cretaceous, and earlier thrusting (Armstrong and Oriel, 1965; Scholten, 1968) of Belt, Precambrian and Cambrian, and Ordovician quartzites probably played some role in elevation and eastward transport of the quartzite later deposited in Jackson Hole. However, the present eastward limit of thrusted Belt quartzites is in extreme southwestern Montana and adjacent Idaho (Ross, 1963, pl. 1), and the present eastward limit of the thrusted Precambrian and Cambrian quartzite sequence of Utah and southeastern Idaho is along a line running roughly from Blackfoot, Idaho, past Bear Lake (Crittenden and others, 1971; S. S. Oriel, oral commun., 1971). Likewise, the Ordovician Kinnikinic and Swan Peak quartzites are found in approximately the same region as the Precambrian quartzites (Ketner, 1968, figs. 1 and 3). Hence, the potential quartzite sources preserved today in the overthrust belt are still more than 100 miles from the nearest conglomerates in Jackson Hole.

Derivation of quartzite from local quartzite terranes (Bengston, 1956, table 1) is probably the weakest hypothesis. Local quartzite terranes are far too small to supply the required quantity of quartzite, and derivation of detritus from local uplifts is not supported by paleocurrent evidence.

DEPOSITIONAL ENVIRONMENT

The conclusion that the Harebell Formation and the Pinyon Conglomerate were deposited in a predominantly continental environment is supported by several lines of evidence:

1. Continental fossils, including vertebrates, freshwater mollusks, leaves, wood, and pollen, are common (Love, 1956b).
2. Sedimentary features, including abundant percussion marks on quartzite roundstones and imbrication inclinations of 28°–29°, correspond very well with modern fluvial environments.
3. The great quantity of well-sorted conglomerate does not have many known analogs in the marine geologic record. At present, the southern facies is a maximum of about 32 miles long (down paleoslope), 17 miles wide (along paleostrike), and from 1,000 to 1,500 feet thick upstream to slightly more than 200 feet thick at the downstream end. Only slides and turbidity currents are thought to be capable of carrying large quantities of coarse detritus very far in marine waters, and these are ruled out by the sorting and shingling of clasts in the conglomerates.
4. The Harebell and Pinyon possess strongly unidirectional paleocurrent systems, in contrast to the greatly dispersed paleocurrents in the underlying mixed marine and continental sandstones.

Evidence for deposition in a marine environment is found in the occurrence of possible marine microfossils (dinoflagellates and acritarchs) and *Mytilus*? clams (Love, 1972) in parts of the Harebell Formation. This evidence suggests that deposition of the Harebell Formation was occasionally at or below sea level.

A subsiding-alluvial-fan model best fits the geometry of the conglomerate deposits. Alluvial fans in the semiarid Southwest range in radius from a few hundred feet to about 7 miles (Blissenbach, 1954; Denny, 1965) and may be as much as 1,000 feet thick (Eckis, 1928). Exceptional alluvial fans are reported with a radius of as much as 40 miles (Grabau, 1913, p. 584). The lobate features outlined by analysis of roundstone length might be explained by the semicircular shape of most alluvial fans noted by Bull (1968). The great thickness of coarse clas-

tics is also explained by the alluvial-fan model. Very coarse detritus, as much as 6 feet in diameter and not uncommonly 3 feet, is reported from some fans in California (Goldman, 1968). Downstream decrease in particle size in alluvial fans is widely noted (Blissenbach, 1954; Eckis, 1928; Goldman, 1968). Although poorly sorted sediments are common in alluvial fans, Blissenbach (1954) stressed the variability found in sorting and rounding of fan deposits and pointed out the strong effects of source rock and reworking on these characteristics. As noted earlier, transport of quartzite roundstones in the Harebell and Pinyon over long distances probably involved considerable reworking. The sedimentary structures observed correspond closely with those seen in fans, except that poorly sorted deposits of possible mudflow origin are not seen in the conglomerates. Blissenbach (1954) noted that mudflow deposits form as much as 40 percent of some alluvial fans in Arizona, but he suggested also that mudflows become less numerous with increased precipitation. Plant remains in the conglomerates suggest a much more humid climate during Harebell and Pinyon time (Love, 1956c) than at present in the Southwest.

The characteristic geographic setting of an alluvial fan is at the base of an imposing mountain front, generally at a fault or fault-line scarp (Blissenbach, 1954). If the alluvial-fan model is correct, then rapidly rising mountain ranges must have been present upstream from each conglomerate deposit at the time of deposition of the fan. Such a mountain range has been postulated for the source of the Divide quartzite conglomerate lithosome (Scholten, 1968). Similarly, a mountain range in the present region of the Teton Range but extending farther north would be needed to supply conglomerate to Jackson Hole. Rapidly rising source areas to the west and northwest of Jackson Hole are prerequisite to transport of the coarse detritus of the Harebell Formation and the Pinyon Conglomerate. Subsidence of the alluvial fans (to below sea level during Harebell time) must have been considerable and prolonged to allow accumulation of the great thickness of conglomerate seen in the Harebell and Pinyon.

The sedimentary features observed within the conglomerates are also consistent with an environment of deposition on alluvial plains. Coarse alluvial deposits with imbrication, crossbedding, and downstream decrease in particle size are well documented (Plumley, 1948; Potter, 1955; Schlee, 1957b). However, the geometry and great thickness of the conglomerates do not favor an alluvial-plain interpretation.

The discussion of depositional models indicates that high mountain ranges west of Jackson Hole (corresponding roughly to the Teton–Gros Ventre arch and the hypothetical Targhee uplift) probably were the immediate source of the coarse detritus seen in the Harebell Formation and the Pinyon Conglomerate. Paleocurrent directions in the conglomerate facies indicate that an ancestral Teton Range must have occupied nearly the same location as the present Teton Range during Late Cretaceous time but that ranges of high relief extended much farther north during Paleocene time. The ancestral Teton Range was not eroded to the Precambrian, as is the present Teton Range, but probably consisted of a thick mantle of quartzite roundstone conglomerates overlying the Paleozoic rocks now present. The mantle of quartzite detritus probably was derived from highlands still farther west where abundant Precambrian and lower Paleozoic quartzites are presently known. The present outliers of Pinyon Conglomerate north of the Teton Range (western facies) may indeed be the remnants of this vast mantle of quartzite detritus. These outliers overlie the Madison Limestone, in harmony with the pictured model of the ancestral Tetons. The lithology of the outliers more closely resembles that of the Divide quartzite conglomerate lithosome farther west than that of the Harebell Formation and the Pinyon Conglomerate to the east (fig. 37). Uplift of the ancestral Teton Range could have been accomplished by activation of the Teton fault (fig. 44*B*). The Teton fault is a major structural feature, and although no geologic evidence has yet been advanced for activity before the Pliocene (Love, 1956c), the intense tectonism evidenced by the conglomerates themselves might suggest a far greater antiquity for the fault.

In summary, the conglomerate facies of the Harebell Formation and the Pinyon Conglomerate were deposited as fans of coarse alluvial detritus along the eastern margin of the ancestral Teton Range. The ancestral Tetons rose rapidly and were quickly stripped of their mantle of quartzite detritus. Coarse quartzitic detritus (the northern facies) was shed directly east from the region of the present Teton Range during Late Cretaceous and early Paleocene time; an extensive region north of the ancestral Teton Range rose rapidly during Paleocene time, shedding coarse quartzitic and volcanic detritus (the southern facies) southeastward into Jackson Hole.

REFERENCES CITED

Andrews, D. A., Pierce, W. G., and Eargle, D. H., 1947, Geologic map of the Bighorn Basin, Wyoming and Montana, showing terrace deposits and physiographic features: U.S. Geol. Survey Oil and Gas Inv. Prelim. Map 71.

Andrews, J. T., and Shimizu, K., 1966, Three-dimensional vector technique for analyzing till fabrics—Discussion and Fortran program: Canada Dept. Mines and Tech. Surveys Geog. Br. Bull., v. 8, no. 2, p. 151–165.

Antweiler, J. C., and Love, J. D., 1967, Gold-bearing sedimentary rocks in northwest Wyoming—A preliminary report: U.S. Geol. Survey Circ. 541, 12 p.

Armstrong, F. C., and Oriel, S. S., 1965, Tectonic development of Idaho-Wyoming thrust belt: Am. Assoc. Petroleum Geologists Bull., v. 49, no. 11, p. 1847–1866.

Barnes, H. H., Jr., 1967, Roughness characteristics of natural channels: U.S. Geol. Survey Water-Supply Paper 1849, 213 p.

Behrendt, J. C., Tibbetts, B. L., Bonini, W. E., and Lavin, P. M., 1968, A geophysical study in Grand Teton National Park and vicinity, Teton County, Wyoming, *with sections on* Stratigraphy and structure, by J. D. Love, *and* Precambrian rocks, by J. C. Reed, Jr.: U.S. Geol. Survey Prof. Paper 516–E, 23 p.

Bengston, C. A., 1956, Structural geology of the Buffalo Fork area, northwestern Wyoming, and its relation to the regional tectonic setting, *in* Wyoming Geol. Assoc. Guidebook 11th Ann. Field Conf., Jackson Hole, 1956: p. 158–168.

Blissenbach, Erich, 1954, Geology of alluvial fans in semiarid regions: Geol. Soc. America Bull., v. 65, no. 2, p. 175–190.

Bull, W. B., 1968, Alluvial fans: Jour. Geol. Education, v. 61, no. 3, p. 101–106.

Cailleux, Andre, 1945, Distinction des galets marins et fluviatiles: Soc. géol. France Bull., v. 15, ser. 5, p. 375–404.

Clifton, H. E., 1965, Tectonic polish of pebbles: Jour. Sed. Petrology, v. 35, no. 4, p. 867–873.

Crittenden, M. D., Jr., Schaeffer, F. E., Trimble, D. E., and Woodward, L. A., 1971, Nomenclature and correlation of some upper Precambrian and basal Cambrian sequences in western Utah and southeastern Idaho: Geol. Soc. America Bull., v. 82, no. 3, p. 581–602.

Denny, C. S., 1965, Alluvial fans in the Death Valley region, California and Nevada: U.S. Geol. Survey Prof. Paper 466, 62 p.

Dorr, J. A., Jr., 1956, Post-Cretaceous geologic history of the Hoback Basin area, central western Wyoming, *in* Wyoming Geol. Assoc. Guidebook 11th Ann. Field Conf., Jackson Hole, 1956: p. 99–108.

Eardley, A. J., 1960, Phases of orogeny in the deformed belt of southwestern Montana and adjacent areas of Idaho and Wyoming, *in* Billings Geol. Soc. 11th Ann. Field Conf., West Yellowstone—earthquake area, 1960: p. 86–91.

———1962, Structural geology of North America (2d ed.): New York, Harper and Row, 743 p.

Eardley, A. J., Horberg, C. L., Nelson, V. E., and Church, Victor, 1944, [Geologic map, cross sections, and stratigraphic column], *in* Hoback-Gros Ventre-Teton Field Conf.: Privately printed.

Eckis, Rollin, 1928, Alluvial fans of the Cucamonga district, southern California: Jour. Geology, v. 36, no. 3, p. 224–247.

Fahnestock, R. K., 1963, Morphology and hyrology of a glacial stream—White River, Mount Rainier, Washington: U.S. Geol. Survey Prof. Paper. 422–A, 70 p.

Fernald, F. A., 1929, Roundstone, a new geologic term: Science, v. 70, no. 1810, p. 240.

Fisher, R. A., 1953, Dispersion on a sphere: Royal Soc. [London] Proc., ser. A, v. 217, p. 295–306.

Foose, R. M., Wise, D. U., and Garbarini, G. S., 1961, Structural geology of the Beartooth Mountains, Montana and Wyoming: Geol. Soc. America Bull., v. 72, no. 8, p. 1143–1172.

Foster, H. L., 1947, Paleozoic and Mesozoic stratigraphy of the northern Gros Ventre Mountains and Mount Leidy Highlands, Teton County, Wyoming: Am. Assoc. Petroleum Geologists Bull., v. 31, no. 9, p. 1537–1593.

Fraser, G. D., Waldrop, H. A., and Hyden, H. J., 1969, Geology of the Gardiner area, Park County, Montana: U.S. Geol. Survey Bull. 1277, 118 p.

Freund, J. E., 1960, Modern elementary statistics: Englewood Cliffs, N. J., Prentice-Hall, 413 p.

Goldman, H. B., 1968, Sand and gravel in California, an inventory of deposits: California Div. Mines and Geology Bull. 180–C, 56 p.

Grabau, A. W., 1913, Principles of stratigraphy [1960 ed.]: New York, Dover Pubs., Inc., 2 v., 1185 p.

Hague, Arnold, 1896, Yellowstone National Park sheets; general description: U.S. Geol. Survey Geol. Atlas, Folio 30.

Hanson, A. M., 1952, Cambrian stratigraphy in southwestern Montana: Montana Bur. Mines and Geology Mem. 33, 46 p.

Heinrich, E. W., 1960, Geology of the Ruby Mountains and nearby areas in southwestern Montana, pt. 2 *of* Pre-Beltian geology of the Cherry Creek and Ruby Mountains areas, southwestern Montana: Montana Bur. Mines and Geology Mem. 38, p. 14–40.

Heinrich, E. W., and Rabbitt, J. C., 1960, Geology of the Cherry Creek area, pt. 1 *of* Pre-Beltian geology of the Cherry Creek and Ruby Mountains areas, southwestern Montana: Montana Bur. Mines and Geology Mem. 38, p. 1–14.

Hewett, D. F., 1926, Geology and oil and coal resources of the Oregon Basin, Meeteetse, and Grass Creek Basin quadrangles, Wyoming: U.S. Geol. Survey Prof. Paper 145, 111 p.

Hobbs, S. W., Hays, W. H., and Ross, R. J., Jr., 1968, The Kinnikinic Quartzite of central Idaho—Redefinition and subdivision: U.S. Geol. Survey Bull. 1254–J, 22 p.

Horberg, C. L., Nelson, V. E., and Church, Victor, 1949, Structural trends in central western Wyoming: Geol. Soc. America Bull, v. 60, no. 1, p. 183-216.

Judson, Sheldon, and Barks, R. E., 1961, Microstriations on polished pebbles: Am. Jour. Sci., v. 259, no. 5, p. 371–381.

Keefer, W. R., 1957, Geology of the Du Noir area, Fremont County, Wyoming: U.S. Geol. Survey Prof. Paper 294–E, 221 p.

———1965, Stratigraphy and geologic history of the uppermost Cretaceous, Paleocene, and lower Eocene rocks in the Wind River Basin, Wyoming: U.S. Geol. Survey Prof. Paper 495–A, 75 p.

Ketner, K. B., 1966, Comparison of Ordovician eugeosynclinal and miogeosynclinal quartzites of the Cordilleran geosyncline, *in* Geological Survey research 1966: U.S. Geol. Survey Prof. Paper 550–C, p. C54–C60.

———1968, Origin of Ordovician quartzite in the Cordilleran miogeosyncline, *in* Geological Survey research

1968: U.S. Geol. Survey Prof. Paper 600–B, p. B169–B177.

Klein, G. D., 1963, Boulder surface markings in Quaco Formation (Upper Triassic), St. Martin's, New Brunswick, Canada: Jour. Sed. Petrology, v. 33, no. 1, p. 49–52.

Klepper, M. R., Weeks, R. A., and Ruppel, E. T., 1957, Geology of the southern Elkhorn Mountains, Jefferson and Broadwater Counties, Montana: U.S. Geol. Survey Prof. Paper 292, 82 p.

Krumbein, W. C., 1939, Preferred orientation of pebbles in sedimentary deposits: Jour. Geology, v. 47, no. 7, p. 673–706.

———1940, Flood gravel of San Gabriel Canyon, California: Geol. Soc. America Bull., v. 51, no. 5, p. 639–676.

———1942, Flood deposits of Arroyo Seco, Los Angeles County, California: Geol. Soc. America Bull., v. 53, no. 9, p. 1355–1402.

Krumbein, W. C., and Graybill, F. A., 1965, An introduction to statistical models in geology: New York, McGraw-Hill Book Co., 475 p.

LaFehr, T. R., and Pakiser, L. C., 1962, Gravity, volcanism, and crustal deformation in the eastern Snake River Plain, Idaho, *in* Short papers in geology, hydrology, and topography: U.S. Geol. Survey Prof. Paper 450–D, p. D76–D78.

Leopold, L. B., Wolman, M. G., and Miller, J. P., 1964, Fluvial processes in geomorphology: San Francisco, W. H. Freeman and Co., 522 p.

Love, J. D., 1939, Geology along the southern margin of the Absaroka Range, Wyoming: Geol. Soc. America Spec. Paper 20, 134 p.

———1947, The Tertiary stratigraphy of the Jackson Hole area, northwestern Wyoming: U.S. Geol. Survey Oil and Gas Inv. Prelim. Chart 27.

———1956a, New geologic formation names in Jackson Hole, Teton County, northwestern Wyoming: Am. Assoc. Petroleum Geologists Bull., v. 40, no. 8, p. 1899–1914.

———1956b, Cretaceous and Tertiary stratigraphy of the Jackson Hole area, northwestern Wyoming, *in* Wyoming Geol. Assoc. Guidebook 11th Ann. Field Conf., Jackson Hole, 1956: p. 76–94.

———1956c, Summary of geologic history of Teton County, Wyoming, during Late Cretaceous, Tertiary, and Quaternary times, *in* Wyoming Geol. Assoc. Guidebook 11th Ann. Field Conf., Jackson Hole, 1956: p. 140–150.

———1968, Late Cretaceous and Cenozoic sedimentation and tectonism, southern Yellowstone–Jackson Hole area, Wyoming (abs.): Geol. Soc. America Spec. Paper 121, p. 611–612.

———1970, Cenozoic geology of the Granite Mountains area, central Wyoming: U.S. Geol. Survey Prof. Paper 495–C, 154 p.

———1972, Harebell Formation (Upper Cretaceous) and Pinyon Conglomerate (uppermost Cretaceous and Paleocene), northwestern Wyoming: U.S. Geol. Survey Prof. Paper 734–A (in press).

Love, J. D., Duncan, D. C., Bergquist, H. R., and Hose, R. K., 1948, Stratigraphic sections of Jurassic and Cretaceous rocks in the Jackson Hole area, northwestern Wyoming: Wyoming Geol. Survey Bull. 40, 48 p.

Love, J. D., and Keefer, W. R., 1969, Basin Creek uplift and Heart Lake Conglomerate, southern Yellowstone National Park, Wyoming, *in* Geological Survey research 1969: U.S. Geol. Survey Prof. Paper 650–D, p. D122–D130.

Love, J. D., and Reed, J. C., Jr., 1968, Creation of the Teton landscape—the geologic story of Grand Teton National Park: Moose, Wyo., Grand Teton Natural History Assoc., 120 p.

Love, J. D., Weitz, J. L., and Hose, R. K., 1955, Geologic map of Wyoming: U.S. Geol. Survey.

Lowell, W. R., and Klepper, M. R., 1953, Beaverhead formation, a Laramide deposit in Beaverhead County, Montana: Geol. Soc. America Bull., v. 64, no. 2, p. 235–243.

Mabey, D. R., 1966, Relation between Bouguer gravity anomalies and regional topography in Nevada and the eastern Snake River Plain, Idaho, *in* Geological Survey research 1966: U.S. Geol. Survey Prof. Paper 550–B, p. B108–B110.

McElhinny, M. W., 1967, Statistics of a spherical distribution, *in* Collinson, D. W., Creer, K. M., and Runcorn, S. K., eds., Methods in palaeomagnetism: Amsterdam, Elsevier, p. 313–321.

McIntyre, D. B., 1963, Rotation of spherical projections: Seaver Lab. Tech. Rept. 7, 7 p.

McKenna, M. C., and Love, J. D., 1970, Local stratigraphic and tectonic significance of *Leptoceratops*, a Cretaceous dinosaur in the Pinyon Conglomerate, northwestern Wyoming, *in* Geological Survey research 1970: U.S. Geol. Survey Prof. Paper 700–D, p. D55–D61.

McMannis, W. J., 1963, LaHood Formation—A coarse facies of the Belt Series in southwestern Montana: Geol. Soc. America Bull., v. 74, no. 4, p. 407–436.

Malde, H. E., 1968, The catastrophic Late Pleistocene Bonneville flood in the Snake River Plain, Idaho: U.S. Geol. Survey Prof. Paper 596, 52 p.

Miesch, A. T., and Connor, J. J., 1968, Stepwise regression and nonpolynomial models in trend analysis: Kansas Geol. Survey Computer Contr. 27, 40 p.

Miller, B. M., 1936, Cambrian stratigraphy of northwestern Wyoming: Jour. Geology, v. 44, no. 2, p. 113–144.

Nockolds, S. R., 1954, Average chemical compositions of some igneous rocks: Geol. Soc. America Bull., v. 65, no. 10, p. 1007–1032.

Pakiser, L. C., and Baldwin, Harry, Jr., 1961, Gravity, volcanism, and crustal deformation in and near Yellowstone National Park, *in* Short papers in the geologic and hydrologic sciences: U.S. Geol. Survey Prof. Paper 424–B, p. B246–B248.

Parkinson, C. R., 1958, The Flathead Formation (middle Cambrian) of the northwestern Wind River Mountains, Wyoming: Miami Univ. of Ohio unpub. M.S. thesis, 106 p.

Pettijohn, F. J., 1957, Sedimentary rocks, 2d. ed.: New York, Harper & Bros., 718 p. (originally pub. 1949).

Pierce, W. G., 1966, Geologic map of the Cody quadrangle, Park County, Wyoming: U.S. Geol. Survey Geol. Quad. Map GQ–542.

Plumley, W. J., 1948, Black Hills terrace gravels—a study in sediment transport: Jour. Geology, v. 56, no. 6, p. 526–577.

Potter, P. E., 1955, Mineralogy and petrology, pt. 1 *of* The petrology and origin of the Lafayette gravel: Jour. Geology, v. 63, no. 1, p. 1–38.

Potter, P. E., and Pettijohn, F. J., 1963, Paleocurrents and basin analysis: New York, Academic Press, 296 p.

Reid, R. R., 1957, Bedrock geology of the north end of the Tobacco Root Mountains, Madison County, Montana: Montana Bur. Mines and Geology Mem. 36, 27 p.

Riccio, J. F., 1962, A geological and geographical appraisal of alluvial fans: Compass, v. 39, no. 2, p. 87–96.

Richmond, G. M., 1945, Geology and oil possibilities at the northwest end of the Wind River Mountains, Sublette County, Wyoming: U.S. Geol. Survey Oil and Gas Inv. Prelim. Map 31.

Roberts, A. E., 1963, The Livingston Group of south-central Montana, *in* Short papers in geology and hydrology: U.S. Geol. Survey Prof. Paper 475–B, p. B86–B92.

Robinson, G. D., 1963, Geology of the Three Forks quadrangle, Montana, *with sections on* Petrography of igneous rocks, by H. F. Barnett: U.S. Geol. Survey Prof. Paper 370, 143 p.

Rohrer, W. L., 1966a, Geologic map of the Kisinger Lakes quadrangle, Fremont County, Wyoming: U.S. Geol. Survey Geol. Quad. Map GQ–527.

———1966b, Geology of the Adam Weiss Peak quadrangle, Hot Springs and Park Counties, Wyoming: U.S. Geol. Survey Bull. 1241–A, 39 p.

———1968, Geologic map of the Fish Lake quadrangle, Fremont County, Wyoming: U.S. Geol. Survey Geol. Quad. Map GQ–724.

———1969, Geologic map of the Sheridan Pass quadrangle, Fremont and Teton Counties, Wyoming: U.S. Geol. Survey open-file map.

Rohrer, W. L., and Obradovich, J. D., 1969, Age and stratigraphic relations of the Tepee Trail and Wiggins Formations, northwestern Wyoming, *in* Geological Survey research 1969: U.S. Geol. Survey Prof. Paper 650–B, p. B57–B62.

Ross, C. P., 1947, Geology of the Borah Peak quadrangle, Idaho: Geol. Soc. America Bull., v. 58, no. 12, pt. 1, p. 1085–1160.

———1963, The Belt Series in Montana, *with a geologic map compiled by* B. A. L. Skipp *and a section on* Paleontologic criteria, by Richard Rezak: U.S. Geol. Survey Prof. Paper 346, 122 p.

Ross, C. P., Andrews, D. A., and Witkind, I. J., 1955, Geologic map of Montana: U.S. Geol. Survey.

Ross, C. P., and Forrester, J. D., 1947, Geologic map of the State of Idaho: U.S. Geol. Survey.

Ryder, R. T., 1967, Lithosomes in the Beaverhead Formation, Idaho-Montana—A preliminary report, *in* Montana Geol. Soc. Guidebook 18th Ann. Field Conf., Centennial basin of southwest Montana, 1967: p. 63–70.

———1968, The Beaverhead Formation—evidence for Late Cretaceous and Paleocene tectonism in southwestern Montana and east-central Idaho (abs.): Geol. Soc. America Spec. Paper 121, p. 259–260.

Ryder, R. T., and Ames, H. T., 1970, Palynology and age of Beaverhead Formation and their paleotectonic implications in Lima region, Montana-Idaho: Am. Assoc. Petroleum Geologists Bull., v. 54, no. 7, p. 1155–1171.

Schlee, J. S., 1957a, Fluvial gravel fabric: Jour. Sed. Petrology, v. 27, no. 2, p. 162–176.

———1957b, Upland gravels of southern Maryland: Geol. Soc. America Bull., v. 68, no. 10, p. 1371–1410.

Scholten, Robert, 1967, Structural framework and oil potential of extreme southwestern Montana, *in* Montana Geol. Soc. Guidebook 18th Ann. Field Conf., Centennial basin of southwest Montana, 1967: p. 7–19.

———1968, Model for evolution of Rocky Mountains east of Idaho Batholith: Tectonophysics, v. 6, no. 2, p. 109–126.

Scholten, Robert, Keenmon, K. A., and Kupsch, W. O., 1955, Geology of the Lima region, southwestern Montana and adjacent Idaho: Geol. Soc. America Bull., v. 66, no. 4, p. 345–404.

Sedimentary Petrology Seminar, 1965, Gravel fabric in Wolf Run: Sedimentology, v. 4, no. 4, p. 273–283.

Siegel, Sidney, 1956, Non-parametric statistics for the behavioral sciences: New York, McGraw-Hill, 312 p.

Smedes, H. W., 1966, Geology and igneous petrology of the northern Elkhorn Mountains, Jefferson and Broadwater Counties, Montana: U.S. Geol. Survey Prof. Paper 510, 116 p.

Smedes, H. W., and Prostka, H. J., 1972, Stratigraphic framework of the Absaroka Volcanic Supergroup in the Yellowstone National Park region: U.S. Geol. Survey Prof. Paper 729–C, 33 p.

Steidtmann, J. R., 1969, Stratigraphy of the early Eocene Pass Peak Formation, central-western Wyoming, *in* Wyoming Geol. Assoc. Guidebook 21st Ann. Field Conf., Tertiary rocks of Wyoming, 1969: p. 55–63.

———1971, Origin of the Pass Peak Formation and equivalent early Eocene strata, central western Wyoming: Geol. Soc. America Bull., v. 82, no. 1, p. 156–176.

Steinmetz, Richard, 1962, Analysis of vectorial data: Jour. Sed. Petrology, v. 32, no. 4, p. 801–812.

Stow, M. H., 1938, Dating Cretaceous-Eocene tectonic movements in Big Horn Basin by heavy minerals: Geol. Soc. America Bull., v. 49, no. 5, p. 731–762.

———1947, Results of some heavy-mineral studies in the Bighorn Basin, Montana and Wyoming, *in* Wyoming Geol. Assoc. Guidebook 2d Ann. Field Conf., Bighorn Basin, 1947: p. 150–164.

Tanner, W. F., 1963, Crushed pebble conglomerate of southwestern Montana: Jour. Geology, v. 71, no. 5, p. 637–641.

Trurnit, Peter, 1968, Pressure solution phenomena in detrital rocks: Sed. Geology, v. 2, no. 2, p. 89–114.

Vandorston, P. L., 1970, Environmental analysis of Swan Peak Formation in Bear River Range, north-central Utah and southeastern Idaho: Am. Assoc. Petroleum Geologists Bull., v. 54, no. 7, p. 1140–1154.

Watson, G. S., 1956, A test for randomness of directions: Royal Astron. Soc. Monthly Notices, Geophys. Supp., v. 7, no. 4, p. 160–161.

Watson, G. S., and Irving, E., 1957, Statistical methods in rock-magnetism: Royal Astron. Soc. Monthly Notices, Geophys. Supp., v. 7, no. 6, p. 289–300.

Weller, J. M., 1960, Stratigraphic principles and practice: New York, Harper and Row, 725 p.

White, W. S., 1952, Imbrication and initial dip in a Keweenawan conglomerate bed [Mich.]: Jour. Sed. Petrology, v. 22, no. 4, p. 189–199.

Williams, Howel, Turner, F. J., and Gilbert, C. M., 1954, Petrography—An introduction to the study of rocks in thin sections: San Francisco, W. H. Freeman and Co., 406 p.

U.S. GOVERNMENT PRINTING OFFICE: 1972 O—479-609